Spring 5-15-2016

The Role of DNMT3A in Acute Myeloid Leukemia Pathogenesis

Christopher Browning Cole
Washington University in St. Louis

WASHINGTON UNIVERSITY IN ST LOUIS

Division of Biology and Biomedical Sciences

Immunology

Dissertation Examination Committee:

Timothy Ley, Chair

John Edwards

Daniel Link

Eugene Oltz

Jacqueline Payton

Matthew Walter

The Role of *DNMT3A* in Acute Myeloid Leukemia Pathogenesis

by

Christopher Browning Cole

A dissertation presented to the

Graduate School of Arts and Sciences

of Washington University in

partial fulfillment of the

requirements for the degree

of Doctor of Philosophy

May 2016

Saint Louis, Missouri

TABLE OF CONTENTS

LIST OF FIGURES

ACKNOWLEDGEMENTS

I would like to thank my mentor Timothy Ley, the members of my thesis committee, and the administration of the Washington University MSTP for their invaluable support and wise guidance. I also thank Mieke Hoock for excellent mouse colony management, Daniel George for expert technical assistance and Bill Eades and the Alvin J. Siteman Cancer Center for the use of the High Speed Cell Sorter Core, which provided high speed cell sorting and analysis. This work was supported by NIH grants CA083962 and CA162086 (to T.J. Ley). I was supported by NIH grant T32 HL007088.

ABSTRACT OF THE DISSERTATION

The Role of *DNMT3A* in Acute Myeloid Leukemia Pathogenesis

by

Christopher Browning Cole

Doctor of Philosophy in Biology and Biomedical Sciences

(Immunology)

Washington University in St. Louis, 2016

Professor Timothy Ley, Chairperson

Loss of function mutations in the DNA methyltransferase *DNMT3A* are highly recurrent in acute myeloid leukemia (AML). *DNMT3A* and the highly homologous gene *DNMT3B* encode the two methyltransferases that are primarily responsible for mediating de novo methylation of specific DNA sequences during cellular differentiation. *DNMT3A* mutations are mutually exclusive of several translocations that create oncogenic fusion genes (*PML-RARA, RUNX1-RUNX1T1, CBFB-MYH11, and MLL-X*), suggesting that these fusions may require functional *DNMT3A* to initiate leukemogenesis. Using bone marrow cells from a constitutive *Dnmt3a* null mouse, we show that loss of *Dnmt3a* caused a striking loss of DNA methylation throughout the genome of bone marrow cells, and a complete loss of methylation at hundreds of specific loci, suggesting that these regions are entirely dependent on *Dnmt3a* for maintaining normal methylation patterns. Using both retroviral vectors and a transgenic model, we demonstrated that the methyltransferase activity of *Dnmt3a* but not *Dnmt3b* is required for aberrant self-renewal *ex vivo* that is driven by *PML-RARA (*but not *RUNX1-RUNX1T1* or *MLL-AF9)*; further, the *PML-RARA* competitive transplant advantage and leukemia generation both required Dnmt3a. In contrast, *Dnmt3a* was not required for leukemia generation caused by *MLL-AF9*, which is known to have a requirement for Dnmt1 activity. Together, these findings demonstrate that *PML-RARA*

is specifically dependent on *Dnmt3a* to drive leukemogenesis, and may explain why *DNMT3A* mutations are mutually exclusive of *PML-RARA* in AML patients.

While the most common mutation in *DNMT3A* in AML patients is the missense mutation R882H, other heterozygous mutations produce frameshifts, premature stop codons, or deletions of the entire coding sequence of the gene, strongly suggesting that these mutations lead to simple haploinsufficiency for DNMT3A. To test the hypothesis that *Dnmt3a* haploinsuffiency may initiate AML, we performed a long-term tumor watch comparing wild-type mice (*Dnmt3a+/+)* to mice carrying one wild-type *Dnmt3a* allele and one targeted allele that contains a neomycin-resistance cassette inserted into the sequence coding for the catalytic domain of the protein, producing a true null allele (*Dnmt3a+/-* mice). At 6 weeks of age, *Dnmt3a+/-* mice have normal hematopoiesis, with no detected differences from wild-type littermates in myeloid, lymphoid, erythroid, or stem/progenitor populations in the bone marrow or spleen. However, after 1.5 years of age, 15/43 *Dnmt3a+/-* mice (35%) became moribund and were euthanized for pathologic evaluation, and at conclusion of the tumor watch at 2 years similar pathologic findings were observed in an additional 9 *Dnmt3a+/-* mice, for an overall disease penetrance of 24/43 (56%). In contrast, 0/20 WT littermate control animals developed myeloid malignancies over the same time period. Based on flow cytometric and morphologic findings, we classified 16 splenic tumors according to the Bethesda criteria: 11/16 had myeloid proliferative disease/MPD, 2/16 had myeloid leukemia with maturation, 2/16 had MPD-like myeloid leukemia, and 1 case had myeloid sarcoma. Six tumors out of 18 tested were able to successfully engraft and lead to lethal disease in sublethally irradiated wild-type recipients, providing further evidence that these tumors represent transplantable, cell-autonomous myeloid malignancies. Exome sequencing of engrafted tumors revealed mutations in the Ras/MAPK pathway, including the canonical gain-of-function mutation *Kras* G12C, a *Ptpn11* E76K mutation, and a missense mutation in the tumor suppressor *Neurofibromatosis 1 (Nf1).* Importantly, 9/51 AML samples with *DNMT3A* mutations

in the TCGA AML cohort also contained activating *NRAS* or *KRAS* mutations. Examination of the *Dnmt3a* locus in 4 sequenced samples revealed no evidence for mutations in or deletions of the residual wild-type *Dnmt3a* allele. These data strongly suggest that Ras/MAPK pathway mutations can cooperate with *Dnmt3a* haploinsufficiency to induce AML in C57Bl/6 mice and in humans.

Chapter 1

Introduction

Section 1: Whole Genome Sequencing and the Genetics of AML

1.1 Historical Background on the Genetics of AML

Acute myeloid leukemia (AML) is a group of heterogeneous hematologic malignancies which are all characterized by the accumulation of immature myeloid "blast" cells in the bone marrow and blood. Aberrantly proliferating blast cells preclude the development of normal hematopoietic cells and lead to cytopenias, immune compromise, and death. No targeted therapy is available for most subtypes of AML, and the 5-year survival for these patients with conventional chemotherapeutic treatment remains at a dismal 45%[1].

Historically, efforts to understand the pathogenesis of acute myeloid leukemia relied on grouping similar cases according to morphology of the leukemic cells, eventually being systematized in the FAB (French-American-British) System[2]. One such example was acute promyelocytic leukemia (APL), which was noted as early as the 1950s to comprise a distinct diagnostic entity marked by blasts resembling normal promyelocytes and an explosive presentation with disseminated intravascular coagulation and rapid lethality[3]. Subsequently, an increased appreciation of the causal role of genetic mutations in oncogenesis led to a focus on the genetics of acute myeloid leukemia and other cancers in the hopes of identifying driver mutations that might be used to stratify risk or ideally result in mutation-specific targeted therapies. In the case of acute promyelocytic leukemia, identification of the causative mutation was greatly facilitated by the observation of a characteristic t(15;17) chromosomal translocation in >90% of APL patients by Janet Rowley and colleagues[4]. The resulting translocation gene product, *PML-RARA,* was cloned and has since been decisively established by our group and others as the key initiating event in the promyelocytic subtype of AML[5–9]. Similar efforts have identified an initiating role for other common AML translocation products, including *RUNX1-RUNX1T1*[10]*, MYH11-CBFB*[11]*,* and a variety of MLL-fusion genes[12–14].

By comparison with leukemias with recurrent chromosomal translocations, AML cases that lack recurrent chromosomal abnormalities (normal karyotype or NK-AML) did not provide a good starting point for finding causative genetic lesions. Recurrent internal tandem duplication mutations in the tyrosine kinase *FLT3* were found serendipitously by Nakao and colleagues when expression studies on AML patients detected an RT-PCR product of aberrantly increased length in several patients[15]. Targeted sequencing efforts subsequently uncovered these *FLT3 ITD* mutations and other mutations in *FLT3* in approximately 25% of AML patients[16–18]. Discovery of another recurrent mutation in NK-AML, a frameshift insertion leading to aberrant cytoplasmic localization of the *NPM1* gene product (*NPMc* mutations), was aided by the fact that the gene had already been implicated as a recurrent fusion partner with various genes in AML cases with recurrent cytogenetic abnormalities[19–21]. A subset of NK-AML patients were also found to display aberrant cytoplasmic localization of the NPM1 protein and targeted sequencing efforts of the *NPM1* gene then uncovered recurrent frame-shift mutations in these patients[22]. Although, these genes were discovered almost serendipitously, approaches to find the other recurrently mutated genes in AML patients needed to be unbiased, and to explore all regions of the genome.

1.2 Application of Next-Generation Sequencing in AML

The advent of whole-genome sequencing has greatly accelerated the search for driver mutations in leukemia, and has led to the discovery of recurrent mutations in several genes which had not previously been implicated in cancer, such as the DNA methyltransferase *DNMT3A*[23], the metabolic enzymes *Isocitrate Dehydrogenase* (*IDH*) *1*[24] and *2*[25], multiple components of the spliceosome complex (including *U2AF1)*[26]*,* and all members of the cohesin complex[27]. The ability of whole-genome sequencing to survey the entire genome in an unbiased manner has been crucial for the discovery of these novel mutations in unsuspected genes, and has implicated entirely new cellular pathways in leukemogenesis.

In addition to allowing the discovery of these new mutations, whole-genome sequencing has provided the ability to focus on the mutational profile of individual patients and determine which genes are affected in a given patient's cancer. This new technology has facilitated two entirely new types of studies that promise to have far-reaching implications for our understanding of leukemia biology, as well as our ability to develop improved therapeutics. The first type of study is the ability of deep sequencing to interrogate the clonality of leukemia. Studies from our lab and others have demonstrated that a given patient's leukemia nearly always consists of multiple clones, including a founding clone and one or more subclones that are derived from it[28–30]. The clonal architecture of a leukemia can be inferred using deep sequencing, in which mutations with similar variant allele frequencies (VAF) form clusters that represent the founding clones or subclones. One study from our group utilized exome sequencing on the progeny of individual hematopoietic stem/progenitor stem cells from normal volunteers to survey to determine how many mutations are "background" mutations present in normal hematopoietic cells prior to transformation[28]. This study discovered that the majority of mutations present in leukemias are likely already present in the hematopoietic stem cell in which the initiating mutation occurred. In addition, the clone with the initiating mutation acquires a small number of cooperating mutations to form the founding clone (in some cases as few as 1 or 2 mutations), and then additional mutations are acquired in the subclones. A subsequent study demonstrated that when transplanted into immunologically impaired mice, individual subclones may be selected for during the engraftment process, and that resultant xenografted leukemias are generally enriched for a single subclone, and thus may not adequately reflect the clonal diversity of the primary tumor[30].

1.3 Mutational Patterns and Clonality in Tumors

Whole genome sequencing has revolutionized studies of the mutational patterns within individual leukemias. It had long been theorized that mutations that tend to occur together have

a cooperative effect, where the second mutation is able to augment the oncogenic effect of the first, providing an additional advantage to the developing cancer which is either additive to or synergistic with the initiating mutation. Elegant targeted sequencing studies by Vogelstein and colleagues provided clinical evidence for this hypothesis, by elucidating one temporal sequence of acquired mutations in colon cancer; the sequential addition of mutations drives disease progression from benign adenoma to full-blown colonic adenocarcinoma in a subset of patients[31]. Direct *in vivo* experimental evidence for cooperativity has come from transgenic mouse models. For example, sequencing of tumors from *PML-RARA* mice uncovered the spontaneous acquisition of *Jak1 V657F* mutations, suggesting that gain-of-function mutations in this tyrosine kinase cooperate with *PML-RARA* to drive leukemogenesis[32]. This hypothesis was experimentally verified by transducing bone marrow from young *PML-RARA+/-* mice with retrovirus encoding the corresponding mutated human gene *JAK1 V678F*, which led to greatly accelerated onset of disease in recipients when compared with *PML-RARA+/-* bone marrow transduced with an empty vector control.

The opposite of cooperativity is mutual exclusivity, i.e. mutations that never occur together in an AML sample. A striking example from whole genome sequencing of AML patients is that *DNMT3A* mutations almost never occur in AML patients with the common AML-initiating fusion genes *MLL-X*, *RUNX1-RUNX1T1, MYH11-CBFB*, and *PML-RARA*[27,28]. This mutual exclusivity suggests several possible interaction scenarios: 1) the two mutations act in the same pathway and are functionally redundant, so there is no selective pressure for a cancer cell to acquire both mutations, 2) the two mutations have antagonistic or synthetically lethal effects, 3) functional DNMT3A enzyme is required for these fusion proteins to drive leukemogenesis. In this thesis, a variety of experiments were performed to assess which of these biological scenarios accounts for the mutual exclusivity of the common AML fusions and *DNMT3A* mutations.

Section 2: DNMT3A Mutations in AML

2.1 DNMT3A Mutations are highly recurrent in AML and Carry a Poor Prognosis

Recent whole genome sequencing efforts by our group have discovered mutations in the *DNA Methyltransferase 3A* (*DNMT3A*) gene in approximately 37**%** of AML patients with a normal karyotype (22% of all cases)[23]. These mutations are almost always heterozygous, and have been demonstrated by our group and others to be associated with high blast count, advanced age, and poor prognosis[23,33–35]. In addition, these mutations have been demonstrated to be stable at relapse[35], indicating that they are probably in the founding clone for most patients. *DNMT3A* mutations are enriched for changes at a single amino acid in the catalytic domain, R882 (37 out of 62 *DNMT3A*-mutated patients in our study), but other patients had nonsense, splice-site, and frame-shift mutations, and in one case, deletion of a 1.5 MB region including *DNMT3A* (**Figure 1)**[23]. Studies from our group and others confirmed that these heterozygous R882 mutations lead to a hypomorphic effect on the methyltransferase activity of the enzyme, and also a dominant negative affect on the WT DNMT3A present in the same AML cells[36–38]. DMNT3A with the R882H mutation forms stable heterodimers with WT DNMT3A, disrupting the ability of the wild-type DNMT3A protein to form active tetramers. The high prevalence, poor prognostic association, and stability throughout the course of disease strongly argue for a key pathogenetic role for *DNMT3A* mutations in AML.

2.2 DNMT3A Haploinsufficiency as a Possible Disease Mechanism

There are two distinct groups of *DNMT3A*-mutated AML patients. The first and most common comprises those with point mutations at amino acid R882. These patients are predicted to have very low DNMT3A activity due to the hypomorphic activity of the R882 mutant protein and the dominant negative effect of the mutated allele[23]. Correspondingly, these cases have been demonstrated to have canonical CpGs that are hypomethylated when compared to the same sequences in AML patients without *DNMT3A* mutations[36]. The other groups consists

of non-R882 mutations. While some are missense mutations in functional domains, others are predicted to have translational effects that would disrupt the coding sequence of one allele by introducing premature stop codons, frameshifts, or whole gene deletions[23]. Many of these mutants would not be predicted *a priori* to have dominant negative activity, suggesting that they create haploinsufficiency for *DNMT3A*. This raises the intriguing possibility that simple haploinsufficiency for *DNMT3A* may also be an initiating event for AML in these patients.

Dnmt3a conditional null mice exhibit an aberrant expansion and loss of differentiation potential in the long-term hematopoietic stem cell compartment when serially transplanted [39](described below). However, conditional *Dnmt3a+/-* mice have not been similarly characterized. Constitutive *Dnmt3a-/-* mice carrying knockout alleles of *Dnmt3a (*which produce no detectable Dnmt3a protein) die with progressive runting at age 3 to 4 weeks, whereas mice with one *Dnmt3a* KO allele do not display runting or early lethality[34]. No gross abnormalities have been reported in *Dnmt3a+/-* mice, except for an increased variation in body size which may reflect instability in quantitative traits induced by DNA hypomethylation[40]. Notably, hematopoiesis in *Dnmt3a+/-* mice has not been fully characterized, and these mice have never been monitored in a long-term tumor watch. Thus the effects of loss of one copy of *DNMT3A* on normal hematopoiesis and leukemogenesis remain to be experimentally tested.

Section 3: DNMT3A and DNMT3B mediate DNA methylation involved in cell differentiation and loss of pluripotency

3.1 Structure and Function of DNMT3A and DNMT3B

DNMT3A and the highly homologous enzyme *DNMT3B* are the two known *de novo* DNA methyltransferases, which are characterized by the ability to introduce DNA methylation to sequences which are not methylated on either strand[41]. In contrast, DNMT1 is the maintenance DNA methyltransferase, and is responsible for methylating the unmethylated strand of a hemimethylated sequence after DNA replication, thus maintaining methylation patterns after cell

divisions. *DNMT3A* and *DNMT3B* share similar domain structures, including a catalytic methyltransferase domain, an ADD domain mediating protein-protein interactions as well as interaction with the unmethylated histone tail of H3K4, and a PWWP domain necessary for targeting to heterochromatin via recognition of H3K36[42]. Both proteins have been primarily studied for their ability to introduce DNA methylation to the C5 carbon of cytosine in CpG-dinucleotides (so-called CpG residues), since this is the most prominent DNA methylation observed in the genome, but the enzymes also possess the ability to methylate cytosine in CA and to a lesser extent CT and CC dinucleotide motifs[43]. The importance of this non-CpG methylation remains unclear. In addition, *DNMT3A* and *DNMT3B* have been shown to physically interact with each other, and with *DNMT1*, *in vitro*[44].

Despite these similarities, *DNMT3A* and *DNMT3B* exhibit differences in flanking sequence specificity both in an *in vitro* cell-free assay and in an "in vivo" yeast episome system[45]. These distinct preferences likely result from differences in the amino acids in the catalytic domain, which have been demonstrated by X-ray crystallography to make contact with the nucleotides flanking the CpG residue[42,46]. Recently ChIP-seq studies have compared genes bound by *DNMT3A* vs *DNMT3B* in NCCIT cells (a mixed germ cell tumor cell line), either undifferentiated or induced to differentiate with retinoic acid. In the undifferentiated cells, there was substantial overlap between the genes bound by *DNMT3A* and *DNMT3B*; after retinoic-acid-induced differentiation, less than 50% of bound genes were shared between the two enzymes[47]. This study was not capable of elucidating cause and effect relationships between binding of the DNMTs and DNA methylation, and an important caveat of ChIP-seq studies like this one is that binding of a DNA methyltransferase does not necessarily correspond to the induction of methylation. Nevertheless, this study indicates that in addition to differences in flanking site preference for the two *de novo* DNA methyltransferase enzymes *in vitro* and in the episomal system, there are also differences in the DNA sequences that are bound. This

suggests that different genes may have different potentials to be regulated by DNA methylation mediated by *DNMT3A* vs *DNMT3B in vivo.*

3.2 Importance of DNMT3A and DNMT3B for de novo DNA Methylation in Development

As the mediators of *de novo* DNA methylation, *DNMT3A* and *DNMT3B* have been demonstrated to play a key role in catalyzing the methylation of genomic DNA required for an organism to normally develop and differentiate[34,42,48]. The phrase "de novo DNA methylation" originally referred to the experimental observation that exogenously induced viral sequences were capable of being methylated and having their expression silenced in mammalian cells[49]; this activity was subsequently discovered to be dependent on *DNMT3A/B*[34]. Later it was observed that after a sweeping phase of demethylation in the fertilized gamete, embryonic cells subsequently exhibited active methylation at specific sequences[50]. This developmental methylation process was termed "de novo" methylation to differentiate it from the process by which newly synthesized strands of DNA have their methylation copied to the daughter strand (primarily by DNMT1) to maintain methylation patterns after cell divisions (so-called maintenance methylation)[51].

De novo DNA methylation is thought to be crucial for an organism's somatic cells to turn off pluripotent stem cell gene expression programs and undergo tissue specific differentiation. Indeed, mouse ES cells that are null for *Dnmt3a* and *3b* lose the ability to differentiate with repeated passages[51]. Both *Dnmt3a* and *Dnmt3b* knockout mice suffer from early lethality, with *Dnmt3b* mice dying in utero due to cardiac defects and hemorrhage, and *Dnmt3a* knockout mice dying at 3-4 weeks of age with severe runting[34]. In humans, biallelic germline mutations in *DNMT3B* lead to the ICF syndrome (Immunodeficiency—Centromeric instability—Facial anomalies), an autosomal recessive syndrome characterized by multiple developmental defects, hypomethylation of satellite repeats, and developmental defects in lymphocytes[52]. The lymphocyte development defects result from hypomethylation of pericentromeric chromatin,

which facilitates the formation of unbalanced translocations and ultimately, the induction of apoptosis resulting in lymphopenias. Several of these mutations have been demonstrated to result in loss of *Dnmt3b* function; knock-in mouse models of two common ICF mutations, A609T and D823G, recapitulated features of the human disease, including low body weight and craniofacial abnormalities, apoptotic death of T cells, and hypomethylation of repetitive genomic sequences.[53] *De novo* germline mutations in *DNMT3A* were recently reported in a cohort of British teenagers, and were associated with a syndrome of developmental intellectual disability, large body size, and distinctive facial features[54]. The translational consequences of these mutations, which are primarily point mutations in all three of the functional domains of the enzyme (ADD, PWWP, and methyltransferase domains) remain to be determined, and the mutational pattern is notably different from that observed in AML patients[23,54]. It is therefore unclear at present unclear whether this syndrome represents *DNMT3A* haploinsufficiency or dominant negative effects of the mutant protein on the residual wild-type allele. It is tempting to speculate that the large body size in these teenagers is mechanistically related to the variability in body size observed in *Dnmt3a+/-* mice discussed above[40]. Because these patients are very young and the mutations are *de novo* rather than inherited, it also remains to be seen whether these individuals have an increased risk of hematologic malignancy.

3.3 DNMT3B Has a Tumor Suppressive Role in Mouse Lymphoma Models

In contrast to the high frequency of*DNMT3A* mutations in AML, *DNMT3B* mutations are rare (2/200 in the TCGA study)[27]. One case had a R538C mutation, and the second had an out-of-frame fusion of *DNMT3B* which presumably inactivated that allele. An expression of a dominant negative isoform of *DNMT3B* lacking the catalytic domain, *DNMT3B7*, has been observed in some lymphoma patients, and is postulated to facilitate oncogenesis by inhibiting the activity of the wild-type *DNMT3B* allele[55]. In order to test this hypothesis, a transgenic mouse was constructed in which lymphomas spontaneously develop due to the overexpression

of Myc in B cells (Eu-*Myc* mice[56] The role of *Dnmt3b* expression was investigated by crossing these mice to a transgenic mouse expressing *DNMT3B7*[55], and then to a mouse with one knockout allele of *Dnmt3b* (*Dnmt3b*+/-)[57]. Constitutive DNMT3B7 overexpression was found to lead to developmental defects reminiscent of the phenotype of *Dnmt3b-/-* mice, whereas conditional expression of the Eu-Myc driver led to an increased incidence of mediastinal lymphomagenesis. The *Dnmt3b+/-* mice likewise exhibited an increased incidence of mediastinal lymphomas, and targeted sequencing indicated that the remaining wild-type allele had not been mutated. Interestingly, mediastinal tumors from the *DNMT3B7* expressing mice were found to have increased 5-meC levels relative to mediastinal tumors from *Eu-Myc* mice with a wild-type *Dnmt3b* allele, and tumors from *Dnmt3b+/-* mice were found to have the highest level of methylation of the three genotypes. Similar results were obtained in another *Eu-Myc* lymphoma model, in which *Dnmt3b* was selectively knocked out in T cells under the control of the EμSR-tTA; the resultant *Dnmt3b-/-* mice developed an increased incidence of T cell lymphoma[58]. In this model, DNA methylation levels by HPLC exhibited the expected pattern, in which *Dnmt3b* loss led to hypomethylation compared to tumors from *Dnmt3b+/+* controls. Collectively, these results demonstrate that loss of one or both copies of *Dnmt3b* is capable of facilitating lymphomagenesis in the context of Eu-Myc mouse models.

These studies of mouse lymphoma models do not address the question of whether *Dnmt3b* loss would contribute to the development of myeloid malignancies; the role of *Dnmt3b* in mouse models of AML pathogenesis remains to be tested. Intriguingly, although *DNMT3B* is highly expressed in AML samples, most patients predominantly express isoforms such as *DNMT3B3* which, like *DNMT3B7 ,* lacks the exons coding for the catalytic domain of the protein (Russler-Germain et al 2014)[36]. This suggests that these isoforms are catalytically inactive, and it is formally possible that they may interact with the DNMT3B and/or DNMT3A proteins in a dominant negative manner.

3.4 Loss of Dnmt3a Leads to Impaired Hematopoietic Differentiation and Increased Self-renewal

Dnmt3a and *Dnmt3b* are highly expressed in murine HSCs, and their expression decreases in more differentiated cells[59]. Surprisingly, a conditional hematopoietic knockout mouse with a large deletion in the catalytic domain of *Dnmt3a* exhibits grossly normal resting hematopoiesis[39]. However, subtle abnormalities in the stem cell population of these mice were discovered when the bone marrow from a *Dnmt3a* -/- mouse was mixed with wild type bone marrow and transplanted into irradiated recipients[29]. Serial competitive transplants resulted in progressive increases in the size of the long-term stem cell compartment, combined with progressive decreases in the ability of the *Dnmt3a-/-* stem cells to develop into mature, differentiated cells. Although these mice did not develop AML (at least in this competitive transplant experiment) their stem cells exhibit impaired differentiation and increased self-renewal, which are two hallmarks of leukemic blasts.

Section 4: Role of DNA Methylation in Modulation of Gene Expression and Cancer

4.1 Relationships between DNA Methylation and Gene Expression

The canonical relationship between DNA methylation and repression of gene expression was based on studies of the promoters of genes that contain a CpG island (a CpG-dense region usually defined as >=1KB with at least a 50% increase in CpG density over the observed ratio in the rest of the genome)[60]. These promoters, known as CpG-island promoters, tend to have a high degree of promoter methylation when repressed, and conversely are mostly unmethylated when the gene is highly expressed. It was subsequently discovered that only a minority of CpG islands, including those in promoters, are methylated in normal cells, and that CpG-island promoters with a high degree of methylation tend to be those which are stably silenced for long periods of time, such as imprinted genes, inactive X chromosome genes, and genes that are specifically expressed in germ cells[61]. Additionally, genes with CpG-island promoters were found to be predominantly housekeeping genes and tumor suppressors. Other genes with more

dynamic, tissue-specific expression usually lack CpG islands, but many have CpG residues near their transcription start site that are capable of being methylated.

The mechanisms by which many heavily methylated CpG-island promoters lead to gene silencing (usually via repressive chromatin remodeling) have been well elucidated[60,62]. Generally, methylated DNA binding proteins stabilize nucleosomes with the repressive H3K9 mark, which in turn recruits histone deacetylases leading to the formation of heterochromatin. In contrast, the mechanisms that lead to DNA methylation in promoters that lack CpG islands appear to be varied and complex. In some cases, such as OCT4 target sites in embryonic stem cells, DNA methylation appears to directly inhibit binding of a transcription factor. In other cases, proteins with methylated DNA binding domains may directly repress transcription by competing with transcription factors for binding sites, or by recruiting co-repressors that lead to the formation of heterochromatin[60,63,64].

Aside from promoters, various other functional units in the genome are capable of being methylated, including gene bodies, insulators, and enhancers. Gene body methylation tends to be positively correlated with gene expression[65], and may also regulate alternative splicing[66]. In addition, some gene bodies possess CpG islands. The function of these CpG island gene bodies is poorly understood, but one possibility is that they serve to regulate the transcription of as yet undiscovered transcripts within genes[65]. Methylation at insulators has been demonstrated to decrease the ability of insulators to repress their target genes (for example, near imprinted loci)[67], but it is unclear whether this principle holds outside of the special case of imprinting. Similarly, enhancer methylation has been demonstrated to lead to gene silencing in reporter assays[68].

Other groups have expanded their methylation analyses from individual CpG islands to larger, surrounding genomic regions. Studies from Andrew Feinberg's group and others have demonstrated a high inverse correlation between the methylation state of the regions directly flanking CpG islands, (called CpG shores) and their neighboring genes[69]. CpG shores from

different normal tissues also displayed a greater degree of differential methylation than CpG islands themselves, and were also more differentially methylated when compared to tumors derived from that same tissue (e.g. colonic adenocarcinoma vs normal colonic tissue). Peggy Goodell's group has used whole genome bisulfite sequencing of hematopoietic stem cells to demonstrate the existence of large hypomethylated regions they termed "canyons", which are enriched for genes involved in transcriptional regulation, including the *HOX* genes[70]. Interestingly, the highly methylated boundaries of these canyons were "eroded" and either expanded or contracted in size in *Dnmt3a*-null hematopoietic stem cells, leading the authors to posit that maintaining these boundaries and thus stabilizing the expression of genes associated with hypomethylated "canyons" is a specific function of *Dnmt3a.*

4.2 Altered DNA Methylation is a Hallmark of Cancer Cells

A pathogenetic role for *de novo* DNA methylation in cancer is supported by the fact that many tumors show marked global DNA methylation abnormalities, which are thought to facilitate their aberrant self-renewal capability and lack of normal differentiation[71]. Studies from different malignancies have noted that tumors can be distinguished by methylation state from normal tissues using unsupervised clustering algorithms[69,72,73]. In general, cancer genomes tend to be globally hypomethylated when compared to the matched normal tissue, but focally hypermethylated at tumor suppressor genes[71]. In stark contrast with normal cells, CpG-island promoters are often hypermethylated in tumor samples. For example *p15*, a cyclin-dependent kinase inhibitor and well-known tumor suppressor that is epigenetically silenced in approximately 60% of AML cases due to hypermethylation in its promoter region, appears to be actively silenced in a manner that is dependent on transcription of an antisense RNA[74]. In most cases, it is unclear whether hypermethylation at tumor suppressors is directly induced by an oncogene, or whether it occurs stochastically and is then selected for by transformation. Direct recruitment of DNA methyltransferase to repress target genes has been suggested

experimentally for various transcription factors important in leukemia including *PU.1*[75] and *MYC*[64], and oncogenic drivers such as *RAS* have been demonstrated to indirectly induce DNA methylation at target genes through the cooperation of a third corepressor protein[76]. As discussed below, there is evidence that *PML-RARA* is capable of directly interacting with *DNMT3A* and thus inducing hypermethylation and gene expression changes, but the importance of this direct induction of methylation for PML-RARA's ability to alter gene expression remains to be established.

The functional importance of DNA methylation in cancer is illustrated by the activity of methylation inhibitors such as 5-Azacytidine in some cancer types, including AML[77]. In addition, the forced expression of genes that are selectively hypermethylated in cancer cells has been shown to result in cancer cell death[78]. The mediators of the aberrant DNA methylation in cancer largely remain to be elucidated, but a role for *DNMT3A* and *DNMT3B* is strongly suggested by the known *de novo* DNA methylation functions of these genes, and the fact that they are both highly expressed in a variety of malignancies, including AML[59]. In the case of *DNMT3A R882H* mutations, DNA methylation arrays have demonstrated the existence of canonical hypomethylated CpGs that distinguish these patients from other NK-AMLs with wild-type *DNMT3A,* strongly suggesting that these specific aberrantly hypomethylated CpGs result directly or indirectly from the *DNMT3A* R882 mutation[36].

4.3 Mutations in the DNA Methylation Pathway are Common in NK-AML

As mentioned above, *DNMT3A* mutations are prevalent in NK-AML, but are mutually exclusive of the common initiating chromosomal translocations, including PML-RARA. Importantly, mutations in several other genes that target the DNA methylation pathway have recently been identified in AML cases. Specifically, the *IDH1* and *IDH2* mutations, which were originally thought to confer a metabolic effect because of their known role in the citric acid cycle, were subsequently demonstrated to produce a neomorphic substrate that inhibits the DNA

methylation pathway and thus leads to hypermethylation in AML cases[79]. Likewise, *TET2* mutations disrupt the removal of methyl-CpGs from DNA by subsequent oxidation steps, resulting in a global increase in CpG methylation in AML patients with this mutation[80]. *IDH* mutations and *TET2* mutations appear to be mutually exclusive[27], which is in line with their predicted antagonistic effects on the DNA methylation pathway, whereas *DNMT3A* mutations and *IDH* mutations tend to co-occur for reasons that are not yet clear.

Collectively, mutations affecting the DNA methylation pathway are rare in cases with the common initiating chromosomal translocations. For example, the TCGA study of AML identified 0/16 *PML-RARA* cases, 1/7 *RUNX1-RUNX1T1* cases, 0/11 *MYH11-CBFB* cases, and 1/*11 MLL-X* fusions with DNA methylation pathway mutations[27]. As discussed above, this raises the intriguing possibility that these chromosomal fusions require a functional DNA methylation pathway in order to drive leukemogenesis. Further support for this hypothesis comes from the fact that each of the four common translocations can be distinguished from each other, and from all other leukemias, by unsupervised clustering of the most differentially methylated CpGs in AML samples[27] (see Figure 2 and related discussion below). The fact that each of these chromosomal fusions is associated with a specific set of methylation changes suggests the importance of DNA methylation for their ability to drive disease, and may provide an explanation for the absence of mutations in the DNA methylation pathway in these cases.

Section 5: PML-RARA and its Relationship to DNA Methylation

5.1 PML-RARA is an Oncogenic Fusion Protein which Represses Myeloid Maturation

Chromosomal translocations involving the transcription factor *Retinoic Acid Receptor Alpha* (*RARA*) are pathognomonic for Acute Promyelocytic Leukemia. The most common of these translocations, t(;15,17)(q22;q21), fuses RARA to the nuclear protein Promyelocytic Leukemia (PML)[81]. Wild type RARA is a key regulator of normal myeloid differentiation[82,83]. By binding to promoters containing Retinoic Acid Response Elements (RAREs) and repressing

them, RARA inhibits myeloid maturation until exposure to its ligand, retinoic acid, causes its release from DNA[84]. In contrast, the PML-RARA fusion protein displays aberrant oligomerization and nuclear localization[85,86], and binds repressively to DNA in a manner that is unresponsive to physiologic concentrations of retinoic acid, but responds to pharmacologic inhibition by the ligand All-Trans-Retinoic Acid (ATRA), which is now a first-line therapy for APL[84]. ATRA binding causes release of PML-RARA protein from target promoters, degradation of PML-RARA, subsequent re-expression of myeloid differentiation genes, and induction of myeloid differentiation.

5.2 PML-RARA is Associated with DNA-Methylation and Silencing of Key Target Genes, and Interacts with DNMT3A and DNMT3B

PML-RARA has been demonstrated to repress gene expression by interacting with several corepressor molecules, including *HDAC3*, *NRCP1*[87], and *MBD 1* [88]. In addition, a physical interaction and colocalization of DNMT3A and PML-RARA has been demonstrated in cell lines[89]. Investigations at known PML-RARA target genes, such as the tumor suppressor *RARB,* have established that PML-RARA causes repression of gene expression and hypermethylation of the *RARB* promoter in the NB4 cell line (which is derived from an APL patient with t(15;17)) and in patient samples. ATRA treatment leads to reduced methylation of DNA near the *RARB* promoter*,* and re-expression of the gene[90,91]. Both *DNMT3A* and *DNMT3B* are highly expressed in NB4 cells, and were found by ChIP-qPCR to be bound (along with PML-RARA) at the *RARB* promoter[91]. Interestingly, ATRA treatment led to a rapid and potent downregulation of both *DNMT3A* and *DNMT3B* expression in NB4 cells and in patient samples (by western blotting). Downregulation was detectable as early as 4 hrs after ATRA addition to NB4 cells, and preceded induction of differentiation, demonstrating that it was not a secondary effect of gene expression changes related to differentiation. The importance of methylation for maintaining repression of *RARB* was demonstrated by the fact that this repression can be

partially relieved by pharmacologic inhibitors of DNA methylation, such as 5-azacytidine, and these synergize with ATRA to cause the release of PML-RARA, reduced promoter methylation, and myeloid differentiation in NB4 cells[91]. These experiments provide support for a model in which PML-RARA recruits DNMT3A and/or DNMT3B to promoters, leading to *de novo* promoter methylation, induction of repressive chromatin changes, and repression of target gene expression.

5.3 The Relationship between PML-RARA binding and DNA methylation remains to be fully elucidated

Recent genome-wide approaches in APL cell lines have confirmed the association between PML-RARA binding at promoter regions, the presence of transcriptionally repressive histone modifications, and repression of gene expression. A ChIP-Chip study of the PR-9 cell line (containing zinc-inducible *PML-RARA*) used an anti-PML antibody with human promoter and CpG arrays to discover 372 genomic regions that are bound when PML-RARA expression is induced[92]. Subsequent ChIP experiments on the same cells revealed that virtually all PR target binding sites exhibited increases in H3-K9 trimethylation, increased HDAC1 binding, and decreases in H3 acetylation. These repressive chromatin changes were accompanied by decreased gene expression for some of the target genes. A ChIP-Seq study of NB4 cells[93] used antibodies against PML and against RARA, and then used a bioinformatics approach to compute overlapping peaks between the two antibodies, which were presumed to correspond to PML-RARA binding sites. This study found 2,722 unique PML-RARA binding sites in NB4 cells, including sites in the gene body of *DNMT3A* and other epigenetic modifier genes such as *HDAC4, HDAC9* and *PRMT3*, as well as in genes encoding hematopoietic transcription factors, such as *RUNX1*, *GATA2*, and *PU.1*. Early (24-48 hours) epigenetic and gene expression changes in response to ATRA were examined using ChIP for histone acetylation and methylation marks, and RNA polymerase II occupancy as a surrogate for gene expression.

Only a small subset of PR target genes were found to be upregulated in response to ATRA at this time point, and upregulated genes were found to be enriched for H3K9 trimethylation and H3 acetylation.

In addition to confirming that PML-RARA binding is associated with repressive chromatin conformations and decreased transcription of target genes, these studies demonstrated the low predictive value of bioinformatically-driven, motif-based approaches to predict PR binding sites. All studies found that only a small subset of bound loci possessed the canonical Retinoic Acid Response Element that typifies wild type RARA targets[92,93]. This finding confirms *in vitro* evidence that PML-RARA possesses novel sequence specificity compared to wild type PML and RARA, and highlights the need for unbiased ChIP-sequencing approaches in order to discover genuine PR targets.

Unsupervised clustering of APL samples based on methylation array data demonstrates that APL samples have a methylation profile which distinguishes them from all other types of AML (**Figure 2, data from the TCGA study on AML, unpublished)**. Importantly, no study has yet assessed the role of DNA methylation on the ability of PML-RARA to repress target genes. In the above-mentioned ChIP-seq paper[93], a GST-methyl DNA binding (methyl-cap) approach coupled with ChIP-seq revealed what the authors describe as “a low level of methylation” near PML-RARA peaks in NB4 cells, but the absence of a control makes their methylation data impossible to interpret. Inferring relationships between the DNA methylation and expression level of a given gene is complicated by the fact that genes have multiple CpG sites both in their promoter and gene body regions, and it is not currently possible to computationally sum the methylation states of all of a gene’s CpG sites to predict whether it will be “on” or “off.” Thus, the most meaningful way to examine DNA methylation is by comparing the methylation state of a given gene under two different conditions. In the case of PML-RARA, comparing the methylation and gene expression status of cells that contain PML-RARA to those of normal

hematopoietic cells that lack PML-RARA will better define the relationships between PML-RARA binding, DNA methylation, and repression of gene expression.

Section 6: Application of Mouse Models to Genetic Studies of AML

6.1 Ctsg-PML-RARA mice develop APL and exhibit aberrant self-renewal ex vivo

To elucidate the role of *PML-RARA* in initiating leukemia, our lab developed a transgenic mouse model in which control of the human *PML-RARA* gene is under control of the endogenous mouse *Cathepsin G* regulatory locus, leading to expression of *PML-RARA* primarily in myeloid progenitor cells (the *Ctsg-PML-RARA* mouse). This mouse spontaneously develops APL with high penetrance (c. 60% in C57Bl/6 mice) and long latency (8-12 months for most APLs), which is preceded by a mild proliferation of myeloid cells with normal maturation in the bone marrow and spleen[6]. The disease phenotype of this mouse faithfully recapitulates salient aspects of human APL, including the acquisition of genetic cooperating events, such as an interstitial deletion of chromosome 2 (with loss of the PU.1 gene)[94], and the ability to cooperate with other mutations observed in APL patients, such as *FLT3*-ITD[95] . The long latency of the disease suggests the need for additional mutations to cooperate with *PML-RARA*, as mentioned above. The cooperative ability of the *Jak1* V657F mutation has been experimentally verified. Intriguingly, when mice with the human *CTSG-PML-RARA* transgene (also made in our lab) were crossed with a transgenic mouse overexpressing *DNMT3A*, the resulting progeny exhibited decreased disease latency[96], suggesting cooperativity between *DNMT3A* and *PML-RARA.* However, the mechanistic nature of this cooperativity and the relationship with DNA methylation was not evaluated.

Young, non-leukemic *Ctsg-PML-RARA* mice exhibit an abnormal “serial replating phenotype”. This phenotype is measured with an assay where whole bone marrow cells are plated in a semi-solid methocellulose medium; rare progenitor cells in the marrow give rise to myeloid colonies that are subsequently replated. In the case of bone marrow from wild-type

mice, the progenitors are not capable of forming colonies after the 2nd or third weekly replating. However, cells from *Ctsg-PML-RARA* mice are capable of being serially replated, and form myeloid colonies week after week. This phenotype has also been detected in other *PML-RARA* mouse models[6,9798], and is thought to be the earliest indicator of aberrant myeloid progenitor self-renewal in these mice. The intimate link between this aberrant self-renewal and the eventual development of leukemia was illustrated by the fact that a *Ctsg-PML-RARA* mouse with mutations preventing sumoylation in PML-RARA lost its replating potential, and in turn, no longer spontaneously developed APL[98].

6.2 Retroviral Models of AML-Initiating Fusion Genes will Allow the Role of DNA Methylation in Aberrant Self-renewal to be Experimentally Defined

In addition to genetically engineered mouse models, the biology of the common AML-initiating translocations has been studied by retroviral overexpression studies, where the fusion gene of interest is introduced into bone marrow cells from a wild-type mouse, and then the transduced cells are studied either *in vitro* or transplanted into irradiated wild-type mice for *in vivo* studies. In *vitro* studies have demonstrated that overexpression of *PML-RARA*[97], *MLL-AF9*[99], or *AML-ETO*[100] is sufficient to induce a replating phenotype similar to that described above for the *Ctsg-PML-RARA* mouse. One appealing feature of these retroviral models is that they quickly induce an aberrant self-renewal phenotype in wild-type cells, which is one hallmark of leukemia initiation. Additionally, the ability of these retroviruses to induce aberrant self-renewal can be tested in the context of bone marrow with deficits in DNA methylation (e.g. Dnmt3a-deficient marrow) in order to determine whether a functional DNA methylation pathway is required for these fusion genes to drive aberrant self-renewal.

Section 7: Summary

In this thesis, we will study mouse models of leukemia to provide a mechanistic explanation for two clinical observations:

1) In addition to recurrent point mutations at amino acid R882, *DNMT3A* mutations include premature stop codons, frameshift mutations, and whole gene deletions that are predicted to lead to haploinsufficiency for the Dnmt3a protein. This suggests that *Dnmt3a* haploinsufficiency may be able to initiate AML.

2) *DNMT3A* mutations are mutually exclusive of the common AML fusion genes, *PML-RARA, MLL-X*, *AML-ETO,* and *CBF-MYH11.* There are multiple scenarios that could explain the mutual exclusivity, including functional redundancy, antagonistic effects, and a requirement of these fusions for functional *DNMT3A* to induce leukemogenesis.

In **Chapter 2**, we will test the common AML fusions for their ability to induce aberrant self-renewal in a *Dnmt3a*-null mouse. We will further characterize the finding that *PML-RARA* cannot induce replating in Dnmt3a deficient marrow by performing additional studies in a *Ctsg-PML-RARA* mouse lacking both copies of *Dnmt3a.*

In **Chapter 3,** we will test the ability of *Dnmt3a* haploinsufficiency to initiate AML in a mouse model, and will further examine the effect of *Dnmt3a* loss on normal hematopoiesis and the ability to induce competitive transplant advantage against wild-type in bone marrow transplantation experiments.

In **Chapter 4**, we will summarize our results and consider future experiments in order to further investigate the role of *DNMT3A* haploinsufficiency in AML and the role of functional *Dnmt3a* in leukemias initiated by the common chromosomal fusions.

Section 8: References

1. Klepin HD, Rao A V, Pardee TS. Acute Myeloid Leukemia and Myelodysplastic Syndromes in Older Adults. *J Clin Oncol*. 2014;32(24). doi:10.1200/JCO.2014.55.1564.

2. Bennett JM, Catovsky D, Daniel MT, et al. Proposals for the classification of the acute leukaemias. French-American-British (FAB) co-operative group. *Br J Haematol*. 1976;33(4):451–8. Available at: http://www.ncbi.nlm.nih.gov/pubmed/188440. Accessed August 7, 2014.

3. HILLESTAD LK. Acute promyelocytic leukemia. *Acta Med Scand*. 1957;159(3):189–94. Available at: http://www.ncbi.nlm.nih.gov/pubmed/13508085. Accessed September 10, 2014.

4. Rowley JD, Golomb HM, Vardiman J, Fukuhara S, Dougherty C, Potter D. Further evidence for a non-random chromosomal abnormality in acute promyelocytic leukemia. *Int J Cancer*. 1977;20(6):869–72. Available at: http://www.ncbi.nlm.nih.gov/pubmed/271143. Accessed September 10, 2014.

5. Grisolano JL, Wesselschmidt RL, Pelicci PG, Ley TJ. Altered myeloid development and acute leukemia in transgenic mice expressing PML-RAR alpha under control of cathepsin G regulatory sequences. *Blood*. 1997;89(2):376–87. Available at: http://www.ncbi.nlm.nih.gov/pubmed/9002938. Accessed September 1, 2014.

6. Westervelt P, Lane A a, Pollock JL, et al. High-penetrance mouse model of acute promyelocytic leukemia with very low levels of PML-RARalpha expression. *Blood*. 2003;102(5):1857–65. doi:10.1182/blood-2002-12-3779.

7. Somervaille TCP, Cleary ML. Identification and characterization of leukemia stem cells in murine MLL-AF9 acute myeloid leukemia. *Cancer Cell*. 2006;10(4):257–68. doi:10.1016/j.ccr.2006.08.020.

8. Brown D, Kogan S, Lagasse E, et al. A PMLRARalpha transgene initiates murine acute promyelocytic leukemia. *Proc Natl Acad Sci U S A*. 1997;94(6):2551–6. Available at: http://www.pubmedcentral.nih.gov/articlerender.fcgi?artid=20126&tool=pmcentrez&rendertype=abstract. Accessed August 31, 2014.

9. He LZ, Tribioli C, Rivi R, et al. Acute leukemia with promyelocytic features in PML/RARalpha transgenic mice. *Proc Natl Acad Sci U S A*. 1997;94(10):5302–7. Available at: http://www.pubmedcentral.nih.gov/articlerender.fcgi?artid=24673&tool=pmcentrez&rendertype=abstract. Accessed September 10, 2014.

10. Grisolano JL, O'Neal J, Cain J, Tomasson MH. An activated receptor tyrosine kinase, TEL/PDGFbetaR, cooperates with AML1/ETO to induce acute myeloid leukemia in mice. *Proc Natl Acad Sci U S A*. 2003;100(16):9506–11. doi:10.1073/pnas.1531730100.

11. Vasen H, Klift H Van Der, Møller P, et al. The fusion gene Cbfb-MYH11. 1999;23(october):12–14.

12. Lavau C, Luo RT, Du C, Thirman MJ. Retrovirus-mediated gene transfer of MLL-ELL transforms primary myeloid progenitors and causes acute myeloid leukemias in mice. *Proc Natl Acad Sci U S A*. 2000;97(20):10984–9. doi:10.1073/pnas.190167297.

13. Corral J, Lavenir I, Impey H, et al. An Mll-AF9 fusion gene made by homologous recombination causes acute leukemia in chimeric mice: a method to create fusion oncogenes. *Cell*. 1996;85(6):853–61. Available at: http://www.ncbi.nlm.nih.gov/pubmed/8681380.

14. Zeisig BB, García-Cuéllar MP, Winkler TH, Slany RK. The oncoprotein MLL-ENL disturbs hematopoietic lineage determination and transforms a biphenotypic lymphoid/myeloid cell. *Oncogene*. 2003;22(11):1629–37. doi:10.1038/sj.onc.1206104.

15. Nakao M, Yokota S, Iwai T, et al. Internal tandem duplication of the flt3 gene found in acute myeloid leukemia. *Leukemia*. 1996;10(12):1911–8. Available at: http://www.ncbi.nlm.nih.gov/pubmed/8946930. Accessed September 10, 2014.

16. Reindl C, Bagrintseva K, Vempati S, et al. Point mutations in the juxtamembrane domain of FLT3 define a new class of activating mutations in AML. *Blood*. 2006;107(9):3700–7. doi:10.1182/blood-2005-06-2596.

17. Yamamoto Y, Kiyoi H, Nakano Y, et al. Activating mutation of D835 within the activation loop of FLT3 in human hematologic malignancies. *Blood*. 2001;97(8):2434–9. Available at: http://www.ncbi.nlm.nih.gov/pubmed/11290608. Accessed September 10, 2014.

18. Fröhling S, Scholl C, Levine RL, et al. Identification of driver and passenger mutations of FLT3 by high-throughput DNA sequence analysis and functional assessment of candidate alleles. *Cancer Cell*. 2007;12(6):501–13. doi:10.1016/j.ccr.2007.11.005.

19. Morris SW, Kirstein MN, Valentine MB, et al. Fusion of a kinase gene, ALK, to a nucleolar protein gene, NPM, in non-Hodgkin's lymphoma. *Science*. 1994;263(5151):1281–4. Available at: http://www.ncbi.nlm.nih.gov/pubmed/8122112. Accessed August 26, 2014.

20. Redner RL, Rush EA, Faas S, Rudert WA, Corey SJ. The t(5;17) variant of acute promyelocytic leukemia expresses a nucleophosmin-retinoic acid receptor fusion. *Blood*. 1996;87(3):882–6. Available at: http://www.ncbi.nlm.nih.gov/pubmed/8562957. Accessed September 10, 2014.

21. Yoneda-Kato N, Look AT, Kirstein MN, et al. The t(3;5)(q25.1;q34) of myelodysplastic syndrome and acute myeloid leukemia produces a novel fusion gene, NPM-MLF1. *Oncogene*. 1996;12(2):265–75. Available at: http://www.ncbi.nlm.nih.gov/pubmed/8570204. Accessed August 23, 2014.

22. Falini B, Mecucci C, Tiacci E, et al. Cytoplasmic nucleophosmin in acute myelogenous leukemia with a normal karyotype. *N Engl J Med*. 2005;352(3):254–66. doi:10.1056/NEJMoa041974.

23. Ley T, Ding L, Walter M. DNMT3A mutations in acute myeloid leukemia. *… Engl J …*. 2010. Available at: http://www.nejm.org/doi/full/10.1056/NEJMoa1005143. Accessed November 25, 2012.

24. Mardis ER, Ding L, Dooling DJ, et al. Recurring mutations found by sequencing an acute myeloid leukemia genome. *N Engl J Med*. 2009;361(11):1058–66. doi:10.1056/NEJMoa0903840.

25. Paschka P, Schlenk RF, Gaidzik VI, et al. IDH1 and IDH2 mutations are frequent genetic alterations in acute myeloid leukemia and confer adverse prognosis in cytogenetically normal acute myeloid leukemia with NPM1 mutation without FLT3 internal tandem duplication. *J Clin Oncol*. 2010;28(22):3636–43. doi:10.1200/JCO.2010.28.3762.

26. Yoshida K, Sanada M, Shiraishi Y, et al. Frequent pathway mutations of splicing machinery in myelodysplasia. *Nature*. 2011;478(7367):64–9. doi:10.1038/nature10496.

27. Genomic and epigenomic landscapes of adult de novo acute myeloid leukemia. *N Engl J Med*. 2013;368(22):2059–74. doi:10.1056/NEJMoa1301689.

28. Welch JS, Ley TJ, Link DC, et al. The origin and evolution of mutations in acute myeloid leukemia. *Cell*. 2012;150(2):264–78. doi:10.1016/j.cell.2012.06.023.

29. Ding L, Ley TJ, Larson DE, et al. Clonal evolution in relapsed acute myeloid leukaemia revealed by whole-genome sequencing. *Nature*. 2012;481(7382):506–10. doi:10.1038/nature10738.

30. Klco JM, Spencer DH, Miller CA, et al. Functional heterogeneity of genetically defined subclones in acute myeloid leukemia. *Cancer Cell*. 2014;25(3):379–92. doi:10.1016/j.ccr.2014.01.031.

31. Fearon ER, Vogelstein B. A genetic model for colorectal tumorigenesis. *Cell*. 1990;61(5):759–67. Available at: http://www.ncbi.nlm.nih.gov/pubmed/2188735. Accessed August 30, 2014.

32. Wartman LD, Larson DE, Xiang Z, et al. Technical advance Sequencing a mouse acute promyelocytic leukemia genome reveals genetic events relevant for disease progression. *J Clin Invest*. 2011;121(4):1445–1455. doi:10.1172/JCI45284DS1.

33. Yan X-J, Xu J, Gu Z-H, et al. Exome sequencing identifies somatic mutations of DNA methyltransferase gene DNMT3A in acute monocytic leukemia. *Nat Genet*. 2011;43(4):309–15. doi:10.1038/ng.788.

34. Okano M, Bell DW, Haber D a, Li E. DNA methyltransferases Dnmt3a and Dnmt3b are essential for de novo methylation and mammalian development. *Cell*. 1999;99(3):247–57. Available at: http://www.ncbi.nlm.nih.gov/pubmed/10555141.

35. Hou H-A, Kuo Y-Y, Liu C-Y, et al. DNMT3A mutations in acute myeloid leukemia: stability during disease evolution and clinical implications. *Blood*. 2012;119(2):559–68. doi:10.1182/blood-2011-07-369934.

36. Russler-Germain D a, Spencer DH, Young M a, et al. The R882H DNMT3A mutation associated with AML dominantly inhibits wild-type DNMT3A by blocking its ability to form active tetramers. *Cancer Cell*. 2014;25(4):442–54. doi:10.1016/j.ccr.2014.02.010.

37. Yamashita Y, Yuan J, Suetake I, et al. Array-based genomic resequencing of human leukemia. *Oncogene*. 2010;29(25):3723–31. doi:10.1038/onc.2010.117.

38. Holz-Schietinger C, Matje DM, Reich NO. Mutations in DNA methyltransferase (DNMT3A) observed in acute myeloid leukemia patients disrupt processive methylation. *J Biol Chem*. 2012;287(37):30941–51. doi:10.1074/jbc.M112.366625.

39. Challen G a, Sun D, Jeong M, et al. Dnmt3a is essential for hematopoietic stem cell differentiation. *Nat Genet*. 2012;44(1):23–31. doi:10.1038/ng.1009.

40. Whitelaw NC, Chong S, Morgan DK, et al. Reduced levels of two modifiers of epigenetic gene silencing , Dnmt3a and Trim28 , cause increased phenotypic noise. *Genome Biol*. 2010;11(11):R111. doi:10.1186/gb-2010-11-11-r111.

41. Fatemi M, Hermann A, Pradhan S, Jeltsch A. The activity of the murine DNA methyltransferase Dnmt1 is controlled by interaction of the catalytic domain with the N-terminal part of the enzyme leading to an allosteric activation of the enzyme after binding to methylated DNA. *J Mol Biol*. 2001;309(5):1189–99. doi:10.1006/jmbi.2001.4709.

42. Jurkowska RZ, Jurkowski TP, Jeltsch A. Structure and function of mammalian DNA methyltransferases. *Chembiochem*. 2011;12(2):206–22. doi:10.1002/cbic.201000195.

43. Gowher H, Jeltsch A. Enzymatic properties of recombinant Dnmt3a DNA methyltransferase from mouse: the enzyme modifies DNA in a non-processive manner and also methylates non-CpG [correction of non-CpA] sites. *J Mol Biol*. 2001;309(5):1201–8. doi:10.1006/jmbi.2001.4710.

44. Van Emburgh BO, Robertson KD. Modulation of Dnmt3b function in vitro by interactions with Dnmt3L, Dnmt3a and Dnmt3b splice variants. *Nucleic Acids Res*. 2011;39(12):4984–5002. doi:10.1093/nar/gkr116.

45. Oka M, Rodić N, Graddy J, Chang L-J, Terada N. CpG sites preferentially methylated by Dnmt3a in vivo. *J Biol Chem*. 2006;281(15):9901–8. doi:10.1074/jbc.M511100200.

46. Jurkowska RZ, Anspach N, Urbanke C, et al. Formation of nucleoprotein filaments by mammalian DNA methyltransferase Dnmt3a in complex with regulator Dnmt3L. *Nucleic Acids Res*. 2008;36(21):6656–63. doi:10.1093/nar/gkn747.

47. Jin B, Ernst J, Tiedemann RL, et al. Linking DNA methyltransferases to epigenetic marks and nucleosome structure genome-wide in human tumor cells. *Cell Rep*. 2012;2(5):1411–24. doi:10.1016/j.celrep.2012.10.017.

48. Okano M, Xie S, Li E. Cloning and characterization of a family of novel mammalian DNA (cytosine-5) methyltransferases. *Nat Genet*. 1998;19(3):219–20. doi:10.1038/890.

49. Niwa O, Yokota Y, Ishida H, Sugahara T. Independent mechanisms involved in suppression of the Moloney leukemia virus genome during differentiation of murine teratocarcinoma cells. *Cell*. 1983. Available at:

http://www.sciencedirect.com/science/article/pii/0092867483902945. Accessed September 10, 2014.

50. Morgan HD, Santos F, Green K, Dean W, Reik W. Epigenetic reprogramming in mammals. *Hum Mol Genet*. 2005;14 Spec No:R47–58. doi:10.1093/hmg/ddi114.

51. Chen T, Ueda Y, Dodge JE, Wang Z, Li E. Establishment and maintenance of genomic methylation patterns in mouse embryonic stem cells by Dnmt3a and Dnmt3b. *Mol Cell Biol*. 2003;23(16):5594–605. Available at: http://www.pubmedcentral.nih.gov/articlerender.fcgi?artid=166327&tool=pmcentrez&rendertype=abstract. Accessed September 10, 2014.

52. Ehrlich M. The ICF syndrome, a DNA methyltransferase 3B deficiency and immunodeficiency disease. *Clin Immunol*. 2003;109(1):17–28. Available at: http://www.ncbi.nlm.nih.gov/pubmed/14585272. Accessed September 10, 2014.

53. Ueda Y, Okano M, Williams C, Chen T, Georgopoulos K, Li E. Roles for Dnmt3b in mammalian development: a mouse model for the ICF syndrome. *Development*. 2006;133(6):1183–92. doi:10.1242/dev.02293.

54. Tatton-Brown K, Seal S, Ruark E, et al. Mutations in the DNA methyltransferase gene DNMT3A cause an overgrowth syndrome with intellectual disability. *Nat Genet*. 2014;46(4):385–8. doi:10.1038/ng.2917.

55. Shah MY, Vasanthakumar A, Barnes NY, et al. DNMT3B7, a truncated DNMT3B isoform expressed in human tumors, disrupts embryonic development and accelerates lymphomagenesis. *Cancer Res*. 2010;70(14):5840–50. doi:10.1158/0008-5472.CAN-10-0847.

56. Adams JM, Harris AW, Pinkert CA, et al. The c-myc oncogene driven by immunoglobulin enhancers induces lymphoid malignancy in transgenic mice. *Nature*. 318(6046):533–8. Available at: http://www.ncbi.nlm.nih.gov/pubmed/3906410. Accessed August 28, 2014.

57. Vasanthakumar A, Lepore JB, Zegarek MH, et al. Dnmt3b is a haploinsuf fi cient tumor suppressor gene in Myc -induced lymphomagenesis. 2013;121(11):2059–2063. doi:10.1182/blood-2012-04-421065.The.

58. Hlady RA, Novakova S, Opavska J, et al. Loss of Dnmt3b function upregulates the tumor modifier Ment and accelerates mouse lymphomagenesis. 2012;122(1):163–177. doi:10.1172/JCI57292DS1.

59. Mizuno S, Chijiwa T, Okamura T, et al. Expression of DNA methyltransferases DNMT1, 3A, and 3B in normal hematopoiesis and in acute and chronic myelogenous leukemia. *Blood*. 2001;97(5):1172–9. Available at: http://www.ncbi.nlm.nih.gov/pubmed/11222358. Accessed September 10, 2014.

60. Deaton AM, Bird A. CpG islands and the regulation of transcription. *Genes Dev*. 2011;25(10):1010–22. doi:10.1101/gad.2037511.

61. Weber M, Hellmann I, Stadler MB, et al. Distribution, silencing potential and evolutionary impact of promoter DNA methylation in the human genome. *Nat Genet*. 2007;39(4):457–66. doi:10.1038/ng1990.

62. Blattler A, Farnham PJ. Cross-talk between site-specific transcription factors and DNA methylation states. *J Biol Chem*. 2013;288(48):34287–94. doi:10.1074/jbc.R113.512517.

63. Velasco G, Hubé F, Rollin J, et al. Dnmt3b recruitment through E2F6 transcriptional repressor mediates germ-line gene silencing in murine somatic tissues. *Proc Natl Acad Sci U S A*. 2010;107(20):9281–6. doi:10.1073/pnas.1000473107.

64. Brenner C, Deplus R, Didelot C, et al. Myc represses transcription through recruitment of DNA methyltransferase corepressor. *EMBO J*. 2005;24(2):336–46. doi:10.1038/sj.emboj.7600509.

65. Jones P a. Functions of DNA methylation: islands, start sites, gene bodies and beyond. *Nat Rev Genet*. 2012;13(7):484–92. doi:10.1038/nrg3230.

66. Maunakea AK, Chepelev I, Cui K, Zhao K. Intragenic DNA methylation modulates alternative splicing by recruiting MeCP2 to promote exon recognition. *Cell Res*. 2013;23(11):1256–69. doi:10.1038/cr.2013.110.

67. Herold M, Bartkuhn M, Renkawitz R. CTCF: insights into insulator function during development. *Development*. 2012;139(6):1045–57. doi:10.1242/dev.065268.

68. Schmidl C, Klug M, Boeld TJ, et al. Lineage-specific DNA methylation in T cells correlates with histone methylation and enhancer activity. *Genome Res*. 2009;19(7):1165–74. doi:10.1101/gr.091470.109.

69. Hansen KD, Timp W, Bravo HC, et al. Increased methylation variation in epigenetic domains across cancer types. *Nat Genet*. 2011;43(8):768–75. doi:10.1038/ng.865.

70. Jeong M, Sun D, Luo M, et al. Large conserved domains of low DNA methylation maintained by Dnmt3a. *Nat Genet*. 2014;46(1):17–23. doi:10.1038/ng.2836.

71. Baylin SB. DNA methylation and gene silencing in cancer. *Nat Clin Pract Oncol*. 2005;2 Suppl 1:S4–11. doi:10.1038/ncponc0354.

72. Hinoue T, Weisenberger DJ, Lange CPE, et al. Genome-scale analysis of aberrant DNA methylation in colorectal cancer. *Genome Res*. 2012;22(2):271–82. doi:10.1101/gr.117523.110.

73. Figueroa ME, Lugthart S, Li Y, et al. DNA methylation signatures identify biologically distinct subtypes in acute myeloid leukemia. *Cancer Cell*. 2010;17(1):13–27. doi:10.1016/j.ccr.2009.11.020.

74. Yu W, Gius D, Onyango P, et al. Epigenetic silencing of tumour suppressor gene p15 by its antisense RNA. *Nature*. 2008;451(7175):202–6. doi:10.1038/nature06468.

75. Suzuki M, Yamada T, Kihara-Negishi F, et al. Site-specific DNA methylation by a complex of PU.1 and Dnmt3a/b. *Oncogene*. 2006;25(17):2477–88. doi:10.1038/sj.onc.1209272.

76. Wajapeyee N, Malonia SK, Palakurthy RK, Green MR. Oncogenic RAS directs silencing of tumor suppressor genes through ordered recruitment of transcriptional repressors. *Genes Dev*. 2013;27(20):2221–6. doi:10.1101/gad.227413.113.

77. McDevitt MA. Clinical applications of epigenetic markers and epigenetic profiling in myeloid malignancies. *Semin Oncol*. 2012;39(1):109–22. doi:10.1053/j.seminoncol.2011.11.003.

78. De Carvalho DD, Sharma S, You JS, et al. DNA methylation screening identifies driver epigenetic events of cancer cell survival. *Cancer Cell*. 2012;21(5):655–67. doi:10.1016/j.ccr.2012.03.045.

79. Figueroa ME, Abdel-Wahab O, Lu C, et al. Leukemic IDH1 and IDH2 mutations result in a hypermethylation phenotype, disrupt TET2 function, and impair hematopoietic differentiation. *Cancer Cell*. 2010;18(6):553–67. doi:10.1016/j.ccr.2010.11.015.

80. Ko M, Huang Y, Jankowska AM, et al. Impaired hydroxylation of 5-methylcytosine in myeloid cancers with mutant TET2. *Nature*. 2010;468(7325):839–43. doi:10.1038/nature09586.

81. Melnick a, Licht JD. Deconstructing a disease: RARalpha, its fusion partners, and their roles in the pathogenesis of acute promyelocytic leukemia. *Blood*. 1999;93(10):3167–215. Available at: http://www.ncbi.nlm.nih.gov/pubmed/10233871.

82. Kastner P, Lawrence HJ, Waltzinger C, Ghyselinck NB, Chambon P, Chan S. Positive and negative regulation of granulopoiesis by endogenous RARalpha. *Blood*. 2001;97(5):1314–20. Available at: http://www.ncbi.nlm.nih.gov/pubmed/11222375. Accessed September 10, 2014.

83. Boylan JF, Lufkin T, Achkar CC, Taneja R, Chambon P, Gudas LJ. Targeted disruption of retinoic acid receptor alpha (RAR alpha) and RAR gamma results in receptor-specific alterations in retinoic acid-mediated differentiation and retinoic acid metabolism. *Mol Cell Biol*. 1995;15(2):843–51. Available at: http://www.pubmedcentral.nih.gov/articlerender.fcgi?artid=231962&tool=pmcentrez&rendertype=abstract. Accessed September 10, 2014.

84. Licht JD. Reconstructing a disease: What essential features of the retinoic acid receptor fusion oncoproteins generate acute promyelocytic leukemia? *Cancer Cell*. 2006;9(2):73–4. doi:10.1016/j.ccr.2006.01.024.

85. Dyck JA, Maul GG, Miller WH, Chen JD, Kakizuka A, Evans RM. A novel macromolecular structure is a target of the promyelocyte-retinoic acid receptor oncoprotein. *Cell*. 1994;76(2):333–43. Available at: http://www.ncbi.nlm.nih.gov/pubmed/8293467. Accessed September 10, 2014.

86. Weis K, Rambaud S, Lavau C, et al. Retinoic acid regulates aberrant nuclear localization of PML-RAR alpha in acute promyelocytic leukemia cells. *Cell*. 1994;76(2):345–56.

Available at: http://www.ncbi.nlm.nih.gov/pubmed/8293468. Accessed September 10, 2014.

87. Hong SH, David G, Wong CW, Dejean A, Privalsky ML. SMRT corepressor interacts with PLZF and with the PML-retinoic acid receptor alpha (RARalpha) and PLZF-RARalpha oncoproteins associated with acute promyelocytic leukemia. *Proc Natl Acad Sci U S A*. 1997;94(17):9028–33. Available at: http://www.pubmedcentral.nih.gov/articlerender.fcgi?artid=23013&tool=pmcentrez&rendertype=abstract. Accessed September 10, 2014.

88. Villa R, Morey L, Raker VA, et al. The methyl-CpG binding protein MBD1 is required for PML-RAR ␣ function. 2006;103(5).

89. Di Croce L, Raker V a, Corsaro M, et al. Methyltransferase recruitment and DNA hypermethylation of target promoters by an oncogenic transcription factor. *Science*. 2002;295(5557):1079–82. doi:10.1126/science.1065173.

90. Fazi F, Zardo G, Gelmetti V, et al. Heterochromatic gene repression of the retinoic acid pathway in acute myeloid leukemia. *Blood*. 2007;109(10):4432–40. doi:10.1182/blood-2006-09-045781.

91. Fazi F, Travaglini L, Carotti D, et al. Retinoic acid targets DNA-methyltransferases and histone deacetylases during APL blast differentiation in vitro and in vivo. *Oncogene*. 2005;24(11):1820–30. doi:10.1038/sj.onc.1208286.

92. Wang K, Wang P, Shi J, et al. PML/RARalpha targets promoter regions containing PU.1 consensus and RARE half sites in acute promyelocytic leukemia. *Cancer Cell*. 2010;17(2):186–97. doi:10.1016/j.ccr.2009.12.045.

93. Martens JH a, Brinkman AB, Simmer F, et al. PML-RARalpha/RXR Alters the Epigenetic Landscape in Acute Promyelocytic Leukemia. *Cancer Cell*. 2010;17(2):173–85. doi:10.1016/j.ccr.2009.12.042.

94. Le Beau MM, Davis EM, Patel B, Phan VT, Sohal J, Kogan SC. Recurring chromosomal abnormalities in leukemia in PML-RARA transgenic mice identify cooperating events and genetic pathways to acute promyelocytic leukemia. *Blood*. 2003;102(3):1072–4. doi:10.1182/blood-2003-01-0155.

95. Kelly LM, Kutok JL, Williams IR, et al. PML/RARalpha and FLT3-ITD induce an APL-like disease in a mouse model. *Proc Natl Acad Sci U S A*. 2002;99(12):8283–8. doi:10.1073/pnas.122233699.

96. Subramanyam D, Belair CD, Barry-Holson KQ, et al. PML-RAR{alpha} and Dnmt3a1 cooperate in vivo to promote acute promyelocytic leukemia. *Cancer Res*. 2010;70(21):8792–801. doi:10.1158/0008-5472.CAN-08-4481.

97. Minucci S, Monestiroli S, Giavara S, et al. PML-RAR induces promyelocytic leukemias with high efficiency following retroviral gene transfer into purified murine hematopoietic progenitors. *Blood*. 2002;100(8):2989–95. doi:10.1182/blood-2001-11-0089.

98. Zhu J, Zhou J, Peres L, et al. A sumoylation site in PML/RARA is essential for leukemic transformation. *Cancer Cell*. 2005;7(2):143–53. doi:10.1016/j.ccr.2005.01.005.

99. Chen W, Kumar AR, Hudson W a, et al. Malignant transformation initiated by Mll-AF9: gene dosage and critical target cells. *Cancer Cell*. 2008;13(5):432–40. doi:10.1016/j.ccr.2008.03.005.

100. Steffen B, Knop M, Bergholz U, et al. AML1/ETO induces self-renewal in hematopoietic progenitor cells via the Groucho-related amino-terminal AES protein. *Blood*. 2011;117(16):4328–37. doi:10.1182/blood-2009-09-242545.

Section 9: Figure Legends

Figure 1.

DNMT3A Mutations are Recurrent in AML**.** 188 bone marrow samples from AML patients were banked at Washington University and all 24 exons of *DNMT3A* were amplified by PCR and Sanger sequenced. Frequency of mutations including those at R882 is indicated by colored dots, and the location of mutations is indicated relative to the methyltransferase (MTase), zinc finger (ZNF), and proline-tryptophan-tryptophan-proline domains.

Figure 2.

Unsupervised Clustering Analysis Demonstrates an APL Methylation Signature. DNA from 178 AML patients was hybridized to Illumina Human Methylation 450 microarrays and unsupervised clustering was performed using a K-means algorithm. Mutation status for common recurrent AML mutations is indicated for each patient. APL patients with *PML-RARA* form a contiguous cluster indicating a common methylation signature (**red arrow**).

Section 10: Figures

Figure 1

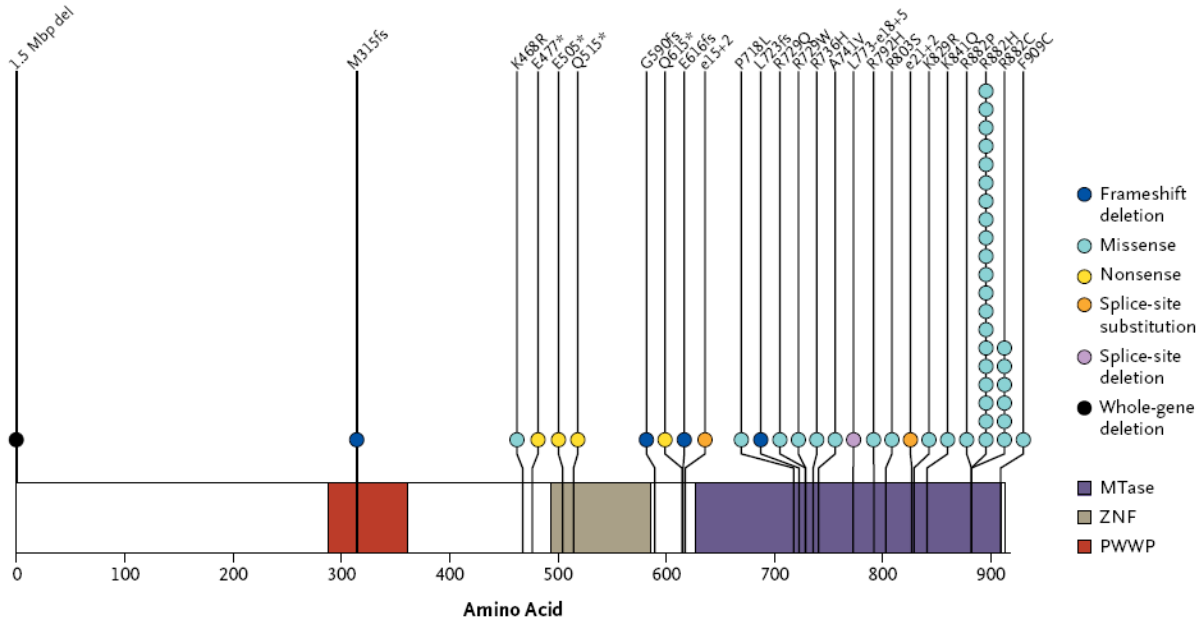

Figure 2

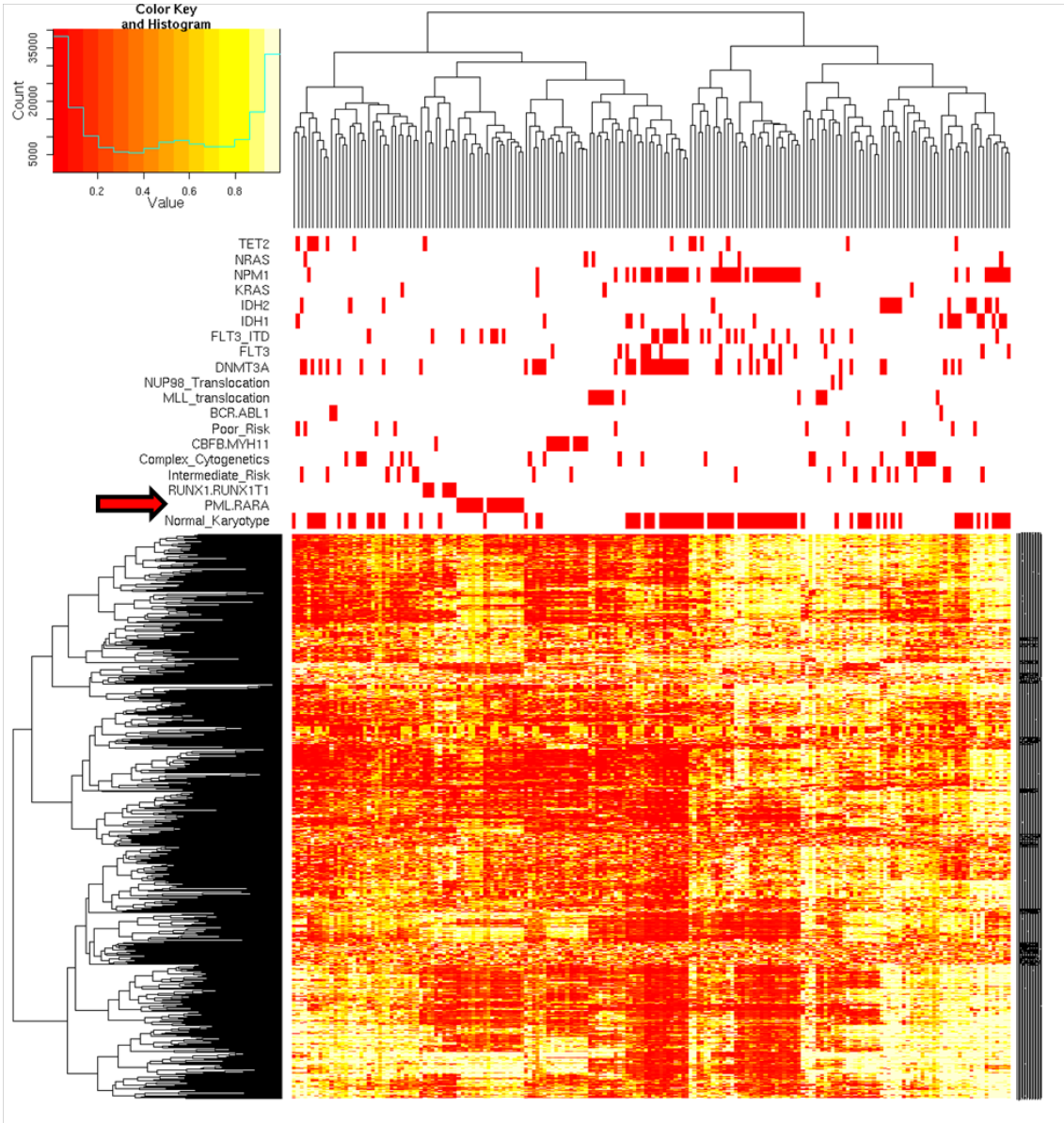

Chapter 2

The *PML-RARA* fusion gene requires Dnmt3a to initiate APL

2.1 Abstract

DNMT3A and *DNMT3B* encode the two DNA methyltransferases that are primarily responsible for the *de novo* methylation of specific cytosine residues in CpG dinucleotides during mammalian cellular differentiation. Loss-of-function mutations in *DNMT3A* are highly recurrent in acute myeloid leukemia (AML), but are almost never found in AML patients with translocations that create oncogenic fusion genes (e.g. *PML-RARA, RUNX1-RUNX1T1,* and *MLL-AF9*). To explore how DNMT3A is involved in the function of these fusion genes, we used retroviral vectors to express *PML-RARA, RUNX1-RUNX1T1,* or *MLL-AF9* in bone marrow cells of wild-type (WT) or Dnmt3a deficient mice; we also examined the phenotypes of hematopoietic cells from *Ctsg-PML-RARA* mice (which express *PML-RARA* in early hematopoietic progenitors and myeloid precursors) with or without Dnmt3a. We demonstrate that the methyltransferase activity of Dnmt3a—but not Dnmt3b—is required for aberrant self-renewal *ex vivo* that is driven by *PML-RARA,* and that Dnmt3a is dispensable for self-renewal driven by *RUNX1-RUNX1T1* and *MLL-AF9*. Furthermore, both the *PML-RARA*-driven competitive transplantation advantage and acute promyelocytic leukemia (APL) development require Dnmt3a. Together, these findings suggest that *PML-RARA* has a unique requirement for Dnmt3a to initiate APL in mice.

2.2 Introduction

Recent efforts by our group and others have identified most of the highly recurrent somatic mutations that are relevant for the pathogenesis of acute myeloid leukemia (1). In addition to discovering recurrent mutations in genes that were not previously known to be important for AML, patterns of mutational co-occurrence and mutual exclusivity are providing important clues regarding the biology of pathways that may contribute to this disease. Mutations in *DNMT3A*, one of the two mammalian *de novo* DNA methyltransferases, occur in ~20% of patients with AML; however, they almost never co-occur with the common chromosomal translocations that create fusion genes such as *PML-RARA, RUNX1-RUNX1T1* (also referred to as *AML-ETO*), and *MLL*-fusions such as *MLL-AF9* (1,2), suggesting a possible relationship between these fusion oncogenes and a fully functional DNMT3A to initiate leukemia.

DNMT3A and the highly homologous enzyme DNMT3B are responsible for inducing specific patterns of *de novo* DNA methylation in bone marrow stem/progenitor cells, which is important for the ability of hematopoietic stem cells to develop into differentiated peripheral blood cells (3-5). The most common *DNMT3A* mutation, which leads to a heterozygous R882H amino acid change in the catalytic domain of the enzyme, reduces DNMT3A methylase activity by 80% and, in a dominant negative fashion, inhibits the ability of wild-type (WT) DNMT3A protein to form active homotetramers (6,7). Although a requirement for functional DNMT3A has not been tested for any of the common chromosomal translocations, all of these translocations are associated with distinct DNA methylation signatures in primary AML samples,

suggesting that alterations in DNA methylation are a common consequence of these chromosomal alterations. In addition, previous studies have suggested a functional relationship between PML-RARA and DNMT3A. PML-RARA is known to act as an oncogenic transcription factor that is capable of initiating leukemia in mouse models (8-14), and has been shown to repress target genes by interacting with a co-repressor complex that includes the methylated DNA binding protein MBD1 and DNMT3A (15-22). At the *RARB* locus, the physical binding of PML-RARA coincides with recruitment of DNMT3A, methylation of the *RARB* promoter, and silencing of gene expression (23). However, it is not yet known whether *PML-RARA* requires *DNMT3A* to act as an oncogene. Recent ChIP-seq studies in AML cell lines have shown that the DNA methylation changes in close proximity to PML-RARA binding sites are relatively subtle (24-25), suggesting that the functional relationship between *PML-RARA* and *DNMT3A* on a whole genome level may be more complex than that observed at the *RARB* locus.

To directly test the hypothesis that AML-initiating fusion genes and DNMT3A mutations are mutually exclusive because the fusions may require DNMT3A to exert their activities, we utilized bone marrow cells from a previously described, constitutive *Dnmt3a* null mouse; we tested the ability of three different fusion oncogenes to induce aberrant self-renewal and leukemia in the absence of Dnmt3a. Our results show that Dnmt3a (but not Dnmt3b) is required only for *PML-RARA* to induce aberrant self-renewal in myeloid progenitor cells, and to initiate APL *in vivo*. It is not required for the leukemogenic potential of *MLL-AF9,* or the self-renewal of myeloid progenitors induced by *RUNX1-RUNX1T1.* These data point out the complexity in understanding the mutual

exclusivity of AML mutations, but demonstrate one mechanism that helps to explain this finding in APL.

2.3 Results

Constitutive loss of Dnmt3a leads to canonical, locus-specific DNA hypomethylation in hematopoietic cells

For the studies of Dnmt3a deficiency in this report, we utilized a constitutive *Dnmt3a* knockout mouse that contains a deletion of part of the catalytic methyltransferase domain of the Dnmt3a enzyme (26). We verified that this allele is a true null for Dnmt3a protein (Supplemental Figure S1A), and that *Dnmt3a* RNA expression is dramatically reduced, with no effects on neighboring genes (data not shown, and see below). Since constitutive *Dnmt3a*$^{-/-}$ mice die of severe runting at about three weeks of age (26), we harvested the bone marrow cells from wild-type (WT) or *Dnmt3a*$^{-/-}$ mice at 2.5 weeks of age, and transplanted them into lethally irradiated C57Bl/6 recipients to study the effects of Dnmt3a loss on hematopoiesis. These mice were allowed to engraft for eight weeks, and were then harvested for morphologic examination, flow cytometry, and DNA methylation studies. Importantly, there were no detectable perturbations in the populations of the stem/progenitor cells or mature cells of any lineage in the engrafted marrow from the *Dnmt3a*$^{-/-}$ donors (see below). Bone marrow cells from three WT and three *Dnmt3a*$^{-/-}$ mice were subjected to CpG-capture and bisulfite sequencing. The targeted genomic regions included all annotated CpG islands, as well as areas of the genome that have been previously established to exhibit differential patterns of

methylation in different tissues, and other regulatory DNA sequences such as enhancers and insulators (Supplemental Table S1). The coverage data for each sample is shown in Supplemental Table S2.

All three *Dnmt3a*$^{-/-}$ bone marrow samples displayed a global decrease in highly methylated CpGs, and a corresponding increase in CpGs that were unmethylated (Supplemental Figure S1B). Nearly all of the CpGs that were differentially methylated were hypomethylated in the *Dnmt3a*$^{-/-}$ samples (231,001 hypomethylated CpGs, vs. 5,488 that were more methylated in *Dnmt3a*$^{-/-}$ samples, Supplemental Figure S1C). This hypomethylation phenotype is in general agreement with previously published studies using a conditional *Dnmt3a* knockout mouse, where the CpGs from purified stem cell and B cell populations of serially transplanted mice were predominantly hypomethylated (3, 27).

Nearly all of the 5,000 most differentially methylated CpGs were hypomethylated in all three *Dnmt3a*$^{-/-}$ samples (Supplemental Figure S1D), and most of the canonically hypomethylated CpGs occurred in defined genomic regions (3, 27). For example, a region on chromosome 16 near the internal (P2) promoter of the *Runx1* gene contains a "canyon" that is completely unmethylated in both WT and *Dnmt3a*$^{-/-}$ bone marrow cells (Supplemental Figure S1E) (27). This canyon is flanked on both sides by regions that are highly methylated in wild-type bone marrow cells, but essentially unmethylated in *Dnmt3a*$^{-/-}$ bone marrow cells.

These results establish that this Dnmt3a deficient mouse strain has a strong focal hypomethylation phenotype in hematopoietic cells, credentialing it for these studies. A complete description of the methylation and expression phenotypes of the bone marrow cells of these mice will be presented elsewhere (Ketkar et al., unpublished observations).

Dnmt3a is required for aberrant self-renewal induced by PML-RARA, but is dispensable for self-renewal caused by RUNX1-RUNX1T1 and MLL-AF9.

We next asked whether Dnmt3a deficiency influenced aberrant self-renewal induced by the AML fusion genes *RUNX1-RUNX1T1, MLL-AF9*, and *PML-RARA*. These oncogenes are capable of inducing an aberrant self-renewal phenotype *ex vivo* when expressed in wild-type mouse bone marrow cells with retroviral vectors (13, 28-29). Whole bone marrow cells, when transduced with MSCV viruses containing cDNAs for *RUNX1-RUNX1T1*, *MLL-AF9*, or *PML-RARA*, and then plated in semi-solid MethoCult media, form CFU-GM (Colony-Forming Unit, Granulocyte-Monocyte) colonies that express CD11b (a marker of terminally differentiated myelomonocytic cells). Progenitor cells from these transductions can be serially replated for several weeks. Wild-type bone marrow cells do not serially replate in this assay, losing the ability to form new myeloid colonies containing cells that express CD11b after one week. To test whether self-renewal in this assay was dependent on *Dnmt3a*, we harvested whole bone marrow cells from 2-2.5 week old WT or *Dnmt3a*$^{-/-}$ littermates, and transduced them with MSCV viruses containing either an empty vector with an IRES-YFP cassette, or with viruses that contain cDNAs for *RUNX1-RUNX1T1, MLL-AF9*, or *PML-RARA* (and an IRES-YFP

cassette to identify the transduced populations). Transduced cells were plated in MethoCult media (Figure 1A). Each week, colonies were quantified, and cells were assessed for expression of CD11b by flow cytometry, and then cells were replated. Both WT and *Dnmt3a*$^{-/-}$ bone marrow cells transduced with "empty" control YFP vector lost the ability to form colonies after one or two replating cycles (Figure 1B). In contrast, both WT and *Dnmt3a*$^{-/-}$ bone marrow transduced with either *MLL-AF9* or *RUNX1-RUNX1T1* gave rise to increasing numbers of colonies over time (Figure 1C-D). In contrast, the *PML-RARA* expressing virus could induce serial replating in WT but not *Dnmt3a*$^{-/-}$ derived marrow cells (Figure 1E). Both WT and *Dnmt3a*$^{-/-}$ bone marrow transduced with either the *MLL-AF9* or *RUNX1-RUNX1T1* viruses maintained expression of the myeloid marker CD11b after three replatings; in contrast, CD11b expression was maintained in WT bone marrow transduced with *PML-RARA,* but lost in the absence of *Dnmt3a* (Figure 1 F-G). Additional flow cytometry and morphologic examination demonstrated that the few remaining cells at week three in the *Dnmt3a*$^{-/-}$ marrow transduced with *PML-RARA* were FcεR positive, c-kit^{high} mast cells, similar to cells transduced with the empty vector GFP (data not shown). Together, these results indicate that in a retroviral transduction system, aberrant myeloid self-renewal by *PML-RARA* requires *Dnmt3a*, whereas self-renewal driven by *MLL-AF9* or *RUNX1-RUNX1T1* does not.

Dnmt3a is required for the aberrant self-renewal of hematopoietic progenitor cells from Ctsg-PML-RARA mice.

To orthogonally validate these results, we crossed *Dnmt3a*$^{+/-}$ mice to a well-characterized *PML-RARA*-expressing transgenic mouse model created in our laboratory (*Ctsg-PML-RARA*, hereafter called *PR*$^{+/-}$) (12), to ultimately generate *PML-RARA* expressing mice lacking both copies of *Dnmt3a* (*PR*$^{+/-}$, *Dnmt3a*$^{-/-}$) as well as all relevant control genotypes (WT, *Dnmt3a*$^{-/-}$, and *PR*$^{+/-}$).

Ctsg-PML-RARA mice express a human *PML-RARA* fusion gene under control of the endogenous mouse *Cathepsin G* locus, which leads to *PML-RARA* expression in early myeloid progenitor cells (with highest expression levels in GMPs, where dysregulation of target genes is most pronounced) (30), and the development of lethal acute promyelocytic leukemia (APL) with long latency and high penetrance (~60% at one year in C57Bl/6 mice) (12). Bone marrow cells derived from these mice display an advantage with competitive transplantation, and give rise to self-renewing myeloid progenitors on semi-solid medium *ex vivo* (30). We reasoned that if functional *Dnmt3a* were required for any of these aberrant self-renewal phenotypes, they would be abrogated in *PR*$^{+/-}$, *Dnmt3a*$^{-/-}$ mice.

We first measured *PML-RARA* expression (by qRT-PCR) in bone marrow cells derived from wild-type, *PR*$^{+/-}$, and *PR*$^{+/-}$, *Dnmt3a*$^{-/-}$ mice (Figure 2A), to determine whether Dnmt3a deficiency altered the expression of *PML-RARA*. No *PML-RARA* transcripts were detected in wild-type bone marrow cells, confirming the specificity of this assay (30). The level of *PML-RARA* expression was not reduced by Dnmt3a deficiency, and was in fact slightly higher than in *PR*$^{+/-}$ mice.

We next assessed the engraftment and differentiation potential of *Dnmt3a*$^{-/-}$ vs. *PR*$^{+/-}$, *Dnmt3a*$^{-/-}$ donor cells (compared to WT and *PR*$^{+/-}$ donor cells) by harvesting whole bone marrow from 2-2.5 week old littermates from all four genotypes, and transplanting these cells into lethally irradiated wild-type recipients. After 8-10 weeks, the engrafted bone marrow cells from all donor genotypes were assessed for their contributions to myeloid and lymphoid lineages (Figure 2B). There was no significant difference in the proportion of mature myeloid (Gr-1+ and/or Cd11b+) or mature lymphoid (B220+ or CD3+) cells regardless of *Dnmt3a* status. Similarly, there were no differences in the numbers of stem and progenitor cells in recipients of marrow with or without Dnmt3a (Figure 2C). At 16 weeks post-transplant, no differences were observed in numbers of peripheral blood leukocytes, red blood cells, or platelets, regardless of the presence or absence of Dnmt3a (Supplemental Figure S2A). Histologic examination of the bone marrow cells of engrafted recipients demonstrated normal cellular morphology with no evidence of dysplastic changes (data not shown). Collectively, these data demonstrate that *Dnmt3a* loss does not lead to impaired engraftment or grossly altered steady-state hematopoiesis for at least four months after transplantation into wild type recipient mice.

We next tested whether *ex vivo* self-renewal was directly altered in bone marrow cells derived from 2-2.5 week old mice from all genotypes (i.e. not transplanted, Figure 2D). WT cells lost the ability to form colonies after one or two replatings, whereas *PR*$^{+/-}$ marrow gave rise to increasing numbers of colonies with serial replating. *PR*$^{+/-}$, *Dnmt3a-/-* cells gave rise to similar numbers of colonies as WT and *PR+/-* with the first

and second platings, but failed to replate thereafter. *PR*$^{+/-}$ cells maintained expression of CD11b with serial replating (Figure 2E). In contrast, replated *PR*$^{+/-}$*, Dnmt3a*$^{-/-}$ cells lost expression of CD11b by the end of the second week (Figure 2E-F). We also tested whether this phenotype was intrinsic to the hematopoietic compartment (as opposed to an effect from *Dnmt3a*$^{-/-}$ stromal cells) by transplanting bone marrow from young (2 to 2.5-week-old) mice into lethally irradiated wild-type C57Bl/6 recipients, and harvesting marrow for replating assays at ten weeks post-transplant (Supplemental Figure S2B). As expected, bone marrow derived from the recipients of *PR*$^{+/-}$ donors formed colonies with serial replating, whereas bone marrow derived from *PR*$^{+/-}$*, Dnmt3a*$^{-/-}$ donors did not (Supplemental Figure S2C). These data demonstrate that this phenotype is due to a cell-autonomous defect in the hematopoietic compartment.

Dnmt3a deficiency attenuates the expression of genes that are normally upregulated by PML-RARA in Granulocyte Monocyte Progenitor cells (GMP cells)

To determine whether Dnmt3a loss affects genes that are specifically dysregulated by *PML-RARA,* we analyzed the expression of genes previously shown to be differentially expressed between WT and *Ctsg-PML-RARA (PR*$^{+/-}$*)* mice (30). In that study, we observed that these genes show the greatest differences in the GMP compartment of *PR*$^{+/-}$ mice, where *Ctsg* is maximally expressed: 112 probesets from the Affymetrix mouse exon ST1.0 arrays were significantly upregulated by PML-RARA in an ANOVA analysis (fold change ≥2.0, FDR <0.05), and 127 probesets were downregulated (30). We therefore performed expression profiling using purified GMP cells from the engrafted marrows of several donor mice from all four genotypes (WT n=4; *PR*$^{+/-}$ n=2;

PR$^{+/-}$, *Dnmt3a*$^{-/-}$ n=4; and *Dnmt3a*$^{-/-}$ *n=3)* harvested 6-8 weeks after transplantation. The results of these analyses are highly concordant with the results of Wartman et al. Of the 112 upregulated probesets (designated as the *PR*$^{+/-a}$ dataset in Figure 3), 96 (86%) exhibited a similar ≥2 fold increase in expression in the data obtained for this study (denoted as the *PR*$^{+/-b}$ dataset, Figure 3, Panel A, and Supplemental Table S3). The average fold change (comparing WT to *PR*$^{+/-}$) for this set of probes in the *PR*$^{+/-a}$ dataset was 8.52 +/- 1.10 (SEM), which was not significantly different from the average fold change of the same genes in the *PR*$^{+/-b}$ dataset (8.71 +/- 1.11; p=0.75; Figure 3A, left panel). GMP cells from the *PR*$^{+/-}$, *Dnmt3a*$^{-/-}$ mice demonstrated significantly less upregulation of many of these probes: the average fold change was 6.24 +/- 0.66 (p = 9.73E-06 compared to *PR*$^{+/-b}$); these data suggest that Dnmt3a loss attenuates the expression of a set of genes that are normally upregulated by PML-RARA in GMP cells. Of the 127 probes that were downregulated at least two-fold in the *PR*$^{+/-a}$ dataset, 107 (84%) were likewise downregulated in the *PR*$^{+/-b}$ dataset, but to a lesser extent (Figure 3, Panel A, right). The average level of downregulation was only -2.91 fold for the *PR*$^{+/-a}$ dataset, and -1.71 fold for the *PR*$^{+/-b}$ dataset. The average expression of these downregulated genes was not appreciably attenuated by Dnmt3a loss, perhaps because the fold changes were relatively small, and therefore more difficult to detect. A heatmap of probeset level data is shown for the 239 dysregulated probes defined by the *PR*$^{+/-a}$ dataset (Figure 3, Panel B), plotting only the average values for the data generated in this study from mice with the designated genotypes. These data extend the fold change data shown in Panel A, and demonstrate that a large number of *PR*$^{+/-}$ dysregulated probesets are affected by Dnmt3a loss. As expected, GMP cells from

Dnmt3a$^{-/-}$ mice had very few changes in expression of the genes that are canonically dysregulated by PML-RARA. We also independently defined differentially expressed genes from the four genotypes using only the data from this study (Supplemental Figure S3, Supplemental Table S4). As expected, this data corroborated the Wartman et al. (30) study for the *PR*$^{+/-}$ dysregulated genes, and identified *Dnmt3a* itself as one of the most downregulated genes in the *Dnmt3a*$^{-/-}$ and *PR*$^{+/-}$*, Dnmt3a*$^{-/-}$ GMP cells. The expression signature for *Dnmt3a* deficient GMP cells was subtle and limited to very few probesets, which is consistent with other studies of both mouse and human hematopoietic cells with reduced or absent *Dnmt3a* expression (1, 2, 3, 5).

DNA methyltransferase activity of DNMT3A is required for aberrant self-renewal by PML-RARA ex vivo.

Both *DNMT3A* and the highly homologous enzyme *DNMT3B* are known to possess *de novo* DNA methyltransferase activities (31). The most common *DNMT3A* mutations in AML occur at residue R882 (2). DNMT3A possessing the R882H mutation has been shown to exhibit reduced DNA methyltransferase activity and produce a dominant negative effect against WT DNMT3A, which leads to a focal DNA hypomethylation phenotype in primary AML samples (6). Some other mutations, such as the Q615* mutation, introduce a premature stop codon that is predicted to form a truncated protein lacking the entire C-terminal methyltransferase domain (Figure 4A) (2). However, DNMT3A has also been reported to influence gene expression by interacting with and stabilizing a co-repressive complex, in a manner that is independent of its methyltransferase activity (32). To determine whether the DNA methyltransferase

activity of DNMT3A is necessary for PML-RARA functions, we conducted complementation experiments where *PR*$^{+/-}$*, Dnmt3a*$^{-/-}$ cells were transduced with retroviruses containing either full-length WT human *DNMT3A*, full-length *DNMT3A* with the R882H mutation, the Q615* truncation mutant, or an empty IRES-YFP vector control. We verified that all constructs were expressed in *PR*$^{+/-}$*, Dnmt3a*$^{-/-}$ bone marrow cells that were sorted for transduced (YFP+) cells using western blotting with an antibody against the N-terminus of DNMT3A (Figure 4B). All proteins were highly expressed, and migrated at their predicted sizes on SDS-PAGE. When sorted YFP+ cells were plated in MethoCult medium, *PR*$^{+/-}$*, Dnmt3a*$^{-/-}$ cells transduced with the empty YFP vector ceased to produce colonies by week four. Reintroduction of wild-type *DNMT3A* was able to restore both colony formation (Figure 4C) and CD11b expression (Figure 4D-E). However, neither of the two mutants known to be deficient for DNA methyltransferase activity (*DNMT3A* R882H and *DNMT3A* Q615*) was able to restore replating ability (Figure 4C), or expression of CD11b (Figure 4D-E).

We also asked whether WT *DNMT3A* was able to restore the normal methylation of a subset of CpG residues in the *Runx1* P2 promoter region shown in Supplemental Figure S1E (green numbers 1-4 shown above the gene). We developed a set of PCR amplicons that each contained a single site for the methylation-sensitive restriction endonuclease HpaII (i.e. a single assayable CpG residue, see Supplemental Table S5). We obtained DNA from the bone marrow cells of *PR*$^{+/-}$*, Dnmt3a*$^{+/-}$ mice transduced with empty YFP, wild-type *DNMT3A,* or the catalytically impaired *DNMT3A* mutants, and cultured the transduced YFP+ cells in MethoCult media for six or seven days. DNA harvested from these cells (and appropriate control mice) was then digested to

completion with HpaII, and qPCR was performed to assess the total level of HpaII cleavage within each amplicon (as a surrogate for the level of cytosine methylation at that particular CCGG cleavage site). Compared to WT or *PR*$^{+/-}$ derived cells, *PR*$^{+/-}$*, Dnmt3a*$^{-/-}$ cells transduced with empty YFP displayed near complete hypomethylation at site 1 (shown in Figure 4F) and site 2 (Supplemental Figure S4B) within the *Runx1* P2 promoter region. Reintroduction of wild-type *DNMT3A*, but not the R882H or Q615* mutants, restored a nearly normal level of methylation to these two sites after only one week, a time frame corresponding to the rapid reintroduction of self-renewal by expression of wild-type *DNMT3A*. Sites 3 and 4, in the hypomethylation "canyon" that is normally unmethylated in bone marrow cells, did not display remethylation with overexpression of DNMT3A for one week (Supplemental Figure S4A-C); these controls demonstrate that HpaII was capable of cleaving unmethylated sites in these DNA samples, and that the overexpression of DNMT3A did not cause abnormal methylation of CpGs that are not normally methylated. Together, these results strongly suggest that it is the DNA methyltransferase activity of DNMT3A *per se* that is required for *PML-RARA* to drive aberrant self-renewal in myeloid progenitor cells.

Dnmt3b is dispensable for the aberrant self-renewal ability of PML-RARA mouse bone marrow ex vivo.

DNMT3B exhibits different sequence specificity from DNMT3A *in vitro* (33), but ChIP-seq studies have demonstrated extensive overlap in the genomic regions bound by DNMT3A and DNMT3B *in vivo* (34). To determine whether PML-RARA also requires Dnmt3b for its ability to induce self-renewal, we generated *PR*$^{+/-}$ mice that were null for

the *Dnmt3b* allele in bone marrow cells. Because *Dnmt3b* loss leads to embryonic lethality, we crossed mice with floxed *Dnmt3b* alleles (35) to mice expressing the pan-hematopoietic *Vav1-Cre* transgene (36) to generate animals with a selective loss of *Dnmt3b* in hematopoietic cells. This conditional null allele of *Dnmt3b* has previously been demonstrated to result in no production of Dnmt3b protein by western blot analysis (37). We intercrossed these three strains of mice to generate *PR$^{+/-}$, Dnmt3b flox/flox* mice with or without *Vav1-Cre* (*PR$^{+/-}$, Dnmt3b flox/flox, Vav1-Cre^{+},* vs. *PR+/-, Dnmt3b flox/flox, Vav-Cre^{-}*), and then compared the ability of bone marrow cells from these mice to self-renew *ex vivo*, as described above (Figure 5A). Importantly, total bone marrow cells from *Dnmt3b flox/flox, Vav1-Cre^{+}* mice demonstrated >95% floxing efficiency of *Dnmt3b* (data not shown), and had a focal hypomethylation phenotype that was overlapping but distinct from that of Dnmt3a deficient mice (7, and Ketkar et al., unpublished observations). *Dnmt3b* was not required for *PML-RARA* to drive self-renewal, since *PR$^{+/-}$, Dnmt3b flox/flox* marrow could be serially replated, and formed equal numbers of colonies regardless of the presence or absence of Cre-mediated *Dnmt3b* excision (Figure 5B). In addition, *Dnmt3b* loss was essentially dispensable for maintaining CD11b expression with serial replating (Figure 5C), although *PR$^{+/-}$, Dnmt3b flox/flox, Vav-Cre^{+}* positive cells did display a slight decrease in CD11b positivity that was statistically significant over time (Figure 5D). We also performed a complementation experiment by transducing *PR$^{+/-}$, Dnmt3a$^{-/-}$* bone marrow cells with a retrovirus expressing a full-length wild-type human *DNMT3B* cDNA (Figure 5E and Supplemental Figure S5). Overexpression of *DNMT3B* was unable to restore colony formation (Figure 5F). These results reinforce the hypothesis that the requirement of

PML-RARA for DNMT3A is specific for the methyltransferase activity of this protein, and it cannot be replaced by DNMT3B.

Dnmt3a is dispensable for leukemia induction by MLL-AF9

The replating results shown above revealed that aberrant self-renewal by *MLL-AF9* and *RUNX1-RUNX1T1* did not require *Dnmt3a*. We next tested whether *MLL-AF9* leukemia induction was *Dnmt3a*-independent *in vivo.* We expressed *MLL-AF9* cDNA in WT or *Dnmt3a*$^{-/-}$ bone marrow cells via retroviral transduction, and then transplanted these cells into lethally irradiated wild-type recipients (Figure 6A). This retroviral model of *MLL-AF9* produces a rapid onset, high-penetrance AML (29). At four weeks post-transplant, recipients of *MLL-AF9* transduced bone marrow exhibited elevated white blood cell counts regardless of the genotype of the transduced donor cells (Figure 6B), and shortly thereafter succumbed to AML (Figure 6C) with identical latency, similar degrees of splenomegaly (Figure 6D) and 100% penetrance (Figure 6E). There were no detectable phenotypic differences between the leukemias that arose in WT vs. *Dnmt3a*$^{-/-}$ bone marrow.

Dnmt3a is required for PML-RARA-driven competitive advantage and APL development in vivo

Previous studies using a conditional *Dnmt3a* deficient mouse model revealed a progressive deficit in hematopoietic maturation in serial competitive transplants (3). In contrast, *PR*$^{+/-}$ derived bone marrow cells have a competitive transplantation advantage,

as demonstrated by an increased ability to contribute to peripheral blood lineages (especially myeloid) over time (38). To determine whether *Dnmt3a* is required for this competitive advantage, we mixed whole bone marrow cells from mice with the indicated genotypes (Figure 7A) in an equal ratio with wild-type competitor marrow, and transplanted the cells into lethally irradiated wild-type mice. Serial analyses of peripheral blood at four week intervals confirmed that *PR*$^{+/-}$ bone marrow is able to outcompete wild-type marrow over time, with 72 +/- 3.7% (SEM) of all peripheral blood cells being derived from *PR+/-* donor marrow at 16 weeks after transplantation (Figure 7B). *Dnmt3a* loss eliminated this competitive advantage, leading to 33.2 +/- 8.6% and 28.7 +/- 7.8% of peripheral blood cells derived from *Dnmt3a*$^{-/-}$ or *PR*$^{+/-}$*, Dnmt3a*$^{-/-}$ donor marrow cells, respectively. To determine whether this reflected a defect in peripheralization rather than a true competitive disadvantage, we sacrificed animals six months post-transplant and examined donor-derived cells from each genotype in the bone marrow and spleen (Figure 7C). The competitive advantage for *PR*$^{+/-}$ derived cells was evident in both of these tissues, with 73.4 +/- 6.4% of bone marrow cells and 67.2 +/- 3.6% of spleen cells derived from *PR*$^{+/-}$ derived donor cells. In contrast, cells derived from *PR*$^{+/-}$*, Dnmt3a*$^{-/-}$ mice comprised only 38.2 +/- 12.8% of total bone marrow cells and 25.9 +/- 7.3% of total spleen cells, with similar competitive deficits observed in the marrow from the *Dnmt3a*$^{-/-}$ donors.

Dnmt3a loss has been shown to have effects at the level of long-term hematopoietic stem cells (3, 39) but *PML-RARA* is primarily expressed in multipotent progenitors and myeloid progenitors in *Ctsg-PML-RARA* mice (30). We therefore performed additional experiments comparing recipients of *PR*$^{+/-}$ versus *PR*$^{+/-}$*, Dnmt3a*$^{-/-}$ marrow to determine

whether Dnmt3a loss in this model might negatively affect the ability of HSPCs to differentiate into more committed progenitors. We evaluated donor-derived long-term HSCs (as well as more committed progenitor populations), and calculated the lineage bias for each genotype, defined as the ratio of donor-derived cells of a given population (e.g. the percentage of long-term HSCs) to the total percentage of donor-derived cells (percentage of Ly5.2+ cells). The expected ratio is 1:1 for cells contributing equally to all lineages. Despite an overall competitive disadvantage (compared to *PR*$^{+/-}$ donor cells), *PR*$^{+/-}$*, Dnmt3a*$^{-/-}$ donor cells were twice as likely to contribute to long-term HSCs (Figure 7D), $p<0.001$, two-way ANOVA. In agreement with previous experiments using conditional *Dnmt3a*$^{-/-}$ mice (3, 39), the ratio of contributions to other downstream populations (such as short-term-HSC, GMP, and CMP) was not different among the genotypes (Figure 7E). Collectively, these results suggest that Dnmt3a is required for the competitive advantage provided by PML-RARA, perhaps by acting upstream from the myeloid progenitor cells that PML-RARA 'reprograms'.

To determine whether Dnmt3a is required for *PML-RARA* to induce APL *in vivo*, we transplanted bone marrow from 2-2.5 week old *PR*$^{+/-}$ or *PR*$^{+/-}$*, Dnmt3a*$^{-/-}$ animals into lethally irradiated wild-type recipients as described in Figure 2A, and performed a long-term tumor watch. Within one year of transplantation, 6/16 *PR*$^{+/-}$ mice developed the typical features of APL, including splenomegaly, an abnormal proliferation of mature myeloid cells, and atypical promyelocytes in the bone marrow and blood, as previously described (12). In contrast, 0/13 *PR*$^{+/-}$*, Dnmt3a*$^{-/-}$ animals developed APL during the

same period of observation (Figure 7D, $p<0.05$ by both Mantel-Cox and Gehan-Breslow-Wilcoxon tests).

2.4 Discussion

In this report, we have explored mechanisms underlying the mutual exclusivity of AML-initiating fusion genes and mutations in *DNMT3A,* both of which are common in AML patients. Although retroviral expression of *RUNX1-RUNX1T1* or *MLL-AF9* induced self-renewal regardless of *Dnmt3a* status, *PML-RARA* required Dnmt3a to induce self-renewal *ex vivo*. Dnmt3a was likewise required for the self-renewal of myeloid progenitor cells derived from *Ctsg-PML-RARA* mice, and also their ability to out-compete wild-type progenitors in a competitive transplant model. We demonstrated that aberrant self-renewal *ex vivo* is specifically dependent on the DNA methyltransferase activity of *DNMT3A*, since neither *DNMT3B* nor mutant *DNMT3A* genes from AML patients that are deficient in catalytic activity were able to restore myeloid self-renewal. Reintroduction of wild-type human DNMT3A was able to restore normal DNA methylation to a canonically hypomethylated locus, and restore aberrant self-renewal ability. Finally, *Ctsg-PML-RARA* mice that were deficient for Dnmt3a had a reduced penetrance of APL *in vivo*.

PML-RARA confers an aberrant self-renewal activity to myeloid progenitors, a finding that is evident long before the development of overt leukemia (30, 38, 40). This property allows myeloid progenitor cells to be serially replated *ex vivo,* and to out-compete wild-type progenitors in competitive transplants (30,38). Aberrant self-renewal may be an essential feature of AML pathogenesis; this phenotype may increase the likelihood that additional, cooperating mutations will occur in cells with increased self-renewal

potential. Our findings demonstrate that functional *Dnmt3a* is required for both the *in vivo* and *ex vivo* myeloid self-renewal phenotypes induced by *PML-RARA*.

The hematopoietic phenotype we demonstrate for $PR^{+/-}$, $Dnmt3a^{-/-}$ marrow displays both similarities and differences from the previously reported phenotypes in serially transplanted hematopoietic cells derived from conditional *Dnmt3a* deficient mice. Like Challen et al. (3), we observed a differentiation bias towards self-renewal in $Dnmt3a^{-/-}$ long-term HSCs. However, we found that loss of *Dnmt3a* decreased the competitive engraftment ability of progenitors derived from the marrow of $PR^{+/-}$ mice. We used whole bone marrow in our study, because it was designed to recapitulate our previous studies (30) that demonstrated that whole bone marrow cells from $PR^{+/-}$ mice display a competitive advantage *in vivo*. There are numerous methodological differences between the two studies, including the use of unfractionated marrow and a single transplantation event in our studies, versus the use of sorted long-term stem cells and serial transplantation in the previous study, which may partially explain apparent discrepancies.

Mayle et al. (39) have shown that sorted hematopoietic stem cells from conditional Dnmt3a deficient mice have an increased propensity to develop both myeloid and lymphoid malignancies after a long latent period, whereas in this study, Dnmt3a deficiency protected *Ctsg-PML-RARA mice* from developing APL. Further, our $PR^{+/-}$, $Dnmt3a^{-/-}$ mice did not spontaneously develop other forms of AML or ALL. In this study,

we transplanted whole bone marrow rather than purified hematopoietic stem cells, the number of animals at risk was small (n=13), and the study was terminated when significance was achieved at one year. It is therefore possible that some of these mice could have developed alternative hematopoietic malignancies had they been followed for a longer period of time. We did not perform an independent tumor watch using the germline *Dnmt3a*$^{-/-}$ mice, so we do not yet know whether there are biologically relevant differences between these two different Dnmt3a deficient models, or whether differences in phenotypes result from the methodological differences described above. Additional studies will be required to better understand the differences between these model systems.

Dnmt3a was not required for the aberrant *ex vivo* self-renewal induced by two common AML-initiating fusions, *RUNX1-RUNX1T1* and *MLL-AF9,* and was not required for MLL-AF9 to induce AML *in vivo.* This data strongly suggests that Dnmt3a loss does not cause a general state of hematopoietic dysfunction that is incompatible with the development of AML. In fact, previous studies have shown that *Dnmt1* (but not *Dnmt3a* or *Dnmt3b)* is highly expressed in a putative leukemic stem cell population from *MLL-AF9* expressing AML cells (L-GMP) (41,42). In this model, haploinsufficiency for *Dnmt1* delayed leukemia progression, suggesting that *MLL-AF9* requires maintenance methylation by Dnmt1 for the induction of leukemia*,* rather than *de novo* DNA methylation by Dnmt3a or Dnmt3b*.* Likewise, *RUNX1-RUNX1T1* has been reported to recruit DNMT1 and histone deacetylases in order to silence gene expression,

suggesting that it also may require Dnmt1 to induce leukemia in mice, instead of Dnmt3a (43,44).

We have shown that Dnmt3a deficiency attenuates the upregulation of several genes that are normally dysregulated by *PML-RARA* expression in GMP cells. Additional studies will be necessary to determine the specific genes and pathways that *PML-RARA* uses to drive aberrant self-renewal, and how these pathways are affected by DNMT3A. Previous studies have suggested that PML-RARA recruits DNMT3A to induce DNA methylation at specific sites in the genome, resulting in the repression of gene expression (18, 20, 23). However, alternative hypotheses have also been proposed: a recent study has suggested that PML-RARA binding to DNA may actually protect target sites from CpG methylation; these findings argue that the characteristic methylation changes of APL cells are not actually required for initiation of APL, but rather occur after transcription factors leave key binding sites (45, 46).

Neither *DNMT3B* nor catalytically inactive mutants of *DNMT3A* were capable of restoring replating to *PR*$^{+/-}$*, Dnmt3a*$^{-/-}$ marrow. This specific requirement for *Dnmt3a* may be due to the fact that the two enzymes have different sequence specificities *in vitro* (33,47) and have been shown to act on overlapping but distinct genomic regions *in vivo* (5,34). Therefore, *Dnmt3a*-specific methylation patterns may be required for *PML-RARA* to induce leukemia.

Collectively, these results suggest an important role for DNMT3A in the development of APL: PML-RARA appears to specifically require DNMT3A to initiate the self-renewal phenotype in myeloid progenitor cells. These findings have helped to define a mechanistic relationship between two recurrent but independent AML driver mutations, and add to the growing body of evidence implicating epigenetic changes in the induction of AML.

2.5 Methods

Mice

The *Ctsg-PML-RARA* and *Dnmt3a*$^{-/-}$ mice have previously been described (12, 26). Both strains have been backcrossed to C57Bl/6 mice for more than ten generations. *Dnmt3a*$^{+/-}$ mice were obtained from the Mutant Mouse Regional Resource Centers repository (MMRRC Strain Name B6.129S4-*Dnmt3a*^{tm2Enl}*/Mmnc*). *PR*$^{+/-}$*, Dnmt3a*$^{-/-}$ mice and all control genotypes were produced by intercrossing *PR*$^{+/-}$*, Dnmt3a*$^{+/-}$ mice. *Dnmt3b* flox/flox mice in the B6 background (B6.129S4(Cg)-Dnmt3btm5.1Enl/Mmnc) were obtained from the Mutant Mouse Regional Resource Center at UNC. *Vav1-Cre* mice in the B6 strain were obtained from the Jackson Laboratory (B6.CG-TG(VAV1-CRE)A2KIO/J). Whenever possible, littermate controls were used for all experiments. .

Bone Marrow Harvest and Transplantation

Bone marrow was harvested from femurs, tibias, pelvi, and humeri of 2 to 2.5-week-old mice. After lysis of red blood cells (ACK buffer: 0.15 M NH4Cl, 10 mM KHCO3, 0.1 mM Na2EDTA), cells were washed with FACS buffer, filtered through 50-µm cell strainers (Partec) and resuspended in PBS at 1 million cells/100 uL for transplantation. For competitive transplant experiments, bone marrow was mixed 50:50 with freshly harvested cells from 6-week-old Ly5.1 mice (The Jackson Laboratory, Bar Harbor, ME). Transplantation was performed by retro-orbital injection of 1×10^6 total bone marrow cells into lethally irradiated Ly5.2 or Ly5.1x5.2 recipients that had received 2 split doses of 550 cGy total body irradiation spaced at 4 hours (Mark 1 Cesium-137 irradiator, JL Shepherd) 24 hours prior to transplantation.

Mouse Analysis and Tumor Watch

Peripheral blood counts were assessed at regular intervals as indicated by automated CBC (Hemavet 950, Drew Scientific Group). For long-term tumor watch experiments, bone marrow transplant recipients were monitored daily and animals displaying signs of illness (lethargy, hunched posture, ruffled fur, dyspnea, or pallor) were euthanized and spleen and bone marrow harvested for analysis. Diagnosis of leukemia was made by light microscopic examination of spleen and/or peripheral blood cells according to the Bethesda criteria (48) and previously published phenotyping of the *Ctsg-PML-RARA* and *MLL-AF9* viral transduction mouse models. Cytospin tissue slides were stained with Wright-Giemsa stain (Sigma-Aldrich) and were imaged using a Nikon MICROPHOT-SA microscope equipped with an oil-immersion 50×/0.90 or 100×/1.30 objective lens (Nikon Corp.) The tumor watch was terminated at one year post-transplantation.

MSCV Vectors

Full-length human *DNMT3A* (NM_175629) and *DNMT3B* (NM_006892) cDNAs (Origene) were cloned into MSCV IRES YFP or MSCV IRES GFP (Addgene) using PCR-introduced EcoRI restriction digest sites and standard ligation techniques. *DNMT3A* R882H and Q615* mutations were introduced using QuikChange II XL mutagenesis kit (Agilent). *PML-RARA* cDNA was prepared from the BCR3 *PML-RARA* cDNA used to create the *Ctsg-PML-RARA* mouse and cloned into MSCV-IRES-YFP as

described above. MSCV *MLL-AF9*-IRES-GFP and MSCV *RUNX1-RUNX1T1*-IRES-GFP vectors were the kind gifts of Dr. Andy Lane. Virus was produced using co-transfection of MSCV vector and EcoPak packaging plasmid (Addgene) into 293T cells, using standard calcium-phosphate transfection, and then harvested at 48 hours post-transfection and stored at -80°C. For transduction of mouse bone marrow, marrow was harvested as above and plated overnight in transplant media containing RPMI +15% FBS + SCF (100 ng/mL), Il-3 (10 ng/mL), FLT-3 (50 ng/mL) and TPO (10 ng/mL). All cytokines were purchased from PeproTech. Cells were transduced by spinfection at 2500 RPM for 90 minutes at 30 degrees in transplant media with the addition of 1M HEPES Buffer/0.85% sodium chloride supplemented with polybrene (10 ug/mL, American Bioanalytical). After two rounds of spinfection, GFP- or YFP-positive cells were sorted using an I-Cyt Synergy II sorter (I-cyt Technologies) and plated in methocellulose for colony formation assays.

Methylcellulose Colony Formation Assay

10,000 cells per plate were plated in triplicate in M3534 MethoCult media containing Il-3, Il-6, and SCF (Stem Cell Technologies) and incubated at 37°C for one week. Each week, clusters of cells meeting the morphologic criteria for CFU-GEMM, CFU-GM, CFU-G, or CFU-M (http://www.stemcell.com/~/media/Technical%20Resources/8/3/E/9/0/28405_methocult%20M.pdf?la=en) were counted as myeloid colonies and cells were lifted using warm DMEM media + 2% FBS, spun down, and replated as before. An aliquot of cells was taken for analysis of myeloid markers by flow cytometry.

Methylation Capture Sequencing

Whole bone marrow was isolated from 2 to 2.5-week-old mice (n=3 per genotype) and transplanted into lethally irradiated wild-type mice and allowed to stably engraft for 8-10 weeks before whole marrow was harvested and DNA isolated using QiaAmp DNA Mini Kit (Qiagen). 12 ug of input DNA from each sample was processed with the SureSelectXT Methyl-Seq Target Enrichment System for the Illumina Multiplexed Sequencing protocol (Agilent Technologies, Santa Clara, CA). DNA was subsequently fragmented using a Covaris S2 (Covaris Inc., Woburn, MA) with the following settings: Duty Cycle: 10%, Intensity: 5, Cycles per Burst: 200, Cycles: 6, Time/Cycle: 6 seconds. Library preparation followed the SureSelect Methyl-Seq Library Prep Kit (Agilent Technologies, Santa Clara, CA) with minor modifications. After end-repair, the DNA was purified using Ampure-XP kit (Beckman-Coulter, Brea, CA) and was recovered in 80µL 10mM Tris-HCl, pH 7.8. Samples were subsequently divided into four A-tailing and adapter ligation reactions following the manufacturer's recommendations for 3µg of input DNA. Post-ligation, all four reactions for each sample were pooled and processed for hybridization using the SureSelect Methyl-Seq Target Enrichment and Methyl-Seq Hybridization Kits (Agilent Technologies, Santa Clara, CA). In the hybridization reactions, we combined the SureSelect Indexing Block #1 and #2 oligonucleotides with 5µg of Mouse C_0t-1 DNA (Invitrogen, Carlsbad, CA). The hybridized probe:library fragment duplexes were immobilized with streptavidin-bound paramagnetic M280 particles (Invitrogen, Carlsbad, CA). The hybridized (captured) ssDNA library fragments were eluted from their duplexes and neutralized using the supplied elution and

neutralization buffers, respectively. The methyl-captured fragments were bisulfite-converted using the DNA Methylation Gold Kit (Zymo Research, Irvine, CA), and the converted ssDNA library fragments were amplified, 8 cycles, with non-indexed primers as described in the manufacturer's protocol. A subsequent amplification incorporated library-specific index sequences during the PCR. The final library amplifications were treated with 0.8:1.0 ratio for AmpureXP beads-to-DNA, eluted with 20µl 10mM Tris-HCl (pH 7.8), quantified by Qubit (Invitrogen, Carlsbad, CA), and sized with the DNA 1000 Chip Kit (Agilent Technologies, Santa Clara, CA) for a molarity determination. All four samples were diluted to 5nM, assayed by qPCR, and based on qPCR results diluted to a 2nM solution. Each 2nM sample was mixed at equal volumes, and the 2nM pool was sequenced, 2x100 bp, across four lanes of an Illumina HS2000 flow cell using V3 chemistry. BSMAP version 1.037 was used to align the bisulfite sequencing reads. Methylation ratios per base were calculated via methratio.py script. The methylation ratios were read into Methylkit package in R to generate coverage and methylation statistics, sample correlation, clustering, and differential methylation analysis. The datasets for the CpG-capture experiments are deposited in the Short Read Archive, with accession number PRJNA283621; the Superseries ID that links the methylation and expression data for this study is Umbrella BioProject PRJNA284138.

Expression profiling

Expression array profiling was performed exactly as described (30). Labeled RNA targets were hybridized to Mouse Exon 1.0 ST arrays (Affymetrix), washed, stained, and

scanned using standard protocols from the Siteman Cancer Center, Molecular and Genomic Analysis Core Facility (http://pathology.wustl.edu/research/cores/lcg/index.php).

Affymetrix CEL files were imported into Partek Genomics Suite™ 6.6 (Partek Inc., St. Louis, MO). Probe-level data were pre-processed, including background correction, normalization, and summarization, using robust multi-array average (RMA) analysis. RMA adjusts for background noise on each array using only the PM probe intensities; and subsequently normalizes data across all arrays using quantile normalization (49,50) followed by median polish summarization to generate a single measure of expression (50). Data was filtered to include only core probesets having raw expression signal greater than 100 in all samples in order to limit the analysis within well-annotated exons.

The Analysis of Variance (ANOVA) and multi-test correction for p-values in Partek Genomic Suite were used to identify differentially expressed genes. Sample genotypes (WT; $PR^{+/-}$; $PR^{+/-}$, $Dnmt3a^{-/-}$; and $Dnmt3a^{-/-}$) were chosen as the candidate variables in the ANOVA model to obtain genotype-specific expression changes. ANOVA p-values were corrected using the Bonferroni method. The list of genes with significant variation in expression level was generated by using a fold change of 2 and a 0.05 FDR criterion as a significant cutoff.

Exon array data for all samples used in this study have been deposited on GEO (http://www.ncbi.nlm.nih.gov/geo/: accession number GSE68844).

HpaII qPCR Assay

DNA was isolated from MethoCult-plated cells after 1 week in MethoCult M3534 media, and genomic DNA was isolated using QiAmp mini kit (Qiagen). 500 ng of genomic DNA was digested with 0.5 uL (5 units) of HpaII enzyme (New England Biolabs) or mock (water) for 90 minutes at 37^{o} C, then heat inactivated at 80^{o} C for 20 minutes. 1.5 microliters of each 30 microliter digest (25 ng gDNA) was amplified using KAPA SYBR FAST qPCR Kit (KapaBiosystems) and PCR primers (IDT). Four amplified regions were selected based on our methylation capture sequencing showing hypomethylation in *Dnmt3a*$^{-/-}$ vs. wild-type cells, and ~200BP amplicons were designed containing HpaII recognition sites (CCGG) using Primer3 software. Each sample was assayed in triplicate. The percentage methylation was calculated at $2^{-\text{delta Ct}}$ where delta Ct is Ct(HpaII digested)-Ct(undigested).

Western Blotting

For blotting of whole embryos, E18 embryos were snap frozen in liquid nitrogen and homogenized with mortar and pestle before lysis in RIPA buffer (50mM Tris pH 8.0, 150 mM NaCl, 0.1% SDS, 0.5% sodium deoxycholate, 1% NP-40) supplemented with protease inhibitor cocktail (Sigma Aldrich). For blotting of retrovirus-transduced bone marrow cells, 250,000 cells were rinsed with PBS and resuspended in urea lysis buffer (7M urea, 2M thiourea, 30mM Tris pH 8.5) supplemented with protease inhibitor cocktail and snap-frozen in liquid nitrogen. Lysates were boiled in 6X SDS loading dye (0.01M

Tris HCl pH 6.8, 8% glycerol, 0.1 mg/ml bromophenol blue, 2% SDS, 1% Beta-mercaptoethanol) for 5 minutes at 95 degrees. Lysates were separated on a 10% SDS-PAGE gel and transferred onto Hybond C Extra nitrocellulose membrane (Amersham). The membrane was probed with an anti-Dnmt3A antibody (1:2000; Cell Signaling, #2160), anti-Dnmt3B antibody (1:2000, Santa Cruz, sc-10236) or anti-αActin (1:5000; Millipore). Immune complexes were revealed by peroxidase-conjugated anti-mouse IgG (1:10,000; GE) or conjugated anti- rabbit IgG (1:2,500; GE) and visualized by chemiluminescence (GE).

Cell Staining and Flow Cytometry

After ACK lysis of red blood cells, peripheral blood, bone marrow,or spleen cells were treated with anti-mouse CD16/32 (clone 93, eBioscience) and stained with the indicated combinations of the following antibodies (all antibodies are from eBioscience unless indicated, see Supplemental Table 6): CD34 FITC (RAM34), CD11b PE or APC-e780 (M1/70), c-kit PerCP-Cy5.5 or APC-e780 (2B8), CD115 APC or PE (AFS98), Gr-1 Pacific-blue (Invitrogen, RM3028), Gr-1 biotin (RB6-8C5), B220 PE, APC, or biotin (RA3-6B2), CD3 e450 or PE (145-2C11), CD71 PE(R17217), Ter-119 Pacific-blue (TER-119), CD16/32 APC (93), Flk2 APC (A2F10). Analysis was performed using a FACScan (Beckman Coulter) or I-Cyt Synergy II sorter (I-cyt Technologies), and data analyzed using FlowJo (Tree Star), Excel (Microsoft), and Prism 5 (Graphpad).

Statistics

All statistical comparisons were made using GraphPad Prism 5 software, except for statistics on sequencing data, which were calculated using the R statistical programming software as described above. Statistical tests employed and significance cut-offs are detailed in each figure legend. When used, Student's T-test was two-tailed and a p value of less than 0.05 was considered significant. All data represent mean plus/minus the standard error of the mean unless indicated.

Study Approval

All mouse procedures were done in accordance with institutional guidelines and approved by the Animal Studies Committee at Washington University in accordance with current NIH policies.

2.6 Acknowledgements

This work was supported by NIH grants CA083962 and CA101937 and the Barnes-Jewish Hospital Foundation grant 00335-0505-02 to T.J. L. The Siteman Cancer Center High Speed Cell Sorter Core was of invaluable assistance, and is supported in part by an NCI Cancer Center Support Grant, P30 CA91842. The Microarray Core is supported by National Center for Research Resources grant UL1 RR024992.

2.7 References

1. Cancer Genome Atlas Research Network. Genomic and epigenomic landscapes of adult de novo acute myeloid leukemia. *N Engl J Med*. 2013;368(22):2059–74.

2. Ley T, Ding L, Walter M. DNMT3A mutations in acute myeloid leukemia. *N Engl J Med.* 2010; 363(25): 2424-33.

3. Challen GA, Sun D, Jeong M, et al. Dnmt3a is essential for hematopoietic stem cell differentiation. *Nat Genet*. 2012;44(1):23–31.

4. Yang L, Rau R, Goodell MA. DNMT3A in haematological malignancies. *Nat Rev Cancer*. 2015;15(3):152–65.

5. Challen GA, Sun D, Mayle A, et al. Dnmt3a and Dnmt3b Have Overlapping and Distinct Functions in Hematopoietic Stem Cells. *Cell Stem Cell*. 2014;15(3):350–64.

6. Russler-Germain DA, Spencer DH, Young MA, et al. The R882H DNMT3A mutation associated with AML dominantly inhibits wild-type DNMT3A by blocking its ability to form active tetramers. *Cancer Cell*. 2014;25(4):442–54.

7. Kim SJ, Zhao H, Hardikar S, Singh AK, Goodell MA, Chen T. A DNMT3A mutation common in AML exhibits dominant-negative effects in murine ES cells. *Blood*. 2013;122(25):4086–9.

8. Grisolano JL, Wesselschmidt RL, Pelicci PG, Ley TJ. Altered myeloid development and acute leukemia in transgenic mice expressing PML-RARalpha under control of cathepsin G regulatory sequences. Blood 1997;89(2):376-87.

9. Brown D, Kogan S, Lagasse E, et al. A PML-RARalpha transgene initiates murine acute promyelocytic leukemia. Proc Natl Acad Sci USA. 1997;94(6):2551-56.

10. He LZ, Tribioli C, Rivi R, Peruzzi D, et al. Acute leukemia with promyelocytic features in PML/RARalpha transgenic mice. Proc Natl Acad Sci USA. 1997;94:5302-07.

11. Kogan SC. Mouse models of acute promyelocytic leukemia. Curr Top Microbiol Immunol. 2007;313:3-29.

12. Westervelt P, Lane AA, Pollock JL, et al. High-penetrance mouse model of acute promyelocytic leukemia with very low levels of PML-RARalpha expression. *Blood*. 2003;102(5):1857–65.

13. Minucci S, Monestiroli S, Giavara S, et al. PML-RAR induces promyelocytic leukemias with high efficiency following retroviral gene transfer into purified murine hematopoietic progenitors. *Blood*. 2002;100(8):2989–95.

14. Kamashev D, Vitoux D, De Thé H. PML-RARA-RXR oligomers mediate retinoid and rexinoid/cAMP cross-talk in acute promyelocytic leukemia cell differentiation. *J Exp Med*. 2004;199(8):1163–74.

15. Hong SH, David G, Wong CW, Dejean A, Privalsky ML. SMRT corepressor interacts with PLZF and with the PML-retinoic acid receptor alpha (RARalpha) and PLZF-RARalpha oncoproteins associated with acute promyelocytic leukemia. *Proc Natl Acad Sci U S A*. 1997;94(17):9028–33.

16. Villa R, Morey L, Raker VA, et al. The methyl-CpG binding protein MBD1 is required for PML-RARalpha function. *Proc Natl Acad Sci U S A*. 2006;103(5):1400–5.

17. Lin RJ, Nagy L, Inoue S, Shao W, Miller WH, Evans RM. Role of the histone deacetylase complex in acute promyelocytic leukaemia. *Nature*. 1998;391(6669):811–4.

18. Fazi F, Travaglini L, Carotti D, et al. Retinoic acid targets DNA-methyltransferases and histone deacetylases during APL blast differentiation in vitro and in vivo. *Oncogene*. 2005;24(11):1820–30..

19. Datta J, Majumder S, Bai S, et al. Physical and functional interaction of DNA methyltransferase 3A with Mbd3 and Brg1 in mouse lymphosarcoma cells. *Cancer Res*. 2005;65(23):10891–900.

20. Morey L, Brenner C, Fazi F, et al. MBD3, a component of the NuRD complex, facilitates chromatin alteration and deposition of epigenetic marks. *Mol Cell Biol*. 2008;28(19):5912–23.

21. Boukarabila H, Saurin AJ, Batsché E, et al. The PRC1 Polycomb group complex interacts with PLZF/RARA to mediate leukemic transformation. *Genes Dev*. 2009;23(10):1195–206.

22. Villa R, Pasini D, Gutierrez A, et al. Role of the polycomb repressive complex 2 in acute promyelocytic leukemia. *Cancer Cell*. 2007;11(6):513–25.

23. Di Croce L, Raker V a, Corsaro M, et al. Methyltransferase recruitment and DNA hypermethylation of target promoters by an oncogenic transcription factor. *Science*. 2002;295(5557):1079–82.

24. Martens JHA, Brinkman AB, Simmer F, et al. PML-RARalpha/RXR Alters the Epigenetic Landscape in Acute Promyelocytic Leukemia. *Cancer Cell*. 2010;17(2):173–85.

25. Wang K, Wang P, Shi J, et al. PML/RARalpha targets promoter regions containing PU.1 consensus and RARE half sites in acute promyelocytic leukemia. *Cancer Cell*. 2010;17(2):186–97.

26. Okano M, Bell DW, Haber DA, Li E. DNA methyltransferases Dnmt3a and Dnmt3b are essential for de novo methylation and mammalian development. *Cell*. 1999;99(3):247–57.

27. Jeong M, Sun D, Luo M, et al. Large conserved domains of low DNA methylation maintained by Dnmt3a. *Nat Genet*. 2014;46(1):17–23.

29. Steffen B, Knop M, Bergholz U, et al. AML1/ETO induces self-renewal in hematopoietic progenitor cells via the Groucho-related amino-terminal AES protein. *Blood*. 2011;117(16):4328–37.

29. Chen W, Kumar AR, Hudson WA, et al. Malignant transformation initiated by Mll-AF9: gene dosage and critical target cells. *Cancer Cell*. 2008;13(5):432–40.

30. Wartman LD, Welch JS, Uy GL, et al. Expression and Function of PML-RARA in the Hematopoietic Progenitor Cells of Ctsg-PML-RARA Mice. *PLoS One*. 2012;7(10):e46529.

31. Jurkowska RZ, Jurkowski TP, Jeltsch A. Structure and function of mammalian DNA methyltransferases. *Chembiochem*. 2011;12(2):206–22.

32. Li H, Rauch T, Chen Z-X, Szabó PE, Riggs AD, Pfeifer GP. The histone methyltransferase SETDB1 and the DNA methyltransferase DNMT3A interact directly and localize to promoters silenced in cancer cells. *J Biol Chem*. 2006;281(28):19489–500.

33. Wienholz BL, Kareta MS, Moarefi AH, Gordon CA, Ginno PA, Chédin F. DNMT3L modulates significant and distinct flanking sequence preference for DNA methylation by DNMT3A and DNMT3B in vivo. *PLoS Genet*. 2010;6(9):e1001106.

34. Jin B, Ernst J, Tiedemann RL, et al. Linking DNA methyltransferases to epigenetic marks and nucleosome structure genome-wide in human tumor cells. *Cell Rep*. 2012;2(5):1411–24.

35. Dodge JE, Okano M, Dick F, et al. Inactivation of Dnmt3b in mouse embryonic fibroblasts results in DNA hypomethylation, chromosomal instability, and spontaneous immortalization. *J Biol Chem*. 2005;280(18):17986–91.

36. Georgiades P, Ogilvy S, Duval H, et al. VavCre transgenic mice: a tool for mutagenesis in hematopoietic and endothelial lineages. *Genesis*. 2002;34(4):251–6.

37. Dodge JE, Okano M, Dick F, et al. Inactivation of Dnmt3b in Mouse Embryonic Fibroblasts Results in DNA Hypomethylation, Chromosomal Instability, and Spontaneous Immortalization. *J Biol Chem.* 2005; 280(18):17986-91

38. Welch JS, Yuan W, Ley TJ. PML-RARA can increase hematopoietic self-renewal without causing a myeloproliferative disease in mice. 2011;121(4).

39. Mayle A, Yang L, Rodriguez B, et al. Dnmt3a loss predisposes murine hematopoietic stem cells to malignant transformation. Blood. 2015;125(4):629-38.

40. Wojiski S, Guibal FC, Kindler T, et al. PML-RARalpha initiates leukemia by conferring properties of self-renewal to committed promyelocytic progenitors. Leukemia 2009;23(8):1462-71.

41. Trowbridge JJ, Snow JW, Kim J, Orkin SH. DNA methyltransferase 1 is essential for and uniquely regulates hematopoietic stem and progenitor cells. *Cell Stem Cell*. 2009;5(4):442–9.

42. Trowbridge JJ, Sinha AU, Zhu N, Li M, Armstrong SA, Orkin SH. Haploinsufficiency of Dnmt1 impairs leukemia stem cell function through derepression of bivalent chromatin domains. *Genes Dev*. 2012;26(4):344–9.

43. Liu S, Shen T, Huynh L, et al. Interplay of RUNX1/MTG8 and DNA methyltransferase 1 in acute myeloid leukemia. *Cancer Res*. 2005;65(4):1277–84.

44. Lasa A, Carnicer MJ, Aventín A, et al. MEIS 1 expression is downregulated through promoter hypermethylation in AML1-ETO acute myeloid leukemias. *Leukemia*. 2004;18(7):1231–7.

45. Schoofs T, Rohde C, Hebestreit K, et al. DNA methylation changes are a late event in acute promyelocytic leukemia and coincide with loss of transcription factor binding. *Blood*. 2013;121(1):178–87.

46. Rohde C, Schoofs T, Müller-Tidow C. The limited contribution of DNA methylation to PML-RARα induced leukemia. 2013;4(1):5–6.

47. Oka M, Rodić N, Graddy J, Chang L-J, Terada N. CpG sites preferentially methylated by Dnmt3a in vivo. *J Biol Chem*. 2006;281(15):9901–8.

48. Morse HC 3rd, Anver MR, Fredrickson TN, et al. Bethesda proposals for classification of lymphoid neoplasms in mice. Blood 2002;100(1):246-58.

49. Bolstad BM, Irizarry RA, Astrand M, Speed TP. A comparison of normalization methods for high density oligonucleotide array data based on variance and bias. *Bioinformatics*. 2003;19(2):185–93.

50. Irizarry RA, Hobbs B, Collin F, et al. Exploration, normalization, and summaries of high density oligonucleotide array probe level data. *Biostatistics*. 2003;4(2):249–64.

2.8 Figure Legends

Figure 1

Dnmt3a is required for aberrant self-renewal ability conferred by PML-RARA on hematopoietic progenitor cells. (**A**) Design of experiments in (**B)** through (**E).** Bone marrow from 2-2.5 week old mice of the indicated genotypes was transduced with the indicated retroviruses, plated in MethoCult media containing IL-3, IL-6, and SCF, and then replated each week. (**B)** A YFP-expressing control vector does not induce replating in WT or *Dnmt3a*$^{-/-}$ cells. **(C)-(D)** *Dnmt3a* is unnecessary for aberrant self-renewal driven by retroviruses expressing *MLL-AF9* **(C)** or *RUNX1-RUNX1T1 (AML-ETO).(***D**). **E)** Loss of *Dnmt3a* eliminates replating driven by a *PML-RARA*-containing retrovirus. **(F)** Representative flow cytometry plots for the myeloid markers Gr-1 and CD11b for week 1 vs. week 4 of replating. (**G)** Flow data for CD11b positivity week 4 of replating, demonstrating loss of myeloid cells in *Dnmt3a*$^{-/-}$ marrow transduced with *PML-RARA.* *N*=3-6 for all experiments. **P*<0.05, *** *P*<0.001 by two-tailed unpaired t-test.

Figure 2

Dnmt3a is required for aberrant self-renewal ability of PML-RARA ("PR") expressing mouse bone marrow cells ex vivo. (**A**) RT-PCR for *PML-RARA* expression in bone marrow cells derived from *Ctsg-PML-RARA* mice (*PR*$^{+/-}$), or *Ctsg-PML-RARA* mice that are also deficient for Dnmt3a (*PR*$^{+/-}$*, Dnmt3a*$^{-/-}$*).* (**B**-**C).** Bone marrow from 2-2.5 week old mice of the indicated genotypes was transplanted into lethally irradiated wild-type recipients in a non-competitive transplant. **(B)** Quantification of cell numbers in the mature myeloid compartment (Gr-1+, left panel) vs. the mature B cell compartment

(B220+, right panel) at ten weeks post-transplant demonstrates ability of *Dnmt3a*$^{-/-}$ donor stem cells to engraft and contribute normally to both myeloid and lymphoid lineages (also see Supplementary Figure S3A). (**C)** Quantification of the indicated progenitor and stem cell compartments shows no significant differences for any genotype at ten weeks post-transplant. (**D-F)** Bone marrow from 2-2.5 week old mice of the indicated genotypes was plated in MethoCult media containing IL-3, IL-6, and SCF, and replated weekly. **(D)** Quantification of colony numbers demonstrates loss of colony formation by *PR*$^{+/-}$*, Dnmt3a*$^{-/-}$ cells. **(E)** Representative flow cytometry for the myeloid markers Gr-1 and CD11b demonstrates loss of myeloid cells from *PR*$^{+/-}$*, Dnmt3a*$^{-/-}$ mice after two weeks of replating in MethoCult media. (**F)** Graph of CD11b positivity over time. *N*=3-6 for all experiments. **P*<0.05, *** *P*<0.001 for *PR*+/- vs. all other genotypes by two-way ANOVA.

Figure 3

Expression analysis of previously identified PML-RARA-dysregulated genes in GMP cells derived from PR$^{+/-}$, PR$^{+/-}$ Dnmt3a$^{-/-}$, and Dnmt3a$^{-/-}$ mice. (**A-B)** Using Affymetrix Mouse Exon 1.0ST arrays, we interrogated gene expression in GMP cells purified from the bone marrow cells of mice transplanted with WT (N=4), *PR*$^{+/-}$ (N=2), *PR*$^{+/-}$*Dnmt3a*$^{-/-}$ (N=4) and *Dnmt3a*$^{-/-}$(N=3) marrow cells, and harvested 6-8 weeks later. **(A)** Mean fold changes for 239 probesets that were previously found to be significantly dysregulated in GMP cells derived from the bone marrow of 6-8 week old *Ctsg-PML-RARA* mice (labeled as *PR*$^{+/-a}$) vs. WT GMP cells (N=4 for each, 30, Supp Table S3). The mean fold changes (compared to WT GMP cells) for the 112 probesets that were

upregulated in the *PR*$^{+/-a}$ are shown in the left panel, and the mean fold changes for the 127 probesets that were downregulated are on the right. Fold changes for the *PR*$^{+/-b}$, *PR*$^{+/-}$ *Dnmt3a*$^{-/-}$, and *Dnmt3a*$^{-/-}$ probesets were calculated by comparing to the WT data from the current set of experimental data. **(B).** Heat map of Z-scored data using the same 239 *PR*$^{+/-}$ dysregulated probesets defined in Wartman et al., and displaying the average values obtained from the arrays generated from GMP purified cells with the designated genotype used in this study. The list of genes with significant variation in expression level was generated by using a fold change of 2 and a FDR criterion of less than or equal to .05.

Figure 4

DNA methyltransferase activity of DNMT3A is required for aberrant self-renewal by PML-RARA ex vivo. (**A**) Schematic of human *DNMT3A* cDNAs used in panels **B** through **E.** Mutations in the methyltransferase domain (MTase) from AML patients induce loss of catalytic function (R882H, red arrow) or lack the methyltransferase domain altogether (Q615*, black arrow) (**B**) Western blot from *PR*$^{+/-}$ or *PR*$^{+/-}$*, Dnmt3a*$^{-/-}$ bone marrow cells transduced with retroviruses containing human *DNMT3A* cDNAs and IRES-YFP, and then sorted for YFP+ cells. Cells were harvested after one week in MethoCult medium. The positions of full length and truncated DNMT3A are indicated on the right. **(C)** Bone marrow from 2-3 week old mice was transduced with the indicated viruses, and GFP+ cells were sorted and serially replated in MethoCult medium. Week 4 colony numbers demonstrate that only wild-type *DNMT3A* with intact DNA methyltransferase activity is able to restore colony formation to *PR*$^{+/-}$*, Dnmt3a*$^{-/-}$ myeloid cells. (**D)** Flow cytometry of week 4 Methocult cells demonstrates persistence of

CD11b expression in *PR*$^{+/-}$*, Dnmt3a*$^{-/-}$ cells, conferred only by wild-type *DNMT3A.* (**E)** Graph of CD11b expression percentages at four weeks of serial replating in MethoCult medium**. (F)** Assay of methylation at a specific HpaII site in the *Runx1* locus that is dependent on Dnmt3a for methylation in wild-type bone marrow cells (Site 1 in Supplemental Figure S1E). Re-expression of WT, full length *DNMT3A* by retroviral transduction restores a normal level of methylation to these sites after seven days in MethoCult media. Retroviruses containing mutant *DNMT3A* (R882H or Q615*) did not restore methylation at this site. *N*=3-4 for all experiments. N.S. Not statistically significant by two-way ANOVA, **P*<0.05, ***P*<0.005, ****P*<0.001.

Figure 5

Dnmt3b is not required for the aberrant self-renewal ability conferred by PML-RARA in mouse bone marrow progenitor cells. (**A**) Design of experiments in (**B)** through (**D).** Bone marrow from 2-2.5 week old mice of the indicated genotypes was plated in MethoCult media containing IL-3, IL-6, and SCF and replated each week. **B)** Quantification of colony numbers demonstrates no difference in colony formation in *PR*$^{+/-}$*, Dnmt3b* $^{fl/fl}$ cells with or without *Vav-Cre*. **(C)** Representative flow cytometry for the myeloid markers Gr-1 and CD11b after week 6 MethoCult replating demonstrates that self-renewal of myeloid cells from *PR*$^{+/-}$ mice is not dependent on *Dnmt3b*. (**D)** Graph of CD11b positivity over time. (**E)** Design of experiment in **(F).** Marrow from 2-2.5 week old mice of the indicated genotypes was retrovirally transduced with MSCV vectors containing WT *DNMT3B-IRES-YFP* or *YFP* only, and then sorted for YFP positive cells and plated in MethoCult media as in (**A).** (**F)** Quantification of colony numbers at week 4 illustrates that overexpression of *DNMT3B* is not able to rescue

aberrant self-renewal in *PR*$^{+/-}$, *Dnmt3a*$^{-/-}$ bone marrow cells. *N*=3-6 for all experiments. N.S. Not statistically significant by two-tailed unpaired t-test, **P*<0.05.

Figure 6

Dnmt3a is dispensable for leukemia induced by MLL-AF9 overexpression. (**A**) Design of experiments in **B** through **E.** Bone marrow from 2-3 week old mice of the indicated genotypes was harvested and transduced with an *MLL-AF9* expressing retrovirus before transplantation into lethally irradiated wild-type mice. (**B**) White blood cell counts at 28 days post-transplant demonstrate an equal degree of leukocytosis in recipients of *MLL-AF9*-transduced *WT* and *Dnmt3a*$^{-/-}$ bone marrow. (**C)** Spleen weights of moribund animals were not significantly different regardless of Dnmt3a status. (**D)** *MLL-AF9* was able to initiate lethal leukemia with 100 percent penetrance and equal latency using bone marrow cells with or without *Dnmt3a* (n = 11 for WT + *MLL-AF9*, n=9 for *Dnmt3a-/-* + *MLL-AF9*). N.S. Not significant by two-tailed unpaired t-test.

Figure 7

Dnmt3a is required for the competitive repopulation advantage conferred by PML-RARA, and its ability to induce APL in vivo. **(A)** Design of competitive transplant experiments in (B)-(E), where marrow from 2-2.5 week old mice of the indicated genotypes was mixed with wild-type competitor marrow and transplanted into lethally irradiated recipients (week zero) for monitoring of relative contribution to peripheral blood cells, bone marrow and spleen (n=4-21 per genotype). (**B)** Flow cytometry at the indicated weeks post-transplant demonstrates that the competitive advantage for *PR*$^{+/-}$ bone marrow in contributing to peripheral blood cells is completely abrogated in *PR*$^{+/-}$,

Dnmt3a$^{-/-}$ bone marrow, and that *Dnmt3a*$^{-/-}$ and *PR*$^{+/-}$*, Dnmt3a*$^{-/-}$ bone marrow cells have a competitive disadvantage versus wild-type marrow cells in this assay. (**C)** Examination of chimerism in bone marrow and spleen at six months after transplantation indicates a decreased contribution of *PR*$^{+/-}$*, Dnmt3a*$^{-/-}$ marrow compared to *PR*$^{+/-}$ marrow in both compartments**.** (**D**) Characterization of the stem/progenitor compartments in chimeric mice 10 weeks after competitive transplantation. The composition of all compartments is the same for both genotypes, except that PR+/-, Dnmt3a-/- donors displayed a significantly increased contribution to the long-term hematopoietic stem cell compartment. (**E**) Quantification of myeloid progenitor compartments demonstrates no significant differentiation biases in either genotype. (**F**) Long-term tumor watch of WT animals transplanted with *PR*$^{+/-}$ or *PR*$^{+/-}$*, Dnmt3a*$^{-/-}$ bone marrow demonstrated that 6/16 recipients of *PR*$^{+/-}$ and 0/13 recipients of *PR*$^{+/-}$, *Dnmt3a*$^{-/-}$ bone marrow had succumbed to APL at one year post-transplant (*P* = 0.0336 by Mantel-Cox Test). N.S. No differences between any two genotypes were statistically significant by two-way ANOVA, ***P*<0.005, ****P*<0.001 by two-way ANOVA.

Figure 1

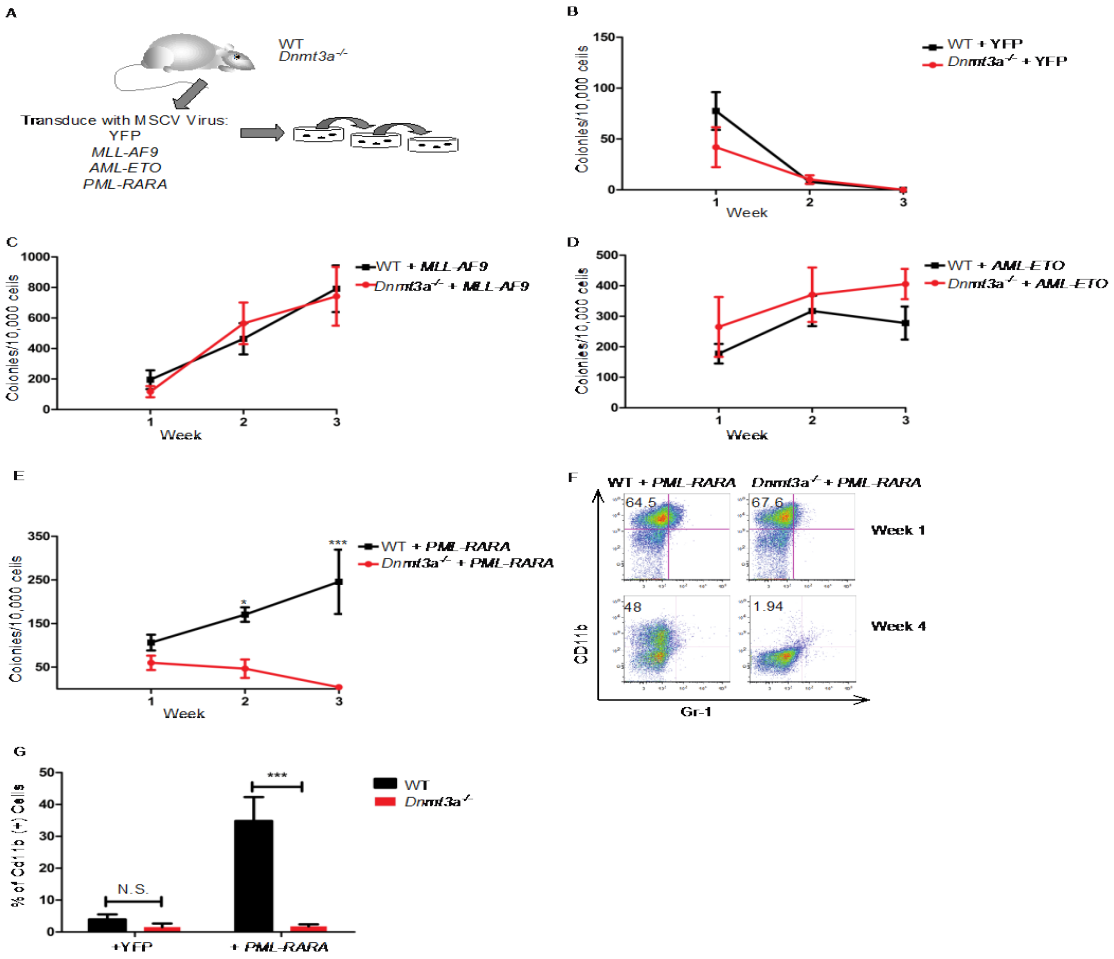

Figure 2

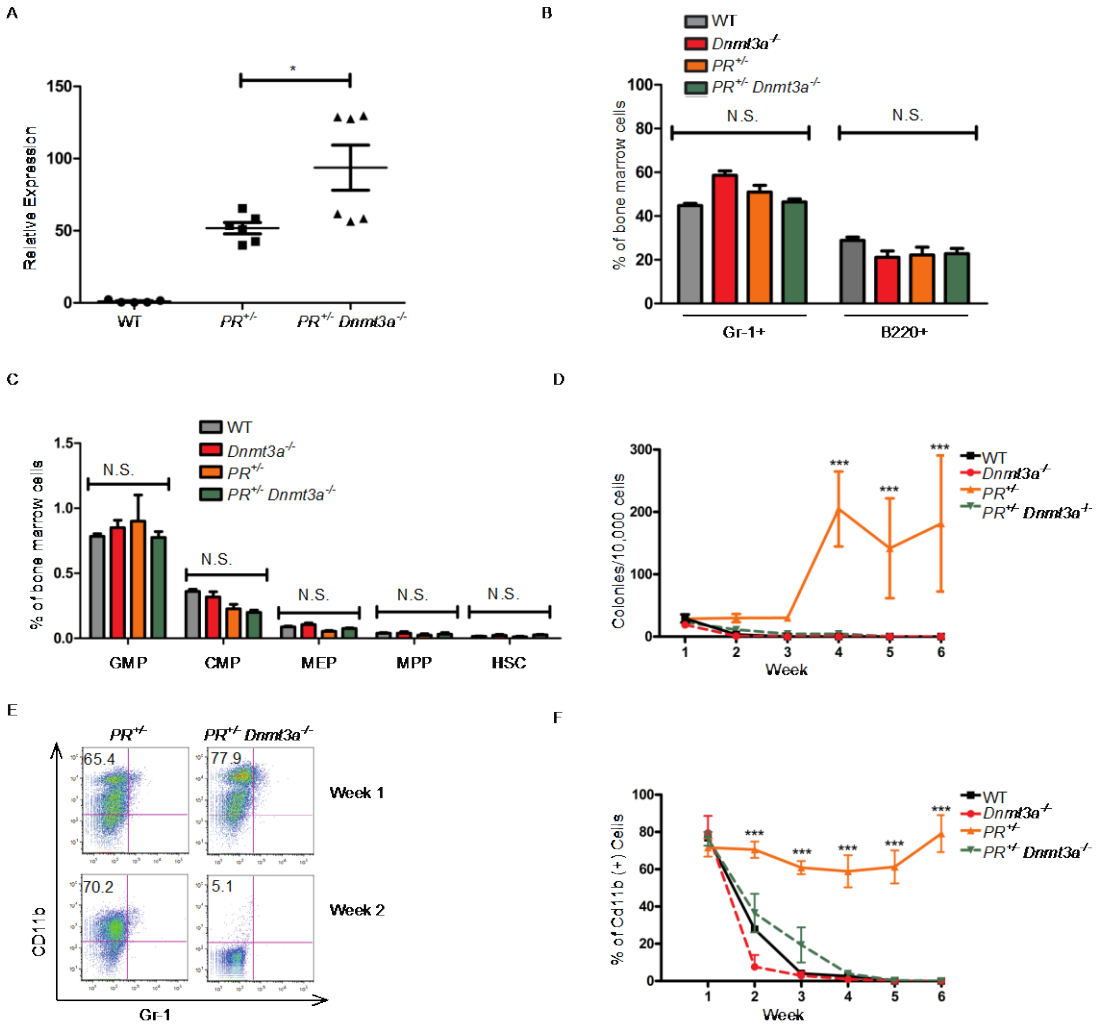

Figure 3

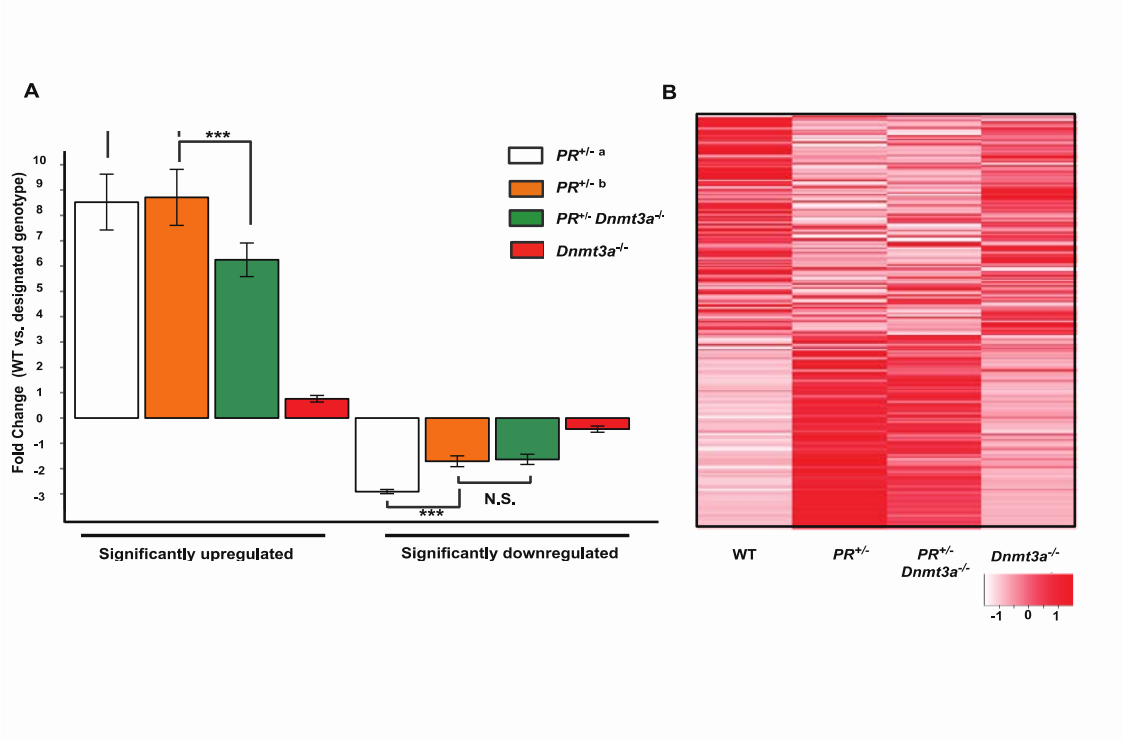

Figure 4

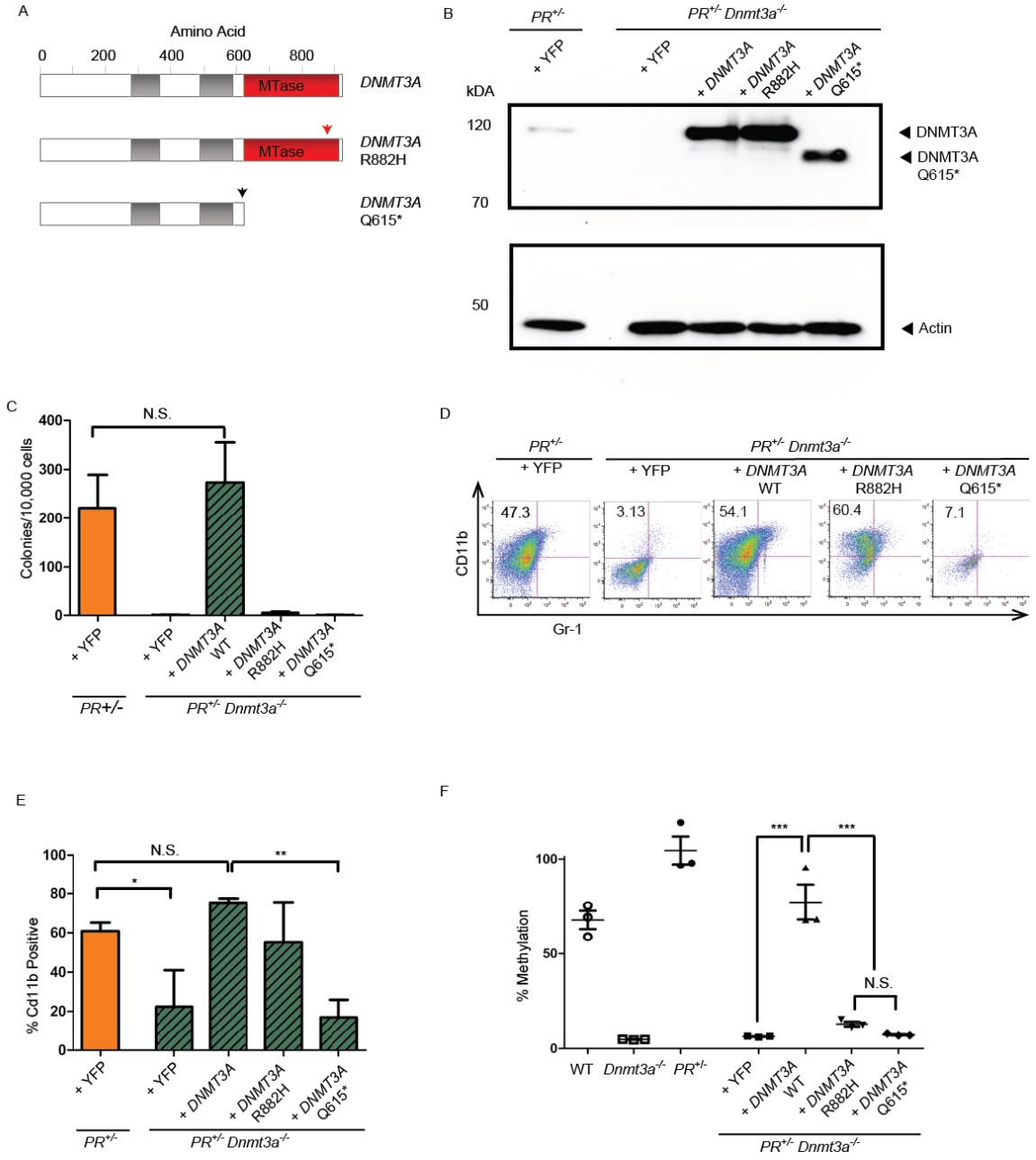

Figure 5

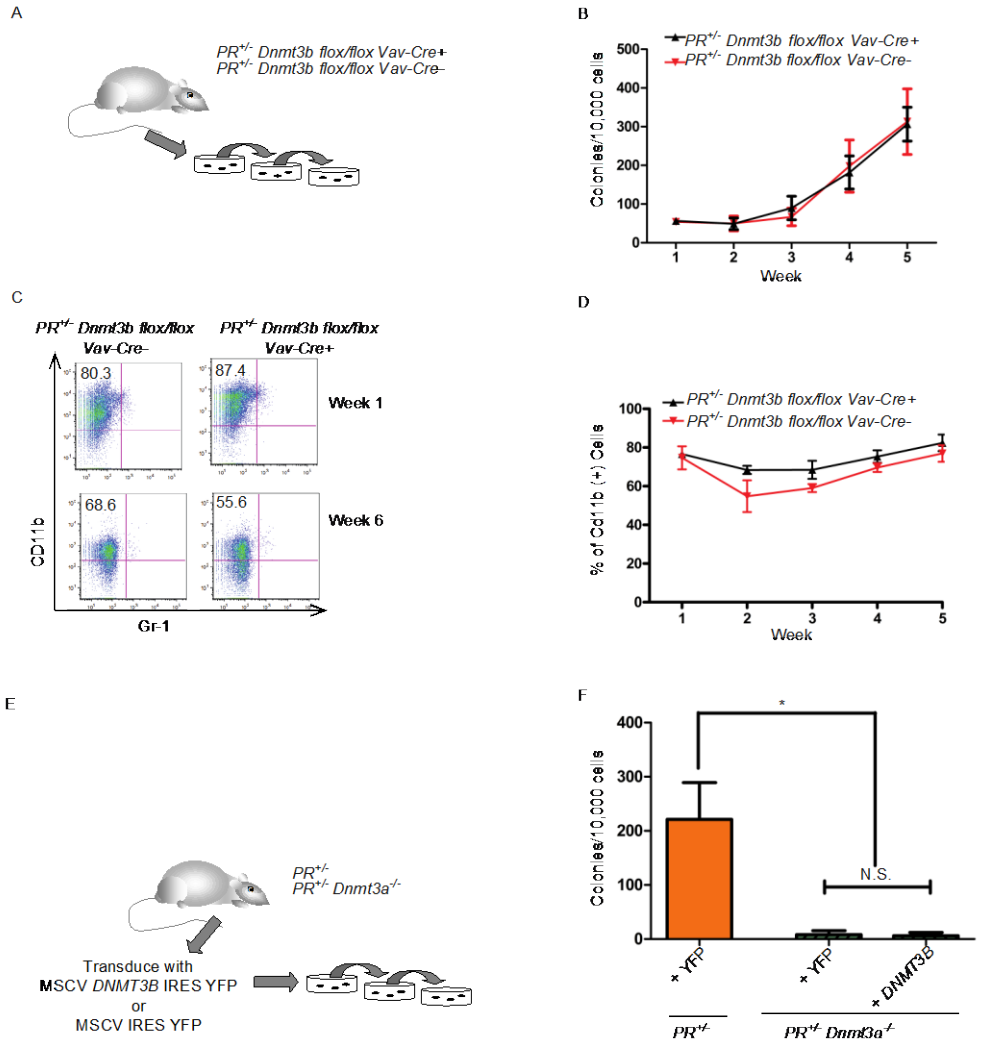

Figure 6

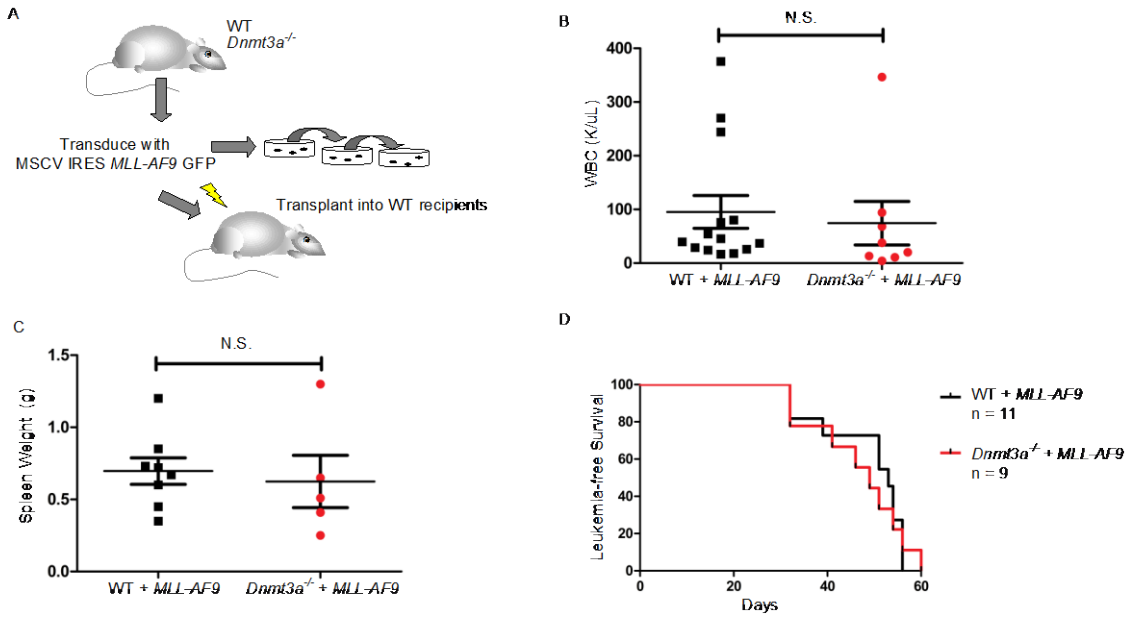

Figure 7

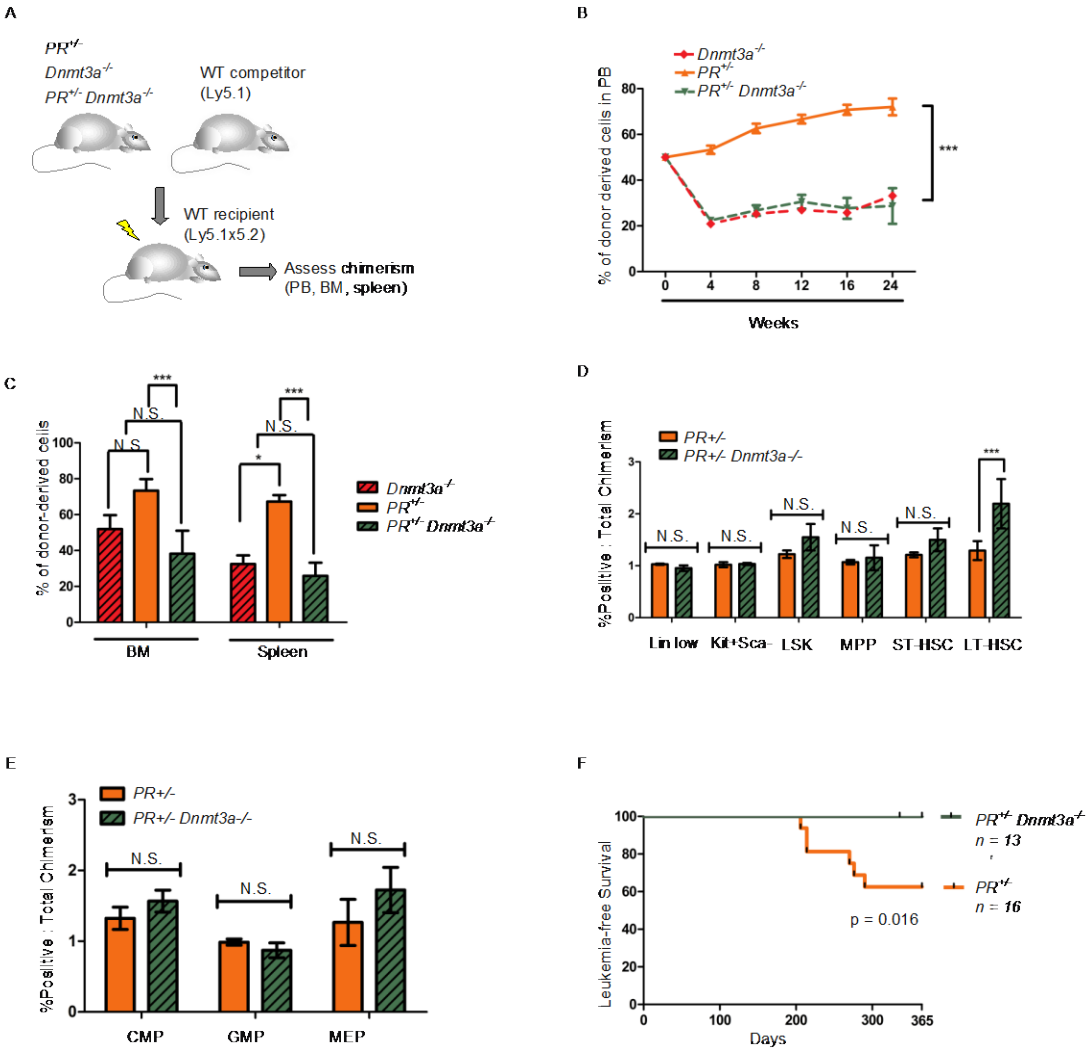

Chapter 3

Myeloproliferation and Myeloid Leukemia in *Dnmt3a+/-* Mice

3.1 Abstract

Recent whole genome sequencing efforts by our group and others have identified recurrent mutations in the DNA methyltransferase *DNMT3A* in various hematologic malignancies, including acute myeloid leukemia (AML), MPN, MDS, CMML, and T-ALL. The most common point mutation in AML, R882H, is nearly always heterozygous in AML, and has been demonstrated to reduce enzyme activity by ~80%; the mutant protein also exerts a potent dominant negative effect on the methylation activity of the wild-type protein. However, other heterozygous mutations produce frameshifts, premature stop codons, or deletions of the entire coding sequence of the gene, strongly suggesting that these mutations lead to simple haploinsufficiency for DNMT3A. To test the hypothesis that *Dnmt3a* haploinsuffiency may initiate AML, we performed a long-term tumor watch comparing wild-type mice (*Dnmt3a+/+)* to mice carrying one wild-type *Dnmt3a* allele and one targeted allele that contains a neomycin-resistance cassette inserted into the sequence coding for the catalytic domain of the protein, producing a true null allele (*Dnmt3a+/-* mice). At 6 weeks of age, *Dnmt3a+/-* mice have normal hematopoiesis, with no detectable differences from wild-type littermates in myeloid, lymphoid, erythroid, or stem/progenitor populations in the bone marrow or spleen. However, after 1.5 years of age, 15/43 *Dnmt3a+/-* mice (35%) became moribund and were euthanized for pathologic evaluation. Affected mice generally exhibited massive splenomegaly with myeloid infiltration of the spleen, liver, and other extramedullary organs. At the conclusion of the tumor watch at two years, all remaining mice were euthanized, and similar pathologic findings were observed in an additional 9 *Dnmt3a+/-* mice, for an overall disease penetrance of 24/43 (56%). In contrast, 0/20 WT littermate control animals developed myeloid malignancies over the same time period. Flow cytometric evaluation of splenic tumors demonstrated positivity for the myeloid markers Gr-1 and CD11b, and the presence of a subpopulation of Gr-1 and CD34 double positive cells. Based on flow cytometric and morphologic findings, we classified 16

splenic tumors according to the Bethesda criteria: 11/16 had myeloid proliferative disease/MPD, 2/16 had myeloid leukemia with maturation, 2/16 had MPD-like myeloid leukemia, and 1 case had myeloid sarcoma. Six tumors out of 18 tested were able to successfully engraft and lead to lethal disease in sublethally irradiated wild-type recipients, providing further evidence that these tumors represent transplantable, cell-autonomous myeloid malignancies. Analysis of exome sequencing data from 5 primary tumor samples is ongoing. One MPD-like myeloid leukemia was engrafted into four separate wild-type recipients, and all 5 tumors were sequenced. Collectively, this set of samples was found to contain mutations in the Ras/MAPK pathway, including the canonical gain-of-function mutation *Kras* G12C, a *Ptpn11* E76K mutation, and a missense mutation in the tumor suppressor *Neurofibromatosis 1 (Nf1).* A second, independent primary tumor was also found to contain an activating *Kras* G13D mutation. Importantly, 9/51 AML samples with *DNMT3A* mutations in the TCGA AML cohort also contained activating *NRAS* or *KRAS* mutations. Examination of the *Dnmt3a* locus in all 5 sequenced samples revealed no evidence for mutations in or deletions of the residual wild-type *Dnmt3a* allele. These data strongly suggest that Ras/MAPK pathway mutations can cooperate with *Dnmt3a* haploinsufficiency to induce AML in C57Bl/6 mice and in humans.

3.2 Introduction

Recent whole genome sequencing efforts by our group have identified mutations in the *DNA Methyltransferase 3A* (*DNMT3A*) gene in approximately 37**%** of AML patients with a normal karyotype (22% of all cases)[1]. These mutations are almost always heterozygous, and have been demonstrated by our group and others to be associated with high blast counts, advanced age, and poor prognosis[1–3]. In addition, these mutations have been demonstrated to be stable at relapse[3], suggesting that they are probably in the founding clone for most patients. *DNMT3A* mutations are enriched for changes at a single amino acid in the catalytic domain, R882 (37 out of 62 *DNMT3A*-mutated patients in our study)[1], but other patients had nonsense,

splice-site, and frame-shift mutations, and in one case, deletion of a 1.5 MB region including *DNMT3A*[1]. Studies from our group and others confirmed that these heterozygous R882 mutations lead to a hypomorphic effect on the methyltransferase activity of the enzyme, and also a dominant negative affect on the WT DNMT3A present in the same AML cells[4,5]. DMNT3A with the R882H mutation forms stable heterodimers with WT DNMT3A, disrupting the ability of the wild-type DNMT3A protein to form active homotetramers, and leading to a canonical hypomethylation signature in *DNMT3A R882H* AML patients[4].

In contrast to the dominant negative effect of R882H mutations, other *DNMT3A* mutations are predicted to have translational effects that would disrupt the coding sequence by introducing premature stop codons, frameshifts, or whole gene deletions[1]. These mutants would not be predicted *a priori* to have dominant negative activity, suggesting that they create simple haploinsufficiency for *DNMT3A*; this raises the possibility that simple haploinsufficiency for *DNMT3A* may also be an initiating event for AML. Remarkably, AML samples with non-R882 mutations also have poor outcomes, but no discrete DNA methylation signature[4].

Dnmt3a conditional null mice exhibit an aberrant expansion and loss of differentiation potential in the long-term hematopoietic stem cell compartment when serially transplanted[6], but hematopoietic abnormalities in *Dnmt3a+/-* mice have not been reported. No phenotypic abnormalities have been reported in *Dnmt3a+/-* mice, except for an increased variation in body size that may reflect instability in quantitative traits induced by DNA hypomethylation[7]. Notably, *Dnmt3a+/-* mice have not been monitored in a long-term tumor watch. Thus the effects of loss of one copy of *DNMT3A* on normal hematopoiesis and leukemogenesis have not yet been experimentally tested.

In the present study, we fully characterize hematopoiesis in *Dnmt3a+/-* mice, and demonstrate that despite minimal effects on hematopoiesis in young mice, older mice succumbed to a variety of myeloid malignancies (including myeloproliferative disease, myeloid sarcoma, and acute myeloid leukemia) after a very long latent period,. Transplantation of these

tumors into sublethally irradiated wild-type recipient mice allowed for studies of the clonality of the tumors using exome sequencing on the primary and secondary tumors. These data revealed mutations in the *RAS-MAPK* pathway in 2/5 samples; these mutations became enriched in secondary tumors. Together, these studies suggest that loss of one copy of *Dnmt3a* can facilitate leukemogenesis in both mice and AML patients.

3.3 Results

Dnmt3a+/- mice exhibit normal hematopoiesis

To characterize the effect of loss of one copy of *Dnmt3a* on hematopoiesis, we used a previously described *Dnmt3a* constitutive knockout mouse with a neomycin resistance cassette inserted into the exons coding for the catalytic domain of *Dnmt3a*[8]. We have verified that this allele produces no detectable Dnmt3a protein, including any truncated forms, by western blotting of whole embryos with an N-terminal Dnmt3a antibody. We intercrossed WT C57Bl/6 mice with *Dnmt3a+/-* mice to generate *Dnmt3a+/-* mice and *Dnmt3a+/+* littermates. *Dnmt3a+/-* mice were born at Mendelian ratios and did not exhibit the severe runting phenotype that leads to premature death in *Dnmt3a-/-* mice (data not shown). 6 week-old *Dnmt3a+/-* and *Dnmt3a+/+* mice were euthanized and bone marrow was harvested for study of mature lineage compartments (myeloid, B and T cells, **Figure 1A**) as well as for myeloid precursors (GMP, CMP, MEP) and long-term hematopoietic cells (KLS-SLAM cells, **Figure 1B)**. No differences between wild-type and *Dnmt3a+/-* bone marrow cells were present in any of these compartments. Microarray analysis of gene expression in an enriched progenitor population of these mice (KLS cells) uncovered no signature for the *Dnmt3a+/-* cells, and unsupervised clustering using the top 5000 genes with the highest variance did not cluster the samples by genotype (**Figure 1C)**.

Loss of one copy of *Dnmt3a* did not lead to an aberrant self-renewal phenotype when whole bone marrow from these mice was serially replated in methocult media (**Figure 1D).** When whole bone marrow cells from 6-week-old *Dnmt3a+/-* animals were competed against wild-type bone marrow in a competitive transplant experiment, there was no advantage for *Dnmt3a+/-* bone marrow over time (**Figure 1E);** no apparent lineage bias was detected in the peripheral blood cells of *Dnmt3a+/-* donor cells (**Figure 1F**). A large cohort of *Dnmt3a+/-* (n=43) and WT mice (n=20) was set up and was bled at regular intervals for studies of peripheral blood counts by automated CBC, and no differences were exhibited between either genotype at any time point up to one year (data not shown**)**. Collectively, these studies demonstrate that loss of one copy of *Dnmt3a* does not grossly perturb hematopoiesis or induce a specific gene expression signature in the progenitor cells of young *Dnmt3a+/-* mice.

Dnmt3a+/- mice develop myeloid malignancies with long latency

To test whether loss of one copy of *Dnmt3a* leads to hematopoietic changes in older mice, we monitored our cohort of *Dnmt3a+/-* and wild-type mice in a tumor watch for two years. Beginning at 1.5 years, some *Dnmt3a+/-* mice (15/43, 35%) became moribund, exhibiting lethargy, abdominal bloating, ruffled fur, and pale extremities (**Figure 2A**). Affected mice were euthanized and were found to have varying degrees of hepatosplenomegaly, with myeloid infiltrates in the spleen, liver, and other organs, including the mediastinal and cervical lymph nodes. At the conclusion of the tumor watch at two years, all remaining mice were euthanized for pathologic examination, and an additional 9 *Dnmt3a+/-* mice were found to display similar pathologic findings, for an overall disease penetrance of 24/43 (56%). "Affected mice" had spleen sizes greater than 5 standard deviations above the mean of spleen size of wild-type mice at 2 years (**Figure 2B).** In addition to splenomegaly, many *Dnmt3a+/-* mice displayed anemia and thrombocytopenia, but not significant leukocytosis. Flow cytometry of the spleen cells of affected animals revealed positivity for the myeloid markers Gr-1 and/or CD11b (**Table1)**. In

addition, many spleens contained sizable populations of cells that were double positive for both the late myeloid marker Gr-1, and the progenitor marker CD34, a hallmark of leukemic myeloid cells. No cases of myeloid disease were observed in 20 wild-type mice during the duration of the tumor watch.

On the basis of flow cytometry and histopathologic findings, 11 of the 16 splenic tumors were classified (Bethesda criteria[9]) as myeloproliferative disease/MPD, two had myeloid leukemia with maturation, two had MPD-like myeloid leukemia, and one had a myeloid sarcoma (**Figure 2C-D** and **Table 1**).

Transplantable Tumors from Dnmt3a+/- mice exhibit mutations in the Ras-MAPK pathway

Six tumors out of 16 that were tested were able to be secondarily transplanted and induce acute disease in sub-lethally irradiated wild-type secondary recipients, with median disease latencies ranging from 26-90 days for each tumor (**Figure 3A**). Flow cytometry and gross pathologic examination demonstrated that tumors derived from the secondary animals were myeloid malignancies that recapitulated the cell surface phenotypes of the primary tumors (**Figure 3B**).

Whole exome sequencing was performed to analyze the mutational spectrum in the primary and secondary tumors from these mice. Tumors were compared against sorted B220+ B cells from the primary animal's spleen, as a normal control population. Sequencing of DNA derived from unsorted spleen cells yielded low variant allele frequencies (VAF) for most putative mutations in the primary tumors, probably because all tumors were heavily contaminated with non-malignant lymphocytes (data not shown). All tumors were therefore resorted for Gr-1 CD34+ double-positive cells to enrich for the myeloid tumor population. In several of these tumors, potential cooperating mutations were identified. In particular, analysis of one primary MPD-like myeloid leukemia (and secondary tumors derived from it) revealed somatic mutations

in the *Ras-MAPK* pathway, including a putative loss-of-function mutation in the tumor suppressor *Nf1* (R1444I), and canonical activating mutations in *SHP2* (E76K) and in *Nras* (G12C) (**Figure 3C**). A second independent primary tumor contained a canonical gain-of-function mutation in *Nras* (G13D).

These mutations were present at a higher VAF in the secondary tumors than the primary tumor, suggesting that they were part of a subclone in the primary tumor that was selected for when engrafted into secondary recipients. Interestingly, 9 of 51 AML patient samples with DNMT3A mutations from the TCGA study also contained *Nras* or *Kras* mutations[10]. This suggests that loss of *Dnmt3a* function and mutations in the *Ras-MAPK* pathway can cooperate in both humans and *Dnmt3a+/-* mice.

Tumors from Dnmt3a+/- mice retain the residual wild-type Dnmt3a allele

We examined the sequence of the residual wild-type *Dnmt3a* allele in all tumors to see whether it was still wild type, or whether loss of heterozygosity (LOH) affected the residual allele. No point mutations or indels in the residual *Dnmt3a* allele were detected by our mutation-calling algorithm, and this result was confirmed by manual review of the *Dnmt3a* coding sequence. A specialized algorithm for detecting copy number changes, CopyCat2, did not detect additional copy number changes at the *Dnmt3a* locus in any of the four sequenced tumors. This result is currently being corroborated by comparing the *Dnmt3a* locus to that in wild-type controls, but our preliminary analyses indicate that the wild-type *Dnmt3a* allele is maintained in these tumors.

3.4 Discussion

In this study, we investigated hematopoiesis and leukemia development in *Dnmt3a+/-* mice. We found that although young *Dnmt3a+/-* mice exhibited no hematopoietic abnormalities or aberrant self-renewal phenotypes, 56% of *Dnmt3a+/-* mice developed myeloid diseases after

a very long latent period. Several of these malignancies were transplantable to sub-lethally irradiated wild-type recipients. Exome sequencing of primary tumors, and corresponding engrafted secondary tumors, revealed that 2/4 tumors tested had mutations in the *Ras-MAPK* pathway, which mimics *NRAS* and *KRAS* mutations in human AML patients with *DNMT3A* mutations. Finally, our sequencing studies revealed that the residual wild-type *Dnmt3a* allele was intact and not mutated in these tumors; these malignancies were therefore haploinsufficient for Dnmt3a, not deficient for this protein.

The motivation for this study was provided by the observation that many mutations at the *DNMT3A* locus in AML cases apparently cause haploinsufficiency (i.e. frameshifts and whole gene deletions)[1]. We discovered that *Dnmt3a+/-* mice developed a variety of myeloid malignancies with very long latencies. These malignancies were often aggressive, with most cases exhibiting massive splenomegaly and leukemic infiltrates into various extramedullary tissues. While *DNMT3A* mutations are found in both myeloid and lymphoid malignancies, they are much more prevalent in myeloid malignancies; likewise, we did not detect any lymphoid malignancies in the *Dnmt3a+/-* mice. This is particularly striking, since C57 Bl/6 mice have a greater tendency to spontaneously develop lymphoid vs. myeloid malignancies[11–13], and it suggests that haploinsufficiency for *Dnmt3a* specifically facilitates myeloid leukemogenesis.

The long latency of leukemia development in *Dnmt3a+/-* mice suggests the need for cooperating mutations for the development of overt leukemia. By performing whole exome sequencing of primary tumors and their corresponding engrafted tumors from wild-type recipients, we were able to identify cooperating hits in the *Ras-MAPK* pathway in two separate tumors. Several of these are well characterized oncogenic mutations that lead to activation of the *RAS-MAPK* pathway, and result in increased proliferative activity in various cell types[14]. Both *NRAS* and *KRAS* mutations frequently occur in human AML patients with mutant *DNMT3A*[10], and studies in mice have demonstrated the ability of *RAS* and *NF1* mutations to

cooperate with other AML-initiating mutations, such as *PML-RARA*[15], *AML-ETO*[16,17] and *MLL* fusions[17,18].

DNMT3A R882H mutations in AML are almost always heterozygous, because this mutation creates a protein that is a potent dominant negative inhibitor of WT DNMT3A[4]. Although rare AML patients appear to have biallellic mutations in DNMT3A, many others appear to have heterozygous mutations that cause simple haploinsufficiency[1]. The development of leukemias in our *Dnmt3a+/-* mice raised the question of whether the residual allele was mutationally inactivated in the manner of a classical "two hit" tumor suppressor. However, we found no evidence for this phenomenon, suggesting that myeloid malignancies that arise in these mice result from simple haploinsufficiency of *Dnmt3a.*

Since their initial discovery in AML patients, *DNMT3A* mutations have been implicated in a variety of hematologic malignancies, including MPN, MDS, CMML, and T-ALL[19]. In this study, we discovered numerous myeloid malignancies in our *Dnmt3a+/-* mice with retention of the wild-type *Dnmt3a* allele. Mutational hits in the *Ras-MAPK* pathway in multiple tumors mirrored similar findings in *DNMT3A*-mutated AML patients, and are suggestive of the ability of *DNMT3A* mutations to cooperate with mutations in the *Ras-MAPK* pathway to drive leukemogenesis. These studies shed light on the clinical observation that many *DNMT3A* mutations are predicted to lead to inactivation of one copy of the gene, and suggest that simple haploinsufficiency for *DNMT3A* facilitates the development of myeloid leukemia in mice and in humans.

3.5 Methods

Mice

The *Dnmt3a-/-* mice have been previously described. *Dnmt3a+/-* mice were obtained from the Mutant Mouse Regional Resource Centers repository (MMRRC Strain Name B5.129S4-*Dnmt3a*^{tm2Enl}*/Mmnc*). Whenever possible, littermate controls were used for all experiments. All mouse procedures were done in accordance with institutional guidelines and approved by the Animal Studies Committee at Washington University in accordance with current NIH policy.

Bone Marrow Harvest and Transplantation

Bone marrow was harvested from femurs, tibias, pelvi, and humeri of 6-week-old mice. After lysis of red blood cells (ACK buffer: 0.15 M NH4Cl, 10 mM KHCO3, 0.1 mM Na2EDTA), cells were washed with FACS buffer, filtered through through 50-μm cell strainers (Partec) and resuspended in PBS at 1 million cells/100 uL for transplantation. For competitive transplant experiments, bone marrow was mixed 50:50 with freshly harvested cells from 6-week-old Ly5.1 mice (The Jackson Laboratory, Bar Harbor, ME). Transplantation was performed by retro-orbital injection of 1×10^6 total bone marrow cells into lethally irradiated Ly5.2 or Ly5.1x5.2 recipients that had received 2 split doses of 550 cGy total body irradiation spaced at 4 hours (Mark 1 Cesium-137 irradiator, JL Shepherd) 24 hours prior to transplantation. For tumor transplants, recipient Ly5.1 mice were sublethally irradiated (600 cGy) and retro-orbitally injected with 1 million tumor cells.

Mouse Analysis and Tumor Watch

Peripheral blood counts were assessed at regular intervals as indicated by automated CBC (Hemavet 950, Drew Scientific Group). For long-term tumor watch experiments, bone marrow transplant recipients were monitored daily and animals displaying signs of illness (lethargy, hunched posture, ruffled fur, dyspnea, or palor) were euthanized and spleen and bone marrow

harvested for analysis. Diagnosis of leukemia was made by light microscopic examination of spleen and/or peripheral blood cells according to the Bethesda criteria. Cytospin tissue slides were stained with Wright-Giemsa stain (Sigma-Aldrich) and were imaged using a Nikon MICROPHOT-SA microscope equipped with an oil-immersion 50×/0.90 or 100×/1.30 objective lens (Nikon Corp.) The tumor watch was terminated after 1 year post-transplant, at which time-point recipients of wild-type marrow begin to succumb to complications related to the irradiation procedure.

Methylcellulose Colony Formation Assay

10,000 cells per plate were plated in triplicate in M3534 Methocult media containing Il-3, Il-6, and SCF (Stem Cell Technologies) and incubated at 37 degrees for 1 week. Each week, clusters of cells meeting the morphologic criteria for CFU-GEMM, CFU-GM, CFU-G, or CFU-M (http://www.stemcell.com/~/media/Technical%20Resources/8/3/E/9/0/28405_methocult%20M.pdf?la=en) were counted as myeloid colonies and cells were lifted using warm DMEM media + 2% FBS, spun down, and replated as before. An aliquot of cells was taken for analysis of myeloid markers by flow cytometry.

Illumina library construction and exome sequencing

Genomic DNA from all tumor samples and/or matched normal samples were fragmented using a Covaris LE220 DNA Sonicator (Covaris, Woburn, MA) within a size range between 100-400bp using the following settings: volume = 50µL, temperature = 4°C, duty cycle = 20, intensity = 5, cycle burst = 500, time = 120 seconds. The fragmented samples were transferred from the Covaris plate and dispensed into a 96 well BioRad Cycle plate by the CyBio-SELMA instrument. Small insert dual indexed Illumina paired end libraries were constructed with the KAPA HTP sample prep kit according to the manufacturer's recommendations (KAPA Biosystems, Woburn, MA) on the SciClone instrument according to the manufacturer's recommendations (Perkin

Elmer, Waltham, MA). Dual indexed adaptors were incorporated during ligation; the same 8bp index sequence is embedded within both arms of the library adaptor. Libraries were enriched with a single PCR reaction for 8 cycles. The final size selection of the library was achieved by a single AMPure XP paramagnetic beads (Agencourt, Beckman Coulter Genomics, Beverly, MA) cleanup targeting a final library size of 300-500bp. The libraries undergo a qualitative (final size distribution) and quantitative assay using the HT DNA Hi Sens Dual Protocol Assay with the HT DNA 1K/12K chip on the LabChip GX instrument (Perkin Elmer, Waltham, MA).

Libraries were captured using the Nimblegen SeqCap EZ Library reagent. The final concentration of each capture pool was verified through qPCR utilizing the KAPA Library Quantification Kit - Illumina/LightCycler® 480 kit according to the manufacturer's protocol (Kapa Biosystems, Woburn, MA) to produce cluster counts appropriate for the Illumina HiSeq2000 platform. Each capture pool was loaded on the HiSeq2000 version 3 flow cell according to the manufacturer's recommendations (Illumina, San Diego, CA). 2 X 101bp read pairs were generated for each sample, yielding approximately 6-7Gb of data per sample.

Variant detection pipeline

Sequence data was aligned to mouse reference sequence mm9 (with the OSK vector sequence added) using bwa version 0.5.9[14] (params: -t 4 -q 5::). Bam files were deduplicated using picard version 1.46.

Single Nucleotide Variants (SNVs) were detected using the union of three callers: 1) samtools version r963[15] (params: -A -B) intersected with Somatic Sniper version 1.0.2[16] (params: -F vcf -q 1 -Q 15) and processed through false-positive filter v1 (params: --bam-readcount-version 0.4 --bam-readcount-min-base-quality 15 --min-mapping-quality 40 --min-somatic-score 40) 2) VarScan version 2.2.6[17] filtered by varscan-high-confidence filter version v1 and processed through false-positive filter v1 (params: --bam-readcount-version 0.4 --bam-readcount-min-

base-quality 15 --min-mapping-quality 40 --min-somatic-score 40), and 3) Strelka version 0.4.6.2[18] (params: isSkipDepthFilters = 1).

Indels were detected using the union of 4 callers: 1) GATK somatic-indel version 5336[19] filtered by false-indel version v1 (params: --bam-readcount-version 0.4 --bam-readcount-min-base-quality 15), 2) pindel version 0.5[20] filtered with pindel false-positive and vaf filters (params: --variant-freq-cutoff=0.08), 3) VarScan version 2.2.6[17] [filtered by varscan-high-confidence-indel version v1 then false-indel version v1 (params: --bam-readcount-version 0.4 --bam-readcount-min-base-quality 15), and 3) Strelka version 0.4.6.2[18] (params: isSkipDepthFilters = 1).

Variants were filtered to remove non-homozygous or heterozygous sites using an R script (https://github.com/genome/gms-core/blob/f00200864a9d0b87e6b6257c5e6bcadab4e6f685/lib/perl/Genome/Model/Tools/Analysis/RemoveContaminatingVariants.R)

Cell Staining and Flow Cytometry

After ACK lysis of red blood cells, peripheral blood, bone marrow,or spleen cells were treated with anti-mouse CD16/32 (clone 93, eBioscience) and stained with the indicated combinations of the following antibodies (all antibodies are from eBioscience unless indicated): CD34 FITC (RAM34), CD11b PE or APC-e780 (M1/70), c-kit PerCP-Cy5.5 or APC-e780 (2B8), CD115 APC or PE (AFS98), Gr-1 Pacific-blue (Invitrogen, RM3028), Gr-1 biotin (RB6-8C5), B220 PE, APC, or biotin (RA3-6B2), CD3 e450 or PE (145-2C11), CD71 PE(R17217), Ter-119 Pacific-blue (TER-119), CD16/32 APC (93), Flk2 APC (A2F10). Analysis was performed using a FACScan (Beckman Coulter) or I-Cyt Synergy II sorter (I-cyt Technologies), and data analyzed using FlowJo (Tree Star), Excel (Microsoft), and Prism 5 (Graphpad).

Exon Array Gene Expression Analysis

For expression array profiling, total cellular RNA was purified using TRIzol reagent (Invitrogen), quantified using UV spectroscopy (Nanodrop Technologies), and qualitatively assessed using an Experion Bioanalyzer. Amplified cDNA was prepared from 20 ng total RNA using the whole transcript WT-Ovation RNA Amplification System and biotin-labeled using the Encore Biotin Module, both from NuGen Technologies, according to the manufacturer's instructions. Labeled targets were then hybridized to Mouse Exon 1.0 ST arrays (Affymetrix), washed, stained, and scanned using standard protocols from the Siteman Cancer Center, Molecular and Genomic Analysis Core Facility (http://pathology.wustl.edu/research/cores/lcg/index.php). Affymetrix Expression Console software was used to process array images, export signal data, and evaluate image and data quality relative to standard Affymetrix quality control metrics. Gene expression analysis was carried out in R using packages available through Bioconductor (www.bioconductor.org).

Statistics

All statistical comparisons were made using GraphPad Prism 5 software, except for statistics on sequencing data, which were calculated using the R statistical programming software as described above. Statistical tests employed and significance cut-offs are detailed in each figure legend. All data represent mean plus/minus the standard error of the mean unless indicated.

3.6 References

1. Ley T, Ding L, Walter M. DNMT3A mutations in acute myeloid leukemia. *N Engl J Med.* 2010. Available at: http://www.nejm.org/doi/full/10.1056/NEJMoa1005143. Accessed November 25, 2012.

2. Yan X-J, Xu J, Gu Z-H, et al. Exome sequencing identifies somatic mutations of DNA methyltransferase gene DNMT3A in acute monocytic leukemia. *Nat Genet*. 2011;43(4):309–15. doi:10.1038/ng.788.

3. Hou H-A, Kuo Y-Y, Liu C-Y, et al. DNMT3A mutations in acute myeloid leukemia: stability during disease evolution and clinical implications. *Blood*. 2012;119(2):559–68. doi:10.1182/blood-2011-07-369934.

4. Russler-Germain D a, Spencer DH, Young M a, et al. The R882H DNMT3A mutation associated with AML dominantly inhibits wild-type DNMT3A by blocking its ability to form active tetramers. *Cancer Cell*. 2014;25(4):442–54. doi:10.1016/j.ccr.2014.02.010.

5. Holz-Schietinger C, Matje DM, Reich NO. Mutations in DNA methyltransferase (DNMT3A) observed in acute myeloid leukemia patients disrupt processive methylation. *J Biol Chem*. 2012;287(37):30941–51. doi:10.1074/jbc.M112.366625.

6. Challen G a, Sun D, Jeong M, et al. Dnmt3a is essential for hematopoietic stem cell differentiation. *Nat Genet*. 2012;44(1):23–31. doi:10.1038/ng.1009.

7. Whitelaw NC, Chong S, Morgan DK, et al. Reduced levels of two modifiers of epigenetic gene silencing , Dnmt3a and Trim28 , cause increased phenotypic noise. *Genome Biol*. 2010;11(11):R111. doi:10.1186/gb-2010-11-11-r111.

8. Okano M, Bell DW, Haber D a, Li E. DNA methyltransferases Dnmt3a and Dnmt3b are essential for de novo methylation and mammalian development. *Cell*. 1999;99(3):247–57. Available at: http://www.ncbi.nlm.nih.gov/pubmed/10555141.

9. Kogan SC, Ward JM, Anver MR, et al. Bethesda proposals for classification of nonlymphoid hematopoietic neoplasms in mice. *Blood*. 2002;100(1):238–45.

10. Genomic and epigenomic landscapes of adult de novo acute myeloid leukemia. *N Engl J Med*. 2013;368(22):2059–74. doi:10.1056/NEJMoa1301689.

11. Frith CH, Highman B, Burger G, Sheldon WD. Spontaneous lesions in virgin and retired breeder BALB/c and C57BL/6 mice. *Lab Anim Sci*. 1983;33(3):273–86.

12. Frith CH. Incidence of hepatic metastases for various neoplasms in several strains of mice. *Toxicol Pathol*. 1983;11(2):120–8.

13. Ward J. *Pathology of genetically engineered mice*. Ames: Iowa State University Press; 2000.

14. Dhillon AS, Hagan S, Rath O, Kolch W. MAP kinase signalling pathways in cancer. *Oncogene*. 2007;26(22):3279–90. doi:10.1038/sj.onc.1210421.

15. Chan IT, Kutok JL, Williams IR, et al. Oncogenic K-ras cooperates with PML-RAR ⎵ to induce an acute promyelocytic leukemia – like disease. *Blood*. 2006;108(5):1708–1715. doi:10.1182/blood-2006-04-015040.

16. Zhao S, Zhang Y, Sha K, et al. KRAS (G12D) Cooperates with AML1/ETO to Initiate a Mouse Model Mimicking Human Acute Myeloid Leukemia. *Cell Physiol Biochem*. 2014;33(1):78–87. doi:10.1159/000356651.

17. Zuber J, Radtke I, Pardee TS, et al. Mouse models of human AML accurately predict chemotherapy response. *Genes Dev*. 2009;23(7):877–89. doi:10.1101/gad.1771409.

18. Tamai H, Miyake K, Takatori M, et al. Activated K-Ras protein accelerates human MLL/AF4-induced leukemo-lymphomogenicity in a transgenic mouse model. *Leukemia*. 2011;25(5):888–91. doi:10.1038/leu.2011.15.

19. Abdel-Wahab O, Levine RL. Mutations in epigenetic modifiers in the pathogenesis and therapy of acute myeloid leukemia. *Blood*. 2013;121(18):3563–72. doi:10.1182/blood-2013-01-451781.

3.7 Figure Legends

Figure 1

Normal hematopoiesis in young *Dnmt3a+/-* mice. (**A)** Quantification of myeloid cells (Gr-1+), B220+ B cells, and CD3+ T cells in bone marrow of 6-week-old wild-type and *Dnmt3a+/-* mice. (**B)** Quantification of myeloid progenitor compartments (GMP, CMP, MEP) and KLS-SLAM cells (HSC) from young mice as in A). **(C)** Unsupervised hierarchical clustering of exon array data from sorted enriched progenitor cells (KLS cells) from 6-week-old mice in which samples are clustering using the 5000 probes with the highest standard deviation demonstrates the lack of a distinct gene expression signature in *Dnmt3a+/-* cells v. wild-type. **(D)** Bone marrow from 6-week-old mice was plated in methocult media containing IL-3, IL-6 and SCF, and replated every 7 days. Quantification of colony numbers demonstrates that *Dnmt3a+/-* cells have no aberrant self-renewal phenotype *ex vivo.* **(E-F)** Bone marrow from 6-week-old wild-type or *Dnmt3a+/-* mice was mixed 50:50 and transplanted into lethally irradiated wild-type mice. **(E)** Chimerism in peripheral blood at 16 weeks demonstrates no competitive advantage for *Dnmt3a+/-* donor cells versus wild-type. **(F)** Lineage bias for each donor genotype was quantified by measuring dividing the number of cells positive for each marker by the total chimerism. No lineage biases were detected for *Dnmt3a+/-* vs wild-type bone marrow cells. N.S. = not significant by two-way ANOVA with Bonferroni post-test. N=3 for all experiments.

Figure 2

Dnmt3a+/- mice develop myeloid malignancies. (**A**) *Dnmt3a+/-* and wild-type mice were monitored in long-term (2 year) tumor watch and mice which became moribund were euthanized for pathologic analysis. (**B)** At 2 years all remaining mice were bled for CBCs, euthanized, and all mice on tumor watch were grouped by spleen size into wild-type, unaffected *Dnmt3a+/-,* and affected *Dnmt3a+/-* (see **Results** for details). Affected *Dnmt3a+/-* mice exhibited anemia and thrombocytopenia but not significant leukocytosis. **(C)** Distribution of pathologic diagnoses

according to Bethesda criteria for all mice that could be definitively classified. (**D)** Representative histology of tissues from affected *Dnmt3a+/-* mice. *$p<0.05$, ***$p<0.001$ by two-tailed t-test.

Figure 3

Transplantable tumors from *Dnmt3a+/-* mice exhibit mutations in the *Ras-MAPK* pathway. (**A**) Kaplan-Meier curve illustrating disease latency for sublethally irradiated wild-type animals engrafted with *Dnmt3a+/-* tumors. (**B)** Representative flow cytometry from primary and secondary tumors demonstrating that secondary tumors recapitulate the immunophenotypes of their corresponding primary tumors. **(C)** Schematic of *Ras-MAPK* pathway illustrating location of mutations in *Dnmt3a+/-* tumors discovered by exome sequencing of sorted Gr-1+Cd34+ cells.

Figure 1

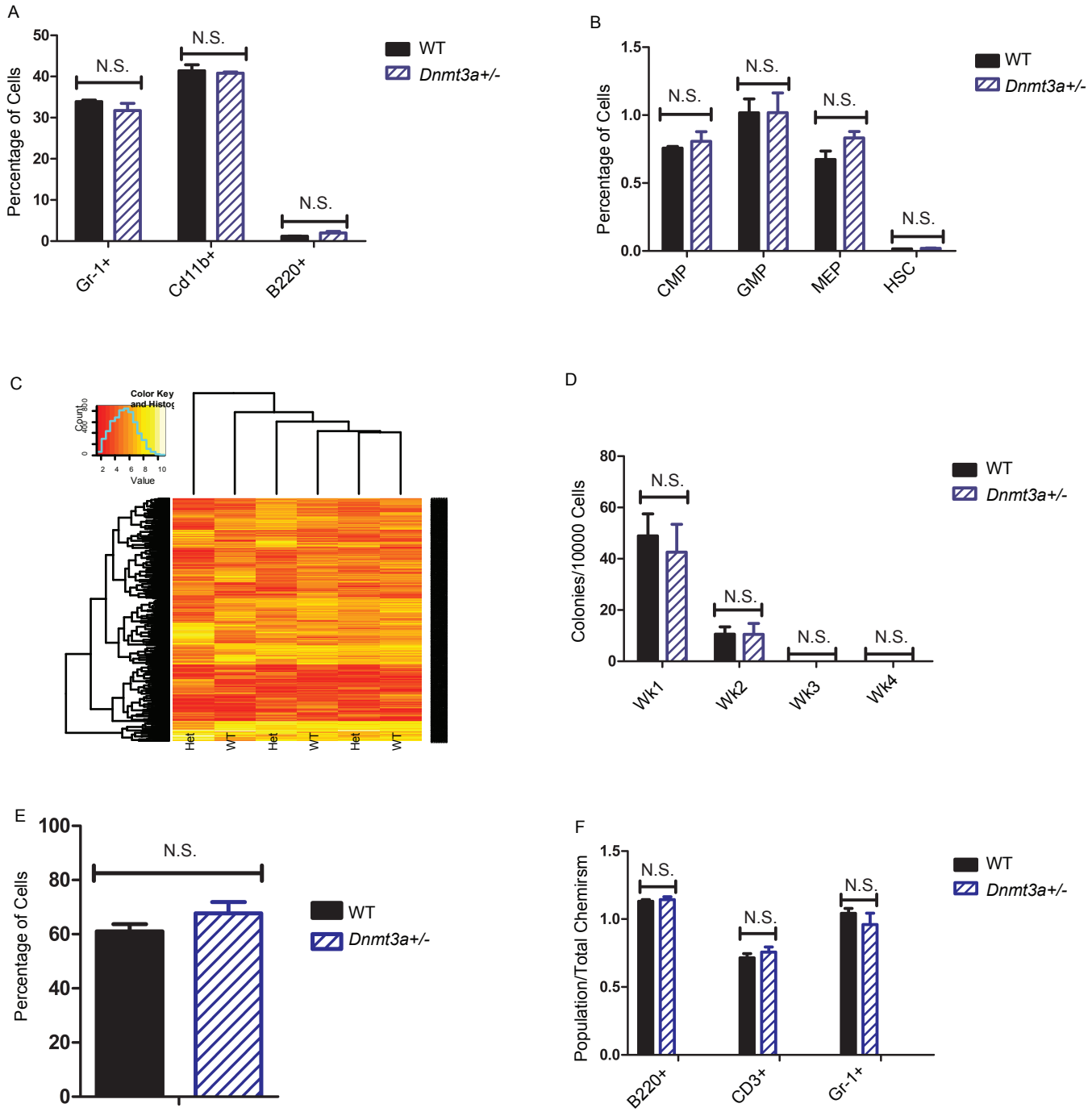

Figure 2

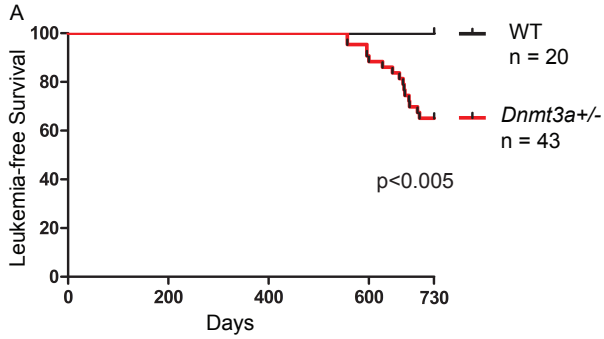

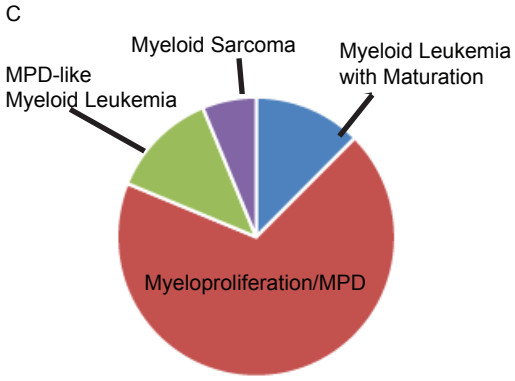

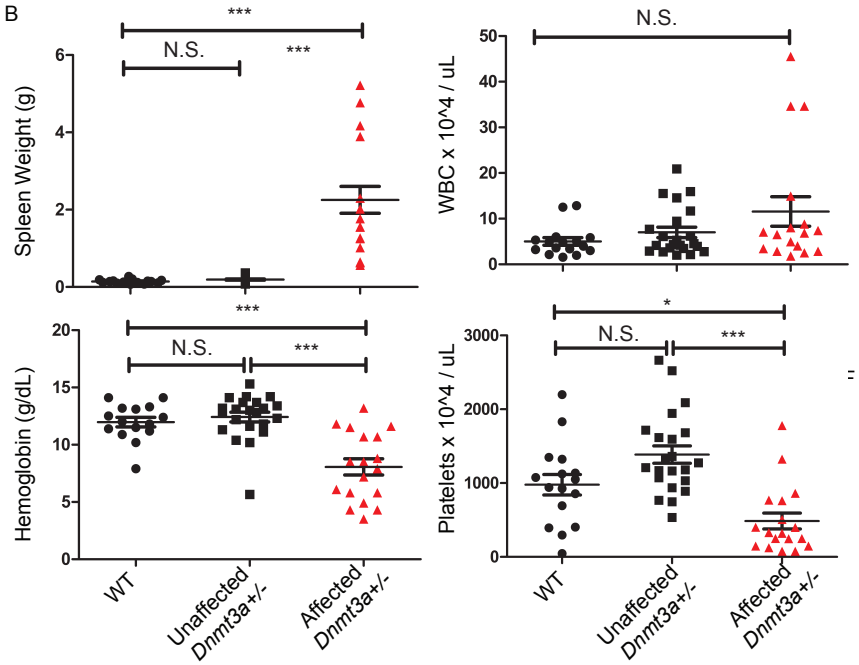

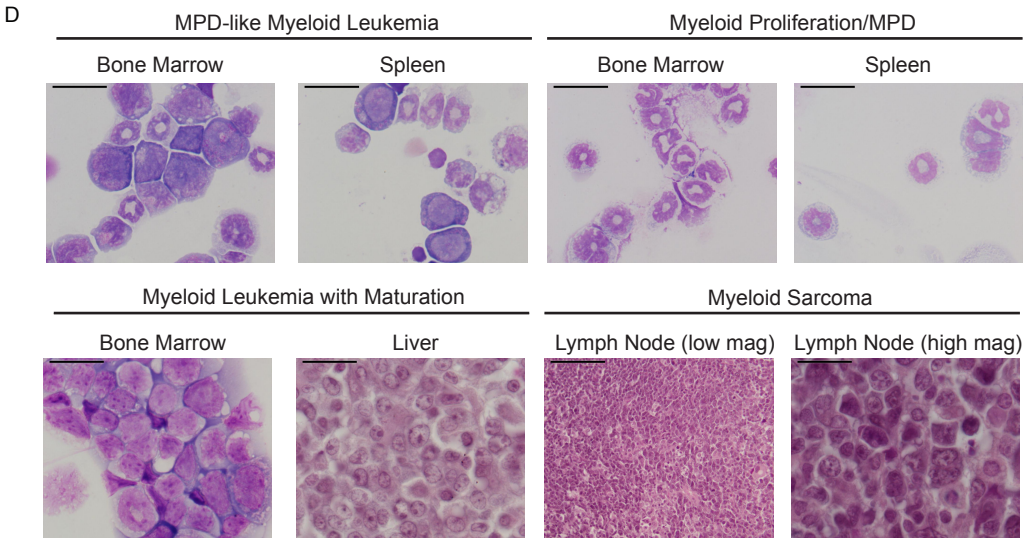

Figure 3

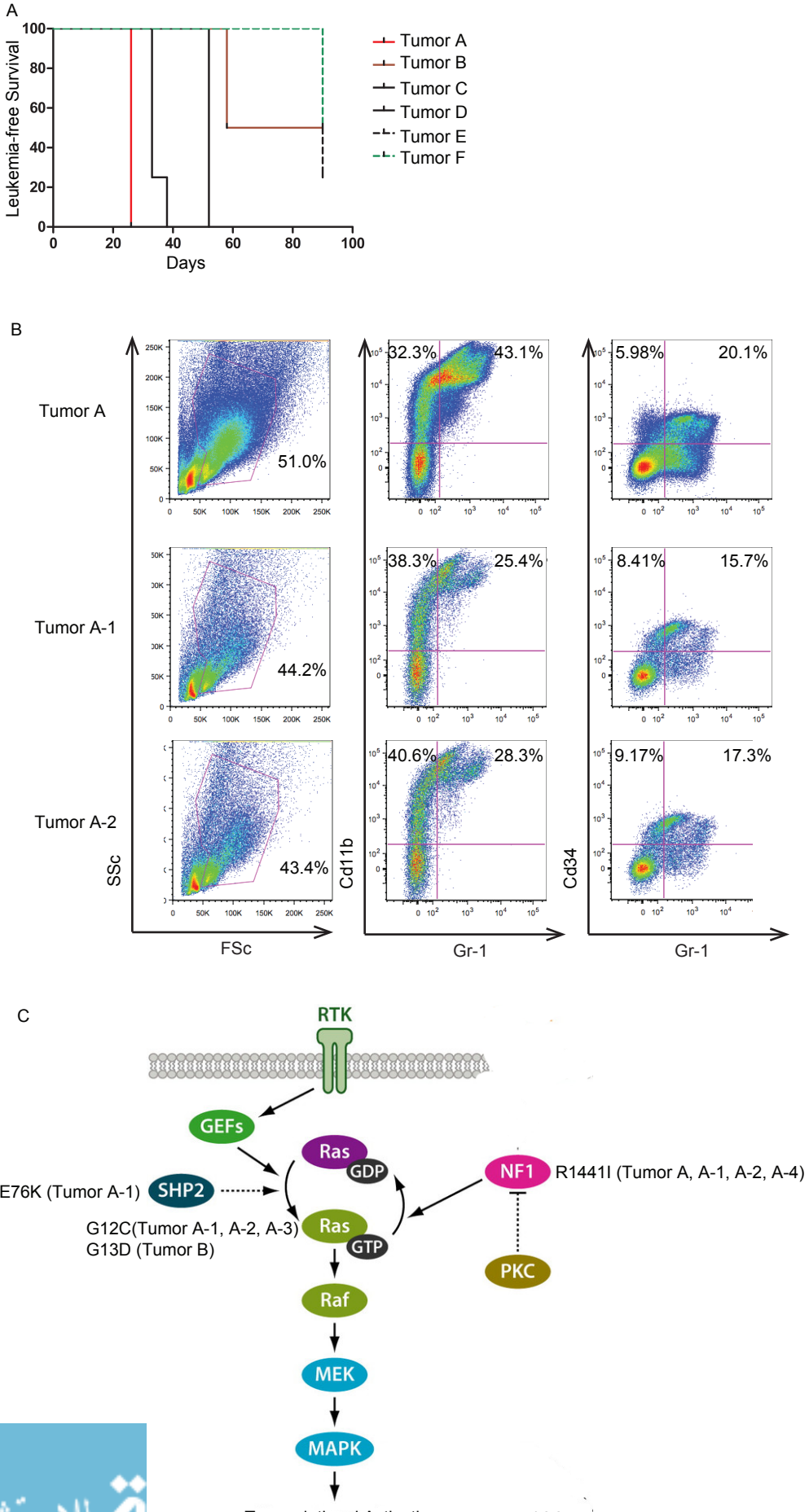

Table 1

Case	Spleen Wgt (g)	Gr-1+	CD11b+	Gr1+CD34+	Gr1+ckit+	B220+	CD3+	Pathologic Diagnosis
1	4	85.7	94.5	**50.4**	3.2	1.0	**23.6**	Myeloid proliferation (nonreactive); Myeloproliferative disease
2	0.82	84.1	99.1	**36.2**	1.6			Myeloid leukemia with maturation
3	2.7	50.3	69.8	**17.9**	4.3	**5.7**	**16.6**	Myeloid proliferation (nonreactive); Myeloproliferative disease
4	0.44	33.1	64.8	**12.1**	1.1	9.7	6.6	Myeloid proliferation (nonreactive); Myeloproliferation (genetic)
5	0.92	43.2	75.4	**20.1**	1.8	1.7	6.8	Myeloid leukemia; MPD-like myeloid leukemia
6	0.5	4.1	24.9	1.3	0.2	**12.1**	**2.9**	Myeloid leukemia; MPD-like myeloid leukemia
7	1.77	1.3	2.3	0.5	0.0	0.1	4.3	Myeloid proliferation (nonreactive); Myeloproliferation (genetic)
8	2.02	1.9	5.8	1.0	0.2	0.1	6.6	Myeloid proliferation (nonreactive); Myeloproliferation (genetic)
9	1.55	3.4	6.0	1.0	0.2	0.3	3.0	Myeloid leukemia with maturation
10	N/A							Myeloid Sarcoma
11	1.56	54.9	71.7	**26.2**	0.5	7.5	**24.2**	Myeloid proliferation (nonreactive); Myeloproliferation (genetic)
12	5.22	52.7	72.6	**41.3**	1.6	0.9	**34.6**	Myeloid proliferation (nonreactive); Myeloproliferation (genetic)
13	4.77	56.3	81.1	**41.7**	1.9	4.9	**16.1**	Myeloid proliferation (nonreactive); Myeloproliferation (genetic)
14	1.27	71.8	92.1	**32.6**	0.4	3.5	9.3	Myeloid proliferation (nonreactive); Myeloproliferation (genetic)
15	0.56	48.6	69.7	**29.3**	0.3	**16.3**	**10.3**	Myeloid proliferation (nonreactive); Myeloproliferation (genetic)
16	4.17	60.1	84.5	**37.7**	1.3	2.3	**21.6**	Myeloid proliferation (nonreactive); Myeloproliferation (genetic)

Chapter 4

Summary and Future Directions

4.1 Summary

In this thesis, we used mouse models of acute myeloid leukemia in order to explain two observed patterns of mutations that have emerged from recent whole genome sequencing of acute myeloid leukemia patients. In **Chapter 2**, we applied well-characterized retroviral and transgenic mouse models to investigate the mechanistic basis for the observation that *DNMT3A* mutations are exclusive of the common fusion proteins *PML-RARA*, *RUNX1-RUNX1T1*, and the *MLL* fusions. We discovered that of these fusion genes, only *PML-RARA* is dependent on *Dnmt3a* for its ability to drive aberrant self-renewal *ex vivo*, and provide a competitive advantage and leukemia *in vivo.* The ability to drive aberrant self-renewal is specifically dependent on the methyltransferase activity of *Dnmt3a*, since neither *DNMT3B* nor catalytically deficient *DNMT3A* mutants are able to restore aberrant self-renewal to *Ctsg-PML-RARA* bone marrow cells lacking Dnmt3a. Using a methylation-sensitive restriction enzyme, we demonstrated that restoration of self-renewal ability by expression of retroviral *DNMT3A* coincides with restoration of DNA methylation at several informative loci. In **Chapter 3**, we studied *Dnmt3a+/-* mice to model a subset of *DNMT3A* mutations observed in AML patients (i.e. heterozygous mutations predicted to create haploinsufficiency for *DNMT3A).* We discovered that although young *Dnmt3a+/-* mice exhibit no detectable hematopoietic abnormalities (including a lack of a competitive transplant advantage, and no aberrant self-renewal phenotype *ex vivo*), a long-term tumor watch demonstrated the development of myeloid malignancies in approximately 60% of animals, with a very long latency (1.5 years or longer). Some of these tumors were transplantable to sublethally irradiated wild-type recipients, and resulted in tumors that were morphologically and immunophenotypically similar to the primary tumors from which they were derived. Whole exome sequencing demonstrated mutations in the *Ras-MAPK* pathway in several tumors, and also verified that the residual *Dnmt3a* wild-type allele was intact, demonstrating that these phenotypes are due to *Dnmt3a* haploinsufficiency. In **Chapter 4**, we

will examine unresolved questions raised by these results, and propose future experiments designed to investigate the role of *DNMT3A* in APL and *DNMT3A* haploinsufficiency in AML.

4.2 Early and late epigenetic changes in Ctsg-PML-RARA mice

The observation that the DNA methylation signature of *APL* patients can distinguish them from cases with the other chromosomal fusions--as well as all other AML cases--is striking and has been observed by multiple groups[1,2]. This finding, and our observation of abrogation of aberrant self-renewal and disruption of leukemogenesis in *PR+/-, Dnmt3a-/-* mice, strongly suggest a role for DNA methylation in the pathogenesis of APL, but the nature of the precise methylation changes and their relationship to PML-RARA activity remain unclear. Previous studies of methylation signatures in APL have largely been limited to technologies such as reduced representation bisulfite sequencing, which is capable of interrogating the methylation status of a small fraction of genomic CpGs[3–5]. Further, all studies to date have also focused on fully transformed APL cells. In addition, studies of methylation in APL patient cells have lacked appropriate controls that are critical to determine “normal” methylation patterns.

The gold standard for interrogating genomic methylation is whole genome bisulfite sequencing, which allows a non-biased measurement of CpG methylation across the genome[6]. Presently we are initiating studies of whole genome bisulfite sequencing to examine methylation patterns in 1) the non-leukemic promyelocytes of 6-week-old *mCG-PML-RARA+/-* mice, 2) promyelocytes of wild-type littermates, and 3) APL samples from *mCG-PML-RARA+/-* mice. The promyelocyte compartment was chosen because it is an enriched progenitor compartment with high expression of the *PML-RARA* allele, and well-documented dysregulation of many genes by PML-RARA[7]. Using this system, we will interrogate early methylation changes induced by *PML-RARA* expression relative to a wild-type control, and we will compare these changes to the methylation state of fully transformed tumors from the same mouse model. This

experiment will elucidate early methylation events induced by *PML-RARA* at high resolution. Additional interrogation of chromatin modifications and accessibility, using techniques such as H3K27 and H3K4 ChIP-seq and ATAC-seq[8], will allow for a comprehensive description of the epigenetic changes accompanying *PML-RARA* expression in preleukemic and leukemic mice.

4.3 Elucidation of the Mechanisms by which PML-RARA and Dnmt3a Affect Gene Expression

The classical model of *PML-RARA* function is that fusion to PML disrupts the ability of RARA to release from DNA, thus leading to a repression of gene expression that is unresponsive to endogenous retinoic acid ligand, possibly by recruitment of a co-repressive complex that includes Dnmt3a[9]. However, early gene expression changes in the myeloid progenitor compartment of *mCG-PML-RARA+/-* mice include both down-regulated and up-regulated genes[7]. Further, confirmation of a direct PML-RARA-DNMT3A protein-protein interaction has not yet been reported by any lab. We are currently performing rigorous pull-down experiments to establish whether PML-RARA and DNMT3A are in fact capable of a direct interaction, and also establishing whether this interaction exists between PML-RARA and mouse *Dnmt3a*, since this is directly relevant to understanding the requirement for functional Dnmt3a in our *Ctsg-PML-RARA* mouse.

Another outstanding question concerns the relationship between *PML-RARA* binding and induction of DNA methylation. Although it is clear from our studies that *PML-RARA* needs functional Dnmt3a to drive leukemogenesis, it is still unclear whether this reliance is the direct result of *PML-RARA* recruitment of Dnmt3a to methylate and repress DNA target genes, as has been proposed[9,10]. Efforts to relate *PML-RARA* binding and DNA methylation genome-wide have relied on a correlative approach (using two antibodies against RARA and PML) and have only been able to capture DNA methylation changes in a limited fashion (using RRBS at an

early time point after induction of *PML-RARA* expression, in a transformed cell line)[3]. To circumvent these limitations, we will express a tagged version of *PML-RARA* in mouse bone marrow cells, and allow it to stably engraft in recipients before harvesting expressing cells for PML-RARA ChIP-seq. This approach will allow us to interrogate PML-RARA binding in an endogenous cellular context, and in combination with the above studies of DNA methylation and chromatin conformation, will enable a genome-wide view of how PML-RARA binding relates to local DNA methylation and chromatin conformation changes. Finally, the above data will be combined with comprehensive RNA-sequencing to describe the relationships between PML-RARA binding, the induction of chromatin structure changes, and changes in gene expression.

4.4 Examination of DNA Methylation in *Dnmt3a+/-* Mice

A DNA methylation analysis has not yet been reported for *Dnmt3a+/-* mice. Future research will seek to determine whether loss of one copy of *Dnmt3a* results in hypomethylation at specific canonical loci, for example the Dnmt3a-dependent loci identified in our methylation sequencing studies in **Chapter 2.** Given the lack of detectable hematopoietic abnormalities in young *Dnmt3a+/-* mice, it is possible that a methylation deficit in these mice due to haploinsufficiency for *Dnmt3a* is far more subtle than that in Dnmt3a-null mice, requiring multiple divisions of hematopoietic stem cells throughout the lifespan of the mouse in order to accumulate changes in CpG methylation. This, along with the need for cooperating mutations such as those in the *Ras-MAPK* pathway, might explain the very long latency to leukemia in the *Dnmt3a+/-* mice. One method to examine a possible progressive methylation deficit is to serially examine methylation in *Dnmt3a+/-* bone marrow cells in mice of different ages, using either the HpaII assay we employed in this thesis, or a more comprehensive genome-wide approach. Additional experiments that might support the hypothesis of a progressive methylation deficit would include examining the methylation state in cultured cells induced to rapidly proliferate, e.g. by growth of a small starting number of bone marrow cells expanded on

stromal cells in the presence of cytokines, or in mice treated with 5-FU to induce rapid stem cell expansion. Methylation changes at individual loci observed in these studies will need to be correlated with gene expression changes to determine their role in the development of disease.

4.5 Identification and Phenotyping of *DNMT3A*-Haploinsufficient Patients

Our group has made considerable progress in understanding the dominant negative mechanism of *DNMT3A* R882H mutations, and correlating these with a canonical hypomethylation phenotype in patients[11], but other *DNMT3A* mutations remain poorly understood. While it can be confidently predicted that some *DNMT3A* mutations, such as a whole gene deletion, will result in protein production from only one allele[12], this needs to be empirically tested for other mutations. For many of the frame-shift mutations, it is likely that premature termination leads to induction of nonsense-mediated decay, but it is also formally possible that some of these mutations result in formation of a truncated protein with biochemical activity. For *DNMT3A* nonsense and missense mutations, the effect of expression of the mutated allele on the methylation activity of the wild-type allele remains to be determined. We are currently in the process of creating expression constructs for a number of these *DNMT3A* mutations to determine which lead to production of a DNMT3A protein. The mutant alleles that result in expression of detectable protein will be further evaluated with biochemical studies to quantify their degree of methylation activity and their effects on wild-type *DNMT3A*, using methods previously published by our group[11].

By biochemically characterizing these mutant *DNMT3A* alleles, we will be able to determine which alleles lead to true haploinsufficiency versus a dominant negative effect (or other unexpected effects). By grouping together the haploinsufficient *DNMT3A* patients and comparing them to patients that have dominant negative alleles (e.g. R882), we will be able to use existing data on gene expression and methylation phenotypes to see if there are common

gene expression or methylation signatures that define *DNMT3A* haploinsufficiency in AML. By comparing these signatures to corresponding data from our *Dnmt3a+/-* mice, we hope to be able to arrive at an understanding of the role of *DNMT3A* in AML pathogenesis, which may have important therapeutic implications for this disease.

4.6 References

1. Genomic and epigenomic landscapes of adult de novo acute myeloid leukemia. *N Engl J Med*. 2013;368(22):2059–74. doi:10.1056/NEJMoa1301689.

2. Figueroa ME, Lugthart S, Li Y, et al. DNA methylation signatures identify biologically distinct subtypes in acute myeloid leukemia. *Cancer Cell*. 2010;17(1):13–27. doi:10.1016/j.ccr.2009.11.020.

3. Martens JH a, Brinkman AB, Simmer F, et al. PML-RARalpha/RXR Alters the Epigenetic Landscape in Acute Promyelocytic Leukemia. *Cancer Cell*. 2010;17(2):173–85. doi:10.1016/j.ccr.2009.12.042.

4. Saeed S, Logie C, Francoijs K-J, et al. Chromatin accessibility, p300 and histone acetylation define PML-RARα and AML1-ETO binding sites in acute myeloid leukemia. *Blood*. 2012. doi:10.1182/blood-2011-10-386086.

5. Mikesch J-H, Gronemeyer H, So CWE. Discovery of novel transcriptional and epigenetic targets in APL by global ChIP analyses: Emerging opportunity and challenge. *Cancer Cell*. 2010;17(2):112–4. doi:10.1016/j.ccr.2010.01.012.

6. Bock C. Analysing and interpreting DNA methylation data. *Nat Rev Genet*. 2012;13(10):705–19. doi:10.1038/nrg3273.

7. Wartman LD, Welch JS, Uy GL, et al. Expression and Function of PML-RARA in the Hematopoietic Progenitor Cells of Ctsg-PML-RARA Mice. *PLoS One*. 2012;7(10):e46529. doi:10.1371/journal.pone.0046529.

8. Buenrostro JD, Giresi PG, Zaba LC, Chang HY, Greenleaf WJ. Transposition of native chromatin for fast and sensitive epigenomic profiling of open chromatin, DNA-binding proteins and nucleosome position. *Nat Methods*. 2013;10(12):1213–8. doi:10.1038/nmeth.2688.

9. Di Croce L, Raker V a, Corsaro M, et al. Methyltransferase recruitment and DNA hypermethylation of target promoters by an oncogenic transcription factor. *Science*. 2002;295(5557):1079–82. doi:10.1126/science.1065173.

10. Fazi F, Travaglini L, Carotti D, et al. Retinoic acid targets DNA-methyltransferases and histone deacetylases during APL blast differentiation in vitro and in vivo. *Oncogene*. 2005;24(11):1820–30. doi:10.1038/sj.onc.1208286.

11. Russler-Germain D a, Spencer DH, Young M a, et al. The R882H DNMT3A mutation associated with AML dominantly inhibits wild-type DNMT3A by blocking its ability to form active tetramers. *Cancer Cell*. 2014;25(4):442–54. doi:10.1016/j.ccr.2014.02.010.

12. Ley T, Ding L, Walter M. DNMT3A mutations in acute myeloid leukemia. *… Engl J …*. 2010. Available at: http://www.nejm.org/doi/full/10.1056/NEJMoa1005143. Accessed November 25, 2012.